University of Alberta

Functional Magnetic Resonance Imaging of Repetitive Movement in Healthy Subjects and Patients with Parkinson's Disease

By

Tracy Ann Boyd

©

A thesis submitted to the Faculty of Graduate Studies and Research in partial fulfillment of the requirements for the degree of Master of Science

University Centre for Neuroscience

Edmonton, Alberta

Spring 2002

National Library of Canada
Acquisitions and Bibliographic Services
395 Wellington Street
Ottawa ON K1A 0N4
Canada

Bibliothèque nationale du Canada
Acquisitions et services bibliographiques
395, rue Wellington
Ottawa ON K1A 0N4
Canada

Your file Votre référence

Our file Notre référence

The author has granted a non-exclusive licence allowing the National Library of Canada to reproduce, loan, distribute or sell copies of this thesis in microform, paper or electronic formats.

L'auteur a accordé une licence non exclusive permettant à la Bibliothèque nationale du Canada de reproduire, prêter, distribuer ou vendre des copies de cette thèse sous la forme de microfiche/film, de reproduction sur papier ou sur format électronique.

The author retains ownership of the copyright in this thesis. Neither the thesis nor substantial extracts from it may be printed or otherwise reproduced without the author's permission.

L'auteur conserve la propriété du droit d'auteur qui protège cette thèse. Ni la thèse ni des extraits substantiels de celle-ci ne doivent être imprimés ou autrement reproduits sans son autorisation.

0-612-69795-9

Canada

University of Alberta

Library Release Form

Name of Author: *Tracy Ann Boyd*

Title of Thesis: *Functional Magnetic Resonance Imaging of Repetitive Movement in Healthy Subjects and Patients with Parkinson's Disease*

Degree: *Master of Science*

Year this Degree Granted: *2002*

Permission is hereby granted to the University of Alberta Library to reproduce single copies of this thesis and to lend or sell such copies for private, scholarly or scientific research purposes only.

The author reserves all other publication and other rights in association with the copyright in the thesis, and except as herein before provided, neither the thesis nor any substantial portion thereof may be printed or otherwise reproduced in any material form whatever without the author's prior written permission.

Tracy Boyd

Tracy Ann Boyd
513 Heritage Medical Research Centre
University Centre for Neuroscience
University of Alberta
Edmonton, AB
T6G 2S2

Date: *January 21, 2002*

University of Alberta

Faculty of Graduate Studies and Research

The undersigned certify that they have read, and recommend to the Faculty of Graduate Studies and Research for acceptance, a thesis entitled "Functional magnetic resonance imaging of repetitive movement in healthy subjects and patients with Parkinson's Disease" submitted by Tracy Ann Boyd in partial fulfillment of the requirements for the degree of Master of Science.

Supervisor:

Dr. Wayne Martin, MD

Supervisory Committee:

Dr. Keir Pearson, PhD

Dr. Christian Beaulieu, PhD

Dr. Arthur Prochazka, PhD

Date: 2002-1-17

Abstract

Functional magnetic resonance imaging (fMRI) during repetitive right and left hand finger tapping was used to 1) characterize cortical motor activity in healthy volunteers, and 2) to compare activation in patients with Parkinson's disease (PD) to age-matched controls. Cortical activity associated with repetitive movement was consistently detected in the contralateral sensorimotor cortex in every subject and scanning session. In the first study there was no difference in the reproducibility of data acquired from ten different healthy subjects versus data acquired from a single healthy subject tested in ten independent sessions. Furthermore, while there was no evidence of impaired cortical activation in PD, widespread regions of relatively increased activation were consistently detected in PD patients when compared to age-matched controls. The results of both studies thus demonstrate that fMRI is a valid and reliable strategy for evaluating changes in cortical activation using a repetitive motor task.

Acknowledgements

I would like to begin by extending my thanks and gratitude to my supervisor Dr. Wayne Martin. I would also like to thank the members of my supervisory committee; Dr. Keir Pearson and Dr. Arthur Prochazka from the University Centre for Neuroscience, and Dr. Christian Beaulieu from the Department of Biomedical Engineering, University of Alberta. In addition, my thanks to the staff and students at the University of Alberta In-Vivo NMR Centre for their assistance in a number of areas, in particular Dr. Alan Wilman and Dr. Chris Hanstock for their advice and expertise in NMR, and Beau Sapach for computer support. Administrative support was provided by Marguerite Wieler, Pam King, and Germaine McInnes from the Movement Disorder Clinic at the Glenrose Rehabilitation Hospital (Edmonton, Alberta), and Carol-Ann Johnson from the University Centre for Neuroscience, University of Alberta. This project was funded through grants to Dr. Wayne Martin from the Parkinson's Society of Alberta. Finally, this thesis would not have been possible without the support and patience of a now expert finger tapping volunteer, my husband Gordon Boyd.

Table of Contents

Chapter 1: Introduction

1.1. General Introduction....1

1.2. Experimental Applications of fMRI....1

1.2.1. FMRI and motor activation....1

1.2.2. Pathophysiology of PD....2

1.2.3. Supplementary motor area (SMA)....4

1.2.4. Impaired SMA activity in PD....5

1.2.5. Functional dissociation of rostral and caudal SMA....7

1.2.6. SMA activation following medication and surgery in PD....8

1.2.7. Lateral premotor pathways in PD....9

1.2.8. Increased cortical activity in PD....10

1.3. Basic Principles of Nuclear Magnetic Resonance Imaging....12

1.3.1. Nuclear spin and alignment....12

1.3.2. Nuclear spin resonance and radiofrequency excitation....13

1.3.3. MR signal and spin relaxation....15

1.3.4. Spatial encoding....19

1.3.5. Spin echo and gradient echo imaging....21

1.4. Basic Principles of Blood Oxygen Level Dependent (BOLD) fMRI.....24

1.5. Reliability of fMRI.....26

1.5.1. Reproducibility of size and location of fMRI activation.....26

1.5.2. Regional patterns of variability.....27

1.5.3. Probabilistic models of variance.....29

1.5.4. Random effects analysis.....30

1.6. General Summary and Research Objectives.....31

1.7. References.....33

Chapter 2: Functional Magnetic Resonance Imaging of Cortical Motor Activity at 3 Tesla

2.1. Introduction.....42

2.2. Methods.....44

2.2.1. Subjects.....44

2.2.2. Motor task.....44

2.2.3. Experimental design.....45

2.2.4. fMRI data acquisition.....45

2.2.5. Data pre-processing.....47

2.2.6. Statistical analysis.....50

2.2.7. Single subject/ single session analyses 52

2.2.8. Multi subject/ session analyses 53

2.3. Results 54

2.3.1. Task performance 54

2.3.2. Single subject-/ session-analyses 54

2.3.2.1. Primary somatosensory and motor cortex activation 55

2.3.2.2. Other regions of activity 59

2.3.2.3. Consistency of motor activation 60

2.3.2.4. Spatial extent of activation 60

2.3.2.5. Amplitude of BOLD response 63

2.3.3. Multi subject-/ session-analyses 66

2.3.3.1. Fixed effects analyses 74

2.3.3.2. Random effects analyses 75

2.4. Discussion 77

2.4.1. Activation of the motor cortex 78

2.4.2. Activation of the somatosensory cortex 78

2.4.3. Activation of other cortical regions 79

2.4.4. Variability 80

2.4.5. Conclusions 82

2.5. References 83

Chapter 3: FMRI of Motor Activity in Patients with Parkinson's Disease and Healthy Age Matched Control Subjects

3.1. Introduction 87

3.2. Methods 89

3.2.1. Subjects 89

3.2.2. Motor task, experimental design, data acquisition, and analyses 89

3.3. Results 91

3.3.1. Task performance 91

3.3.2. Head movement 91

3.3.3. Single subject analyses 92

3.3.3.1. Location of activity 92

3.3.3.2. Spatial extent of activation 95

3.3.3.3. Amplitude of BOLD response 98

3.3.4. Group analyses 100

3.3.4.1. Fixed effects analyses 108

3.3.4.2. Random effects analyses 109

3.3.5. Between group analysis 110

3.4. Discussion 110

3.4.1. Repetitive finger tapping 111

3.4.2. Single subject versus group analyses 112

3.4.3. Functional compensation 114

3.4.3.1. Lateral premotor and parietal cortex 114

3.4.3.2. Caudal SMA 115

3.4.3.3. Anterior cingulate 116

3.4.4. Conclusions 116

3.5. References 119

Chapter 4: General Discussion

4.1. Technical issues and limitations 124

4.1.1. Image artifacts and distortion 124

4.1.2. Inflow effects, draining veins, and physiological noise 126

4.2. Limitations of standard block-design fMRI experiments 128

4.3. General conclusions 129

4.3.1. Feasibility of investigating motor activity using fMRI at 3T 129

4.3.2. Changes in cortical activation in PD 129

4.4. References 132

List of Tables

Chapter 2: Functional Magnetic Resonance Imaging of Cortical Motor Activity at 3 Tesla

Table 2-1. Anatomical localization of activity associated with right hand finger tapping within the individual data set....67

Table 2-2. Anatomical localization of activity associated with left hand finger tapping within the individual data set....68

Table 2-3. Anatomical localization of activity associated with right and left hand finger tapping within the group data set....69

Chapter 3: FMRI of Motor Activity in Patients with Parkinson's Disease and Healthy Age Matched Control Subjects

Table 3-1. Clinical characteristics of patients with Parkinson's disease....90

Table 3-2. Anatomical localization of activity associated with right hand finger tapping within the group of PD patients....101

Table 3-3. Anatomical localization of activity associated with left hand finger tapping within the group of PD patients....102

Table 3-4. Anatomical localization of activity associated with right and left hand finger tapping within the group of control subjects....103

List of Figures

Chapter 1: Introduction

Figure 1-1. Schematic representation of changes in striatal pathways in PD.....3

Figure 1-2. Proton alignment, precession, and excitation 14

Figure 1-3. T_2 decay of transverse magnetization and T_1 recovery of longitudinal magnetization.....18

Figure 1-4. Spatial encoding of magnetic resonance images 20

Figure 1-5. Spin echo formation following 180^0 RF pulse 23

Chapter 2: Functional Magnetic Resonance Imaging of Cortical Motor Activity at 3 Tesla

Figure 2-1. FMRI experimental design 46

Figure 2-2. EPI template image (SPM 99) 49

Figure 2-3. MIP images of activity associated with right and left hand finger tapping from each session in the individual data set 56

Figure 2-4. MIP images of activity associated with right and left hand finger tapping from each session in the group data set 57

Figure 2-5. The change in BOLD signal associated with a time series of alternating blocks of rest and repetitive finger tapping.....58

Figure 2-6. The mean spatial extent of activity associated with right and left hand finger tapping in the individual and group data sets 62

Figure 2-7. The mean estimated BOLD signal change associated with right and left hand finger tapping in the individual and group data sets 65

Figure 2-8. Fixed and random effects analysis of activity associated with right and left hand finger tapping across sessions in the individual data set 70

Figure 2-9. Fixed and random effects analysis of activity associated with right and left hand finger tapping across sessions in the group data set 71

Figure 2-10. Fixed and random effects analysis of activity associated with right hand finger tapping in the individual and group data sets 72

Figure 2-11. Fixed and random effects analysis of activity associated with left hand finger tapping in the individual and group data sets 73

Chapter 3: FMRI of Motor Activity in Patients with Parkinson's Disease and Healthy Age Matched Control Subjects

Figure 3-1. Maximum and mean estimated head movement associated with right and left hand finger tapping in PD patients and control subjects 93

Figure 3-2. MIP images of activity associated with right and left hand finger tapping from each subject in the PD and controls groups 94

Figure 3-3. The mean spatial extent of activity associated with the right and left hand finger tapping in PD patients and control subjects 96

Figure 3-4. The mean estimated BOLD signal change associated with right and left hand finger tapping in PD patients and control subjects 99

Figure 3-5. Fixed and random effects analysis of activity associated with right and left hand finger tapping across sessions in the group of PD patients 104

Figure 3-6. Fixed and random effects analysis of activity associated with right and left hand finger tapping across sessions in the group of healthy control subjects 105

Figure 3-7. Fixed and random effects analysis of activity associated with right hand finger tapping in the group of PD patients and the group of control subjects 106

Figure 3-8. Fixed and random effects analysis of activity associated with left hand finger tapping in the group of PD patients and the group of control subjects 107

List of Abbreviations

FMRI: functional magnetic resonance imaging

BOLD: blood oxygen level dependent

PD: Parkinson's disease

PET: positron emission tomography

SPECT: single photon emission computed tomography

T: telsa

SMA: supplementary motor cortex

rCBF: regional cerebral blood flow

NMR: nuclear magnetic resonance

MR: magnetic resonance

B_0: applied magnetic field

RF: radiofrequency

T_1: spin-lattice relaxation

T_2: spin-spin relaxation

T_2^*: spin-spin relaxation (due to local magnetic field inhomogeneity)

EPI: echo planar imaging

SPM: statistical parametric mapping

TR: repetition time

TE: echo time

MIP: maximum intensity projection images

I. INTRODUCTION

1.1 General Introduction

Non-invasive functional brain mapping techniques including positron emission tomography (PET) and functional magnetic resonance imaging (fMRI) are widely used to investigate change in neural activity associated with cognition, motor control and sensory stimulation. Although both of these techniques are useful, fMRI is often preferred since does not require the use of contrast agents or radioactive substances and has been shown to have spatial and temporal resolution that is significantly better than those achieved by PET (see Ogawa et al., 1998).

1.2 Experimental Applications of fMRI

1.2.1. FMRI and motor activation

Blood oxygen level dependent (BOLD) contrast fMRI has provided valuable information about many aspects of human motor control (reviewed by Mattay and Weinberger, 1999). Verification of observed fMRI activation through direct motor mapping during surgery (Jack et al., 1994; Puce et al., 1995; Yousry et al., 1995; Pujol et al., 1996, 1998; Tomczak et al., 2000) support the validity of this technique. In addition to identifying the neural regions associated with various movement parameters, fMRI studies can also provide insight into the functional impairments in diseases such as Parkinson's disease (PD). While only two fMRI studies of motor activation in PD have been published to date (Sabatini et al., 2000; Haslinger et al., 2001), the results both support and build upon the findings from previous electrophysiological (Deecke et al., 1977; Dick et al., 1987, 1989), single photon emission tomography (SPECT) (Rascol et

al., 1992, 1994, 1997), and PET (Playford et al., 1992; Jahanashahi et al., 1995; Samuel et al., 1997a) investigations of motor activation in PD.

1.2.2. Pathophysiology of PD

Parkinson's disease is a progressive neurodegenerative disorder that disrupts the synergy of central motor pathways. Specifically, the characteristic symptoms of Parkinson's disease, which include bradykinesia, ridigity and resting tremor have been found to be associated with a diminished supply of the neurotransmitter dopamine (DeLong, 1990). The loss of dopamine in Parkinson's disease originates from the progressive degeneration of dopaminergic neurons in the substantia nigra pars compacta in the midbrain, and resulting overactivity of the internal segment of the globus pallidus (GPi) and subthalamic nucleus (DeLong, 1990). As outlined in Figure 1-1, the GPi is largely inhibitory and projects to the major portions of the thalamus and brainstem through two separate motor circuits within the striatum, the direct and indirect pathways (Alexander and Crutcher, 1990).

The direct pathway in the striatum begins with inhibitory GABAergic projections (co-localized with substance P), from the putamen to the GPi. From the GPi, inhibitory GABAergic projections extend both to the thalamus and the substantia nigra pars reticulata, which in turn projects to the thalamus and brainstem (Alexander and Crutcher, 1990). When the direct pathway is stimulated both by excitatory dopaminergic input from the substantia nigra pars compacta, and excitatory glutamatergic projections from the sensorimotor cerebral cortex, the activity of the GPi is inhibited. This results in disinhibition of thalamic neurons and heightened excitation of precentral motor regions. It is thought that the net effect of this enhanced premotor excitation is the facilitation of

Figure 1-1. *Schematic representation of changes in striatal pathways in Parkinson's Disease*

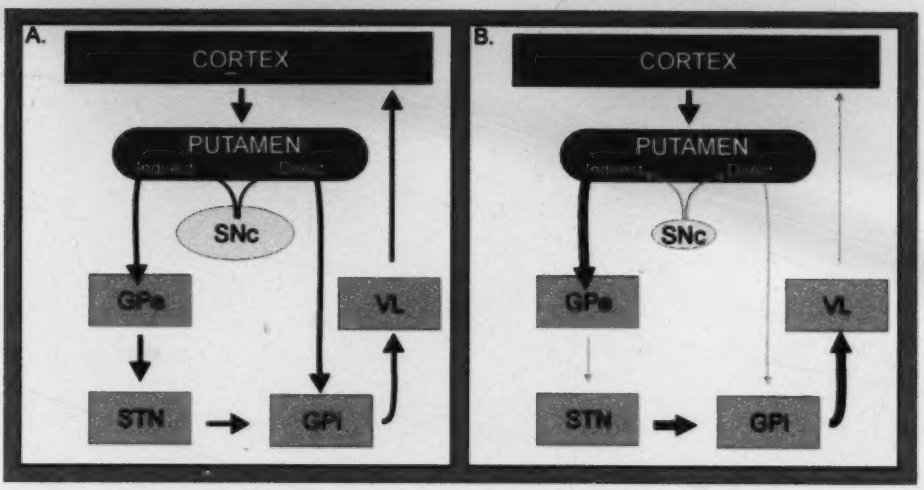

Figure 1-1. Schematic representation of changes in striatal pathways in Parkinson's Disease. (A) In normal striatal circuitry, output from the internal segment of the globus pallidus (GPi) exerts a chronic inhibitory effect on thalamocortical neurons (ventral lateral thalamus, VL). Activation of the direct pathway inhibits firing of the GPi, whereas activation of the indirect pathway (through the external segment of the globus pallidus (GPe) and subthalamic nucleus, STN) stimulates it. Therefore dopamine from the substantia nigra pars compacta (SNc) stimulates the direct and inhibits the indirect pathway. (B) In PD, loss of striatal dopaminergic input secondary to degeneration of SNc neurons diminishes inhibition of the GPi by the direct pathway and increases excitation of the GPi by the indirect pathway. Thus increased GPi output results in excessive inhibition of thalamocortical pathways and subsequent diminished output to cortical motor regions.

cortically initiated movement. Thus, reduced dopaminergic output from the degenerating substantia nigra pars compacta in PD, would limit the disinhibition of the thalamus and interfere with movement initiation (reviewed by Albin et al., 1989).

The indirect pathway in the striatum begins with inhibitory GABAergic projections (co-localized with enkephalin), from the putamen to the external segment of the globus pallidus (GPe). The GPe in turn, sends inhibitory GABAergic projections to the subthalamus. From the subthalamus excitatory glutamatergic projections extend to the GPi (Alexander and Crutcher, 1990). Stimulation of the indirect pathway inhibits the excitatory input from the subthalamus to the GPi, reducing the inhibition from the GPi to the thalamus, thereby facilitating cortical initiation of movement. In PD, reduced dopaminergic innervation from the substantia nigra pars compacta, releases the subthalmic nucleus from its tonic inhibiton by the GPe. This enhances excitatory subthalamic drive to the GPi, leading to increased inhibition of thalamic targets and reduced activity in precentral motor fields. Therefore, impaired dopaminergic input as seen in PD, would both reduce positive feedback from the direct system, and increase the negative feedback from the indirect system (reviewed by Albin et al., 1989).

1.2.3. Supplementary Motor Area (SMA)

While the primary motor area is thought to be predominantly associated with movement execution, there is considerable evidence that supplementary motor area (SMA) is particularly critical for the production planning and preparation of self initiated movements (Brinkman, 1984; Mushiake et al., 1990; Tanji and Shima, 1994; Chen et al., 1995). Self-initiated movement includes both well-learned movement sequences that are initiated from memory, as well as movement that is freely selected. For example,

microelectrode recording studies with non-human primates identified a subset of SMA neurons that responded preferentially during performance of sequences of arm movements that had previously been memorized, as opposed to movements guided by visual cues (Mushiake et al., 1990; Tanji and Shima, 1994). In addition, SMA lesions in non-human primates have also been shown to result in impaired performance of remembered sequences of movements while retaining normal ability for learning new motor sequences using external visual cues (Brinkman, 1984; Chen et al., 1995).

1.2.4. Impaired SMA activity in PD

The role of the SMA in PD is of particular interest, as this region is significantly affected by input from the striatum, and the motor impairments of patients with SMA lesions are known to be similar to those associated with PD (Laplane et al., 1977; Dick et al., 1986; Gentilucci et al., 2000). These motor impairments include difficulty executing self-initiated movements, while movement that is guided by sensory cues typically remains relatively unaffected (Benecke et al., 1997; Georgiou et al., 1994). Indeed, electrophysiological studies demonstrated that the amplitude of a scalp recorded electrical potential previously shown to be associated with SMA activity (Deecke et al., 1969; Shibasaki et al., 1980), was lower in patients with PD than in healthy controls during self-initiated movement (Deecke et al., 1977; Dick et al., 1987, 1989).

In one of the earliest functional imaging studies of motor activation in PD, Playford et al., (1992) measured rCBF changes using PET while subjects moved a joystick in trials cued by a regularly paced tone in both 'free' and 'fixed' conditions. In the 'free' condition, subjects were free to move the joystick either forward, backwards, right or left, avoiding repetitive sequences. In the 'fixed' condition, subjects were

instructed to move the joystick forward in every trial. During the 'free' condition, PD patients showed significantly impaired levels of task-related activation in the SMA, anterior cingulate gyrus, dorsolateral prefrontal cortex (DLPFC), and putamen when compared to healthy controls (Playford et al., 1992). In contrast, there was no difference between controls and PD patients in the levels of neural activation during movements in the 'fixed' condition.

Impaired SMA activity in PD has also been reported in patients that were required to select the timing of repetitive movements. In a PET study, Jahanashahi et al., (1995) investigated rCBF changes while subjects repetitively moved the right index finger, either self-paced or paced by an auditory cue. Compared to healthy controls, PD patients showed significantly impaired activation of the SMA, anterior cingulate, putamen, DLPFC, and right parietal cortex, while performing self-paced movements. When the movements were paced by an auditory cue, there were no significant rCBF differences between the control group and PD patients (Jahanashahi et al., 1995). The lack of measured activation differences during finger movements paced by an auditory cue, as well as the fact that both subject groups performed the movements at an average of once every 3 seconds, indicates that factors related to movement execution alone did not affect the results (Jahanashahi et al., 1995).

In summary, the SMA, which receives substantial input from the striatum, has been shown to be selectively impaired in PD patients both when the direction of movement (Playford et al., 1992) and the timing of movement (Jahanashahi et al., 1995) were not guided by external cues. When external cues were provided, PD patients

exhibited both relatively normal patterns of neural activation and motor ability (Playford et al., 1992; Jahanashahi et al., 1995).

1.2.5. Functional dissociation of rostral and caudal SMA

Although PET studies have clearly established the relative hypoactivity of the SMA in PD, SMA was shown to be comprised of two anatomically and functionally distinct regions. A dissociation between the rostral SMA, which is located anterior to the anterior commissure (AC), and the caudal SMA, located posterior to the AC, has been described both in primates (Matsuzaka et al., 1992; Rizzolatti et al., 1996), and in humans using both PET (Deiber et al., 1991, 1996, 1998) and fMRI (Tyszka et al., 1994; Humberstone et al., 1997; Van Oostende et al., 1997; Boecker et al., 1998; Samuel et al., 1998; Deiber et al., 1999; Lee et al., 1999).

Anatomical studies found that while the caudal SMA is closely linked with the primary motor cortex, the rostral SMA has been shown to be interconnected with several cortical regions including the basal ganglia, anterior cingulate cortex, dorsolateral prefrontal cortex, lateral premotor cortex and posterior parietal regions (Luppino et al., 1993). This is consistent with reports that the rostral SMA is involved more with the planning and preparation for movement, while the caudal SMA is associated more with movement execution. For example, greater activation was detected in the rostral SMA both during self-initiated movement (Deiber et al., 1991, 1996, 1999; Humberstone et al., 1997; Van Oostende et al., 1997; Boecker et al., 1998), and during movement that was simply imagined and not actually performed (Tyszka et al., 1994; Dieber et al., 1998).

In a more recent fMRI study of the temporal nature of activity in the SMA, Lee et al., (1999) demonstrated that the rostral SMA was activated during the preparation of movement, while the caudal SMA was active more during the execution phase of the task. Similarly, Samuel et al., (1998) reported that while the rostral SMA was highly active during the early stage of the motor task, this activity decreased during repetitive execution of the movement. Consistent with both the pathophysiology and the motor impairments in PD, fMRI studies have more precisely localized impaired motor activation in PD to the rostral SMA (Sabatini et al., 2000; Haslinger et al., 2001).

1.2.6. SMA activation following medication and surgery in PD

Functional imaging studies have also provided insight into the effect of various pharmacological or surgical treatments in PD. SPECT (Rascol et al., 1992) and PET (Jenkins et al., 1992) studies demonstrated improved motor performance and normalization of impaired SMA activity during self-directed voluntary movement in PD patients following subcutaneous administration of a dopamine agonist, apomorphine. Normalization of SMA activation has also been reported following an oral dose of the dopaminergic medication levodopa, both in PD patients who were previously non-treated and those who had been receiving levodopa (Rascol et al., 1994; Haslinger et al., 2001). Similar results have been demonstrated in PD patients who underwent surgical procedures to restore striatal output. Impaired SMA activity in patients with PD has been shown to improve following pallidotomy (Ceballos-Baumann et al., 1994; Grafton et al., 1995; Samuel et al., 1997b), stimulation of the subthalamic nucleus (Davis et al., 1997; Ceballos-Baumann et al., 1999), and fetal tissue neurotransplantation (Bluml et al., 1999; Piccini et al., 2000).

Impaired activation of the SMA during self-directed voluntary movement in PD patients (Playford et al., 1992; Jahanashahi et al.,1995; Sabatini et al., 2000; Haslinger et al., 2001), and the normalization of SMA activation following dopaminergic medication (Jenkins et al., 1992; Rascol et al., 1992; 1994; Haslinger et al., 2001), or surgical treatment (Ceballos-Baumann et al., 1994; 1999; Grafton et al., 1995; Samuel et al., 1997b; Davis et al., 1997; Bluml et al., 1999; Piccini et al., 2000), provides compelling evidence that in contrast to movements that are determined by external cues, the SMA is critical for self-directed movement.

1.2.7. Lateral premotor pathways in PD

While many studies have demonstrated that SMA is important for self-directed movement (Brinkman, 1984; Mushiake et al., 1990; Tanji and Shima, 1994; Chen et al., 1995), microelectrode recordings from cells in the lateral premotor cortex in non-human primates have revealed that approximately half of the premotor neurons increase their activity preferentially or exclusively in relation to movements made in response to visual cues (Godschalk et al., 1981; Halsband et al., 1994). Removal of the lateral prefrontal cortex in non-human primates results in impaired ability to perform movements that are visually cued, while the ability to perform remembered movement sequences remains intact (Petrides, 1982; Passingham, 1985). The lateral premotor cortex is thus primarily involved in the control of movements that are guided by external cues.

The lateral premotor cortex is ideally situated to process sensory guided movement. The major source of input to the lateral premotor cortex is the cerebellum which receives somatosensory input from muscle spindles and tendon receptors, and information about visual location and motion through the pons from parietal area 7 and

area V5 (Schell and Strick, 1984; Stein and Glickstein, 1992). The lateral premotor also receives input from the inferior and superior parietal association areas. However, although the parietal association cortex also has connections with the SMA, and prefrontal cortex, it does not receive input from the striatum (Pandya and Yeterian, 1985). Activation of the lateral premotor cortex through either cerebellar or parietal regions should therefore be unaffected by striatal impairment in PD.

As expected, there is no evidence of impaired activity in the cerebellum, parietal or lateral premotor regions in PD patients. However, more recent functional imaging studies have revealed that these regions may contribute to functional compensation in PD. In addition to impaired SMA activity, there are now reports of diffuse cortical overactivity in PD patients during performance of self-initiated sequential movements (Samuel et al., 1997a; Sabatini et al., 2000; Haslinger et al., 2001).

1.2.8. Increased cortical activity in PD

A number of regions have been shown to be significantly more activated during self-initiated movement in PD patients compared to healthy control subjects. Using SPECT, increased cerebellar activity was reported during performance of a pre-learned sequence of finger movements in non-medicated patients, relative to both patients tested while on medication, and healthy control subjects (Rascol et al., 1997). Samuel and colleagues (1997a) also demonstrated using PET, that along with the expected impaired activation of SMA, the lateral premotor cortex and inferior parietal areas were significantly overactive bilaterally during performance of a pre-learned sequence of finger movements in PD patients compared to healthy controls (Samuel et al., 1997a). There were no significant differences in the mean motor response times or the error rates

between the control subjects and PD patients groups in these studies, indicating that performance factors alone did not affect the results.

In the first published fMRI study of PD, Sabatini et al. (2000) reported that in addition to relatively impaired activity of the rostral SMA, PD patients exhibited significantly increased activation bilaterally in the primary sensorimotor cortex, lateral premotor cortex, inferior parietal cortex, caudal SMA, and anterior cingulate cortex during performance of a pre-learned sequence of finger movements. A similar pattern of impaired rostral SMA activity, with more widespread cortical hyperactivity bilaterally, was also observed in PD patients while performing joystick movements in freely selected directions (Haslinger et al., 2001). In addition, Haslinger et al. (2001) confirmed that both the hypo- and hyperactivity partially recovered to normal levels in patients with PD following a single dose of levodopa.

It has been proposed that heightened cortical activity in PD during movement is associated with functional compensation for impaired striatal motor pathways in PD patients (Rascol et al., 1997; Samuel et al., 1997a; Sabatini et al., 2000; Haslinger et al., 2001). This idea is largely based upon functional imaging studies of patients recovering from stroke which suggested that the motor system has the capacity to reorganize (Chollet et al., 1991; Weiller et al., 1993; Cramer et al., 1997; Cao et al., 1998; Pineiro et al., 2001). Overall, it is evident that understanding how various components of the motor system are affected in PD using fMRI, will be increasingly useful for evaluating and optimizing pharmacological and surgical treatment options for patients with PD.

1.3. Basic Principles of Nuclear Magnetic Resonance Imaging

The basic principles of nuclear magnetic resonance (NMR) imaging that will be discussed throughout this section have been recently reviewed (Bushong, 1996; Brown and Semelka, 1999; Haacke, 1999; Zimmerman et al., 2000), and will be briefly summarized below.

1.3.1. *Nuclear spin and alignment*

NMR imaging is a technique that relies on the properties of nuclear spin in the presence of an external magnetic field. A small magnetic dipole moment is present in nuclei with either an odd number of protons or neutrons. These nuclei therefore behave like tiny magnets, and are thus susceptible to the forces of other magnetic fields. Although several different types of atoms exhibit this phenomenon, standard NMR imaging of human soft tissue is based on the single proton of the hydrogen atom (^{1}H), which is abundant in the human body and exhibits a strong magnetic moment.

In the absence of an external magnetic field, the phase of the individual magnetic dipoles of the nuclei in a sample will be randomly oriented producing a net magnetic moment of zero (Figure 1-2a). However, in the presence of a large external magnetic field (B_0), the magnetic dipoles of the individual nuclei will orient either parallel (low energy state) or anti-parallel (high energy state) to the magnetization of the of the applied field. At any given time, a slightly greater proportion of the magnetic dipoles of the nuclei will be oriented parallel to the applied magnetic field. The combined magnetization of the individual nuclei is additive, with the vector of net magnetization aligned parallel to the applied field (Figure 1-2b).

When discussing NMR, magnetization is conventionally described using a three dimensional coordinate system in which the z axis is represented along the vertical direction, the x axis is represented along the horizontal axis, and the axis oriented perpendicular to the xz plane is labeled as the y axis. Within this coordinate system, the vector of the applied static magnetic field (B_0) is located along the vertically oriented z axis. The z axis is also referred to as the longitudinal axis, while the xy plane is referred to as the transverse plane.

In standard MR imaging the external magnetic field is produced from a large superconducting magnet. The strength of the magnetic field is measured in units of tesla (T), where 1 T is equal to 10 000 gauss (the magnetic field of the earth is about 0.5 gauss). Standard clinical scanners operate at 1.5 T; however many research centres are now using higher field strength magnets. While the strength of the external magnetic field ultimately determines the magnetization of tissue, the degree to which tissue acquires magnetization, referred to as the tissue's magnetic susceptibility, varies in different types of tissue.

1.3.2. Nuclear spin resonance and radiofrequency excitation

In addition to the alignment of the magnetic moments of individual nuclei and the magnetization of a sample, force from the external magnetic field will transform some of the angular momentum of the continual motion of nuclei into precessional, or rotational motion. The nuclei will therefore also precess around the axis of the external magnetic field, at a frequency referred to as the Larmor frequency. The Larmor frequency, symbolized by ω_o (omega), is proportional to the applied magnetic field with

Figure 1-2. *Proton alignment, precession, and excitation*

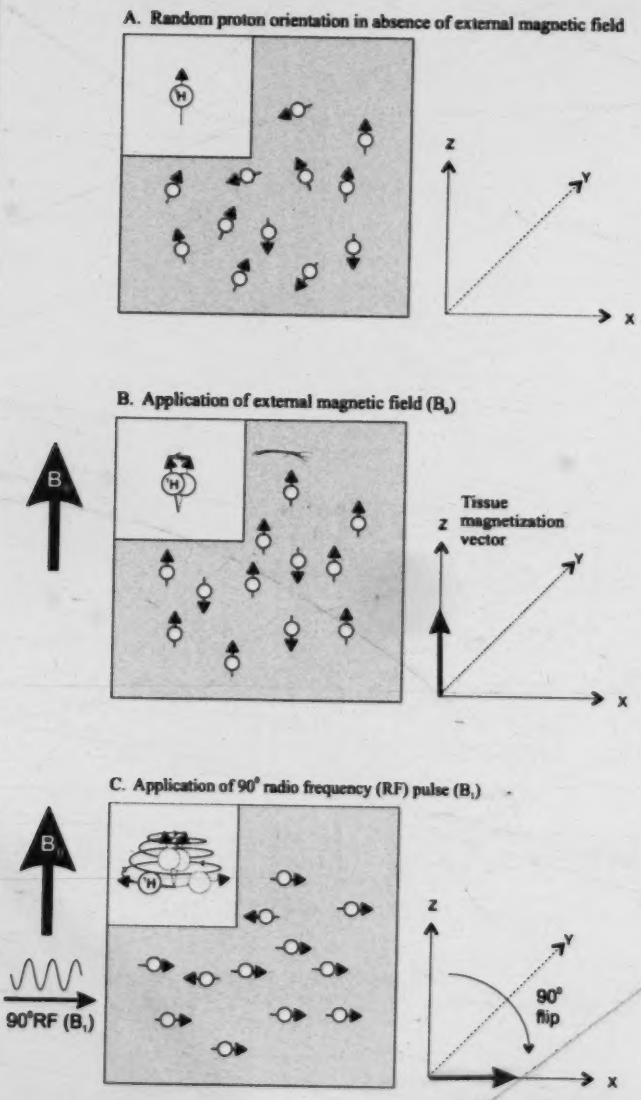

Figure 1-2. In the absence of an external magnetic field the small magnetic dipoles of individual nuclei in tissue, such as the single proton of the hydrogen atom as shown in the corner inset, are oriented randomly (A). In the presence of an external magnetic field (B_o), the dipoles of the individual protons become aligned with B_o and as shown in the corner inset precess around the z axis. The dipoles of individual protons therefore summate creating a net tissue magnetization vector along the longitudinal plane (z axis) (B). Following the application of a 90° radiofrequency magnetic pulse (B_1) that is oriented at a right angle to B_o, as shown in the corner inset the angle of proton precession increases through to the xy, or transverse plane, which flips the net tissue magnetization vector into the transverse plane (C).

a proportionality constant termed the gyromagnetic ratio (γ) which is unique for each nucleus, i.e. $\omega_o = \gamma B_o$. For example, the gyromagnetic ratio of hydrogen protons is 42 MHz/Tesla. In the presence of an external magnetic field, hydrogen protons will therefore precess at a frequency of 42 MHz/Tesla.

The fact that the precessional frequency of each type of atom is known is essential for NMR. The observed MR signal is induced by disrupting longitudinal magnetization by briefly applying an oscillating magnetic field (B_1) that is typically oriented along the plane perpendicular to B_0. The oscillating magnetic field used in standard ^1H MR imaging is a pulse of radiofrequency (RF) energy that oscillates at a frequency equal to the precessional frequency of the hydrogen proton. Since the oscillations of the RF pulse and the precessional frequency of the hydrogen nuclei are in resonance, energy from the RF pulse will be absorbed by the nuclei. As the precessing protons (also referred to as spins) become excited by this energy, the precessional angle of the net longitudinal magnetization of the sample increases (Figure 1-2c). If the RF energy is strong enough, the net longitudinal magnetization will actually rotate away from B_0 into the transverse (xy) plane. Because the magnetic field produced along the transverse plane is oscillating it will induce an alternating current in a radio receiver antenna. The current induced in the receiving coil is proportional to the magnetization in the transverse plane and is the basis for the MR signal that is used to generate images.

1.3.3. MR signal and spin relaxation

Although immediately after the brief RF pulse protons will be precessing at the same frequency and phase along the transverse plane, giving rise to a strong MR signal, the excitation energy will gradually dissipate. The net transverse magnetization, which is

the source of the MR signal, diminishes as the excitation energy dissipates and the phase of the spins become dispersed throughout the transverse plane. As the phase of the spins become dispersed throughout the xy plane, transverse magnetization diminishes until the point when the phase of spins become evenly distributed and net transverse magnetization reaches zero. The exponential loss of transverse magnetization that is measured over time is referred to as the free induction decay (FID).

Due to the continuous presence of the static magnetic field B_0 along the z axis, the spins of protons will gradually return to an equilibrium state aligned with B_0. The recovery of longitudinal magnetization associated with the return of spins from a high energy excited state to a low energy state along the z-axis is referred to as relaxation. There are two main components to spin relaxation, T_1 and T_2 relaxation.

T_1 is a time constant characterizing the recovery of longitudinal magnetization along the z-axis. More specifically, T_1 is defined as the time required for 63% of the MR signal elicited from nuclei that are excited in a state of high-energy expenditure to relax or return to a low-energy state at equilibrium with the external magnetic field (Figure 1-3b). T_1 relaxation is mediated by the loss of energy from excited proton spins to the surrounding macromolecule lattice. Since T_1 relaxation is mediated by the transfer of energy between spins and the surrounding lattice of macromolecules, it is also often referred to as spin-lattice relaxation.

In contrast to T_1 relaxation which characterizes the recovery of longitudinal magnetization, T_2 relaxation describes the decay of transverse magnetization and is therefore defined accordingly as the time required for transverse magnetization to reach 37% of its initial magnetization (Figure 1-3a). While T_1 processes are associated with

the transfer of energy from excited protons to the lattice of macromolecules in the surrounding environment, T_2 relaxation is associated with the transfer of energy between the spins of excited protons and thus is also referred to as spin-spin relaxation. This transfer in energy is due to both small intermolecular and intramolecular interactions as well as small inhomogeneities in local magnetic field. Phase dispersion or decay of transverse signal associated with the presence of local magnetic field inhomogeneity is referred to more specifically as T_2^*, and will be discussed in later sections of this introduction.

Both T_1 and T_2 relaxation rates depend on the concentration of proteins and other macromolecules in an image voxel. Any differences in the strength of the MR signal acquired at a pre-determined time point are therefore attributed to the specific characteristics of the soft tissue. For example, in tissue such as brain white matter, interactions between protons, lipid membranes and intracellular organelles facilitate the dephasing of the nuclear spins which thereby enhances the rate at which longitudinal magnetization recovers. Similarly, as the amount of free water increases (i.e., inflamed, edematous tissue) both T_1 and T_2 relaxation times increase. Differences in T_1 and T_2 relaxation therefore provide a valuable source of contrast in MR images.

While both T_1 and T_2 relaxation processes are important aspects of the NMR phenomenon, the imaging parameters that are chosen for data acquisition determine which relaxation process dominates the observed signal contrast. The most important imaging feature is the length of time between the application of the RF pulse and the acquisition of the MR signal, which is referred to as the echo time (TE). Initially following the RF pulse, the MR signal is dominated by T_2 relaxation processes as energy

Figure 1-3. *T_2 decay of transverse magnetization and T_1 recovery of longitudinal magnetization*

A. T_2 Decay Curve

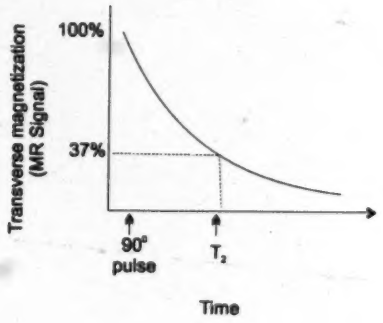

B. T_1 Recovery of Longitudinal Magnetization

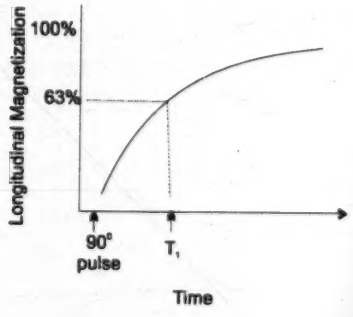

Figure 1-3. Transverse magnetization (MR signal) decays exponentially due to the loss of phase coherence among protons after the 90° rf pulse, while longitudinal magnetization recovers as proton spins realign parallel to B_0. Specifically, T_2 represents the time required for transverse magnetization to decay to 37% of its initial value (A), while T_1 is defined as the time required for 63% of longitudinal magnetization to recover (B).

is transferred between nuclei. Due to this small transfer of energy between nuclei, the precessional frequency of the protons will eventually begin to vary. Since energy cannot be transferred between items that are not precessing in resonance, T_1 processes gradually dominate as the energy is given up to the surrounding macromolecular lattice and net magnetization of the sample returns to alignment with the static applied magnetic field. T_2 relaxation times are therefore always shorter than T_1 times.

1.3.4. Spatial encoding

Spatial encoding is required to localize the MR signal in three dimensions. Spatial encoding is elicited using three separate orthogonal coils that are positioned along each axis within the bore of the magnet. When current is passed through these coils they generate small magnetic fields that are added to the main magnetic field. In contrast to the larger applied magnetic field, which produces a relatively uniform magnetic field, these coils are specifically designed to generate a linearly varying magnetic field gradient so that the strength of the magnetic field along each axis will become position dependent. Since the precessional frequency of nuclei is dependent on magnetic field strength, the precessional frequency of protons within an imaging voxel will also vary depending on their position along the applied gradient.

The first spatial encoding step in conventional imaging is achieved by applying a RF pulse that will selectively excite a narrow range of frequencies (Figure 1-4a). In the presence of a linear field gradient only a select region along the gradient will be excited by this RF pulse. Following slice selective excitation, applied along the z axis, phase encoding is implemented along an orthogonal axis (i.e., y axis). Phase encoding is

Figure 1-4. *Spatial encoding of magnetic resonance images*

A. Selective slice selection

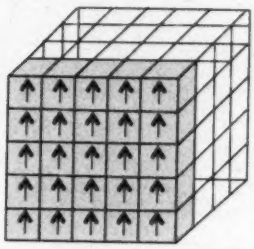

B. Phase encoding

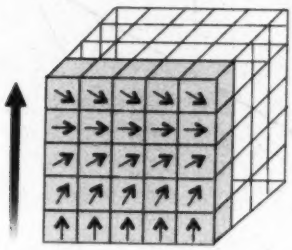

C. Frequency encoding

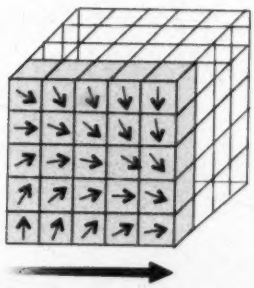

Figure 1-4. Spatial information in MR images is encoded through the application of separate magnetic field gradients along each of the three axes. First, a slice selective rf pulse is applied to define the image plane, in which initially all spins at all locations precess at the same frequency (A). A phase encoding pulse is then applied along an orthogonal axis which produces a spatial variation in spin precessional frequency. This results in spatial variations in the phase of spins as spins that were precessing at faster frequency acquire a phase lead which remains even after the gradient is turned off and spins once again precess at the same frequency (B). Finally, another magnetic field gradient is applied along the remaining axis as the signal is recorded. This results in frequency encoding along that axis (C).

achieved by briefly applying a field gradient that produces spatial variations in the frequency of precession. When the gradient is turned off, the spins will again precess at the same frequency. However, spins that were precessing faster when the gradient was turned on, will have acquired a phase lead compared to more slowly precessing spins. The phase of nuclei that were precessing faster, will therefore be located at a different location than nuclei that were precessing at slower frequencies. Conceptually, phase encoding along the y-axis would divide each selectively excited slice into horizontal rows of voxels that are each identifiable by a particular spin phase (Figure 1-4b).

Along the other spatial axis a frequency encoding gradient is applied. Since this gradient is applied during sampling of the MR signal, it is often referred to as the readout gradient. The readout gradient, which systematically varies the frequency of the spins along the x-axis during the acquisition of the signal, thereby further encodes the selectively excited slice into vertical columns (Figure 1-4c). In combination with the previous phase encoding step, the signal detected at each location within imaging space will then be encoded with a unique combination of phase and frequency. This information is used to assign the MR signal to the corresponding spatial location during image reconstruction.

1.3.5. Spin echo and gradient echo imaging

Despite attempts to improve the uniformity of the external magnetic field, most physiological samples will still have regions of local magnetic field inhomogeneity. Since the precessional frequency of spins is associated with the strength of the magnetic field, variations in the field will be associated with the loss of phase coherence among

spins and the rapid decay of signal. Spin dephasing associated with small magnetic field inhomogenieties is specifically referred to as T_2^* relaxation.

The application of a refocusing pulse that is of sufficient strength to rotate the spins 180° around the transverse plane will essentially reverse the relative phase of spins. For example, the phase of spins that were precessing at a faster frequency, will now lag behind the phase of spins that were precessing at a slower frequency. However, since the relative frequency of precession has not changed, following the 180° pulse the phase of spins that were precessing at a faster frequency will eventually catch up to more slowly precessing spins. As the spins become re-phased, the magnetization of the individual nuclei once again summate resulting in a sharp recovery of transverse magnetization called a spin echo (Figure 1-5). The 180° pulse therefore minimizes the phase dispersal associated with local magnetic field inhomogeneities (T_2^* relaxation). In addition to eliminating the potentially serious loss of signal, spin echo sequences also ensure that the sampled MR signal is sensitive to anatomy, irrespective of magnetic field uniformity.

While spin echo imaging is based on the brief application of a 180° RF pulse, gradient echo imaging sequences refocus spins by reversing the direction of the applied field gradients. When the gradient directions are reversed, the spins that were in a high field will now be in low field and vice versa. As the relative frequency of spins will also be reversed, spins will eventually rephase, thereby producing an increase in signal similar to a spin echo. For example, spins that were initially precessing at a relatively fast rate, will precess at a relatively slow rate following gradient reversal. This allows

Figure 1-5. *Spin echo formation following 180° RF pulse*

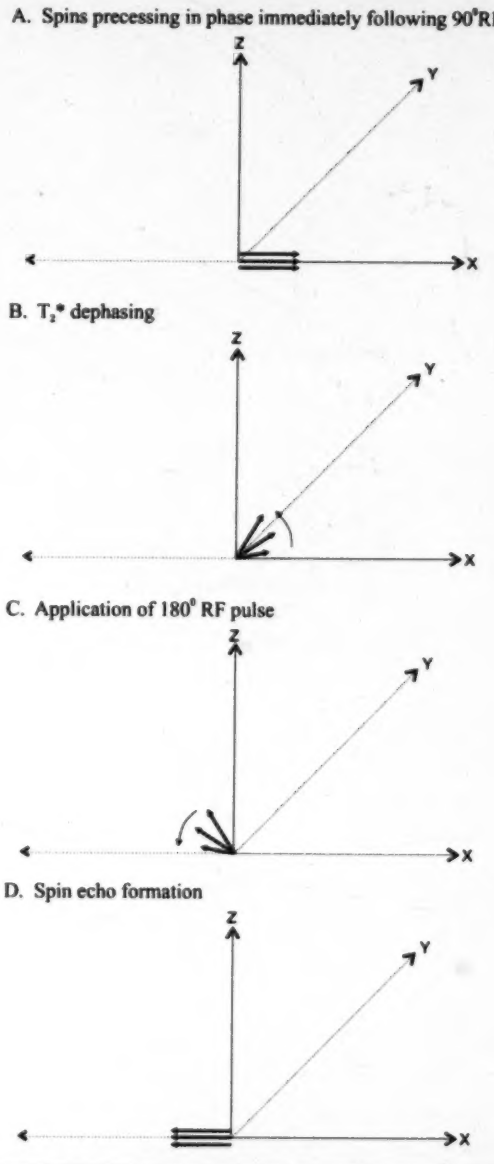

Figure 1-5. Immediately following the 90° RF pulse, spins will be precessing in phase at the same frequency(A). Eventually, the precessional frequency of spins will vary (shorter lines represent spins precessing at a slower frequency), and the phase of spins will become dispersed throughout the xy plane (B). The application of a 180° RF pulse will rotate the phase of spins across the xy plane. As a result, the relative phases of fast and slowly precessing spins are reversed (C). Phase of faster precessing spins will therefore eventually "catch up" with the more slowly precessing spins. As the spins become re-phased, the magnetization of the individual nuclei once again summate resulting in a sharp recovery of transverse magnetization called a spin echo (D).

the phase of spins that were previously lagging behind to catch up. Unlike spin echo imaging, in the presence of gradient reversal the observed MR signal is still dominated by local magnetic field inhomogeneities. Sensitivity to local magnetic field inhomogeneity is particularly important for certain types of imaging including Blood Oxygen Level Dependent (BOLD) fMRI.

1.4 Basic principles of Blood Oxygen Level Dependent (BOLD) fMRI

The basic principles of blood oxygen level dependent (BOLD) fMRI that will be briefly summarized in this section have been described in a number of comprehensive reviews (Posse et al., 1996; Forster et al., 1998; Ogawa et al., 1998; Raichle, 1998; Turner et al., 1998; DiSalle et al., 1999). In contrast to standard anatomical MR imaging which often depend on spin echo to minimize signal loss associated with T_2^* processes, highly localized magnetic field inhomogeneities associated with the presence of paramagnetic substances in the blood can provide a valuable source of contrast in functional MR images. This is due to the fact that the MR signal in images sensitive to T_2^*, will decrease as the relative concentration of a paramagnetic contrast agent increases. This T_2^* effect was first described in studies of laboratory animals which showed that the non-toxic exogenous contrast agent gadolinium could be tracked as it flowed throughout the cerebral vasculature (Villringer et al., 1986; Belliveau, 1988).

In 1991, Belliveau and colleagues published a study that looked at functional activity in humans using T_2^* weighted imaging to track an exogenous contrast agent in the visual cortex. In this study, subjects viewed a visual stimulus while a bolus of gadolinium was injected intravenously. The passage of the contrast agent through the visual cortex was monitored by repeatedly acquiring single slice images of the region.

The relative increase in blood volume associated with visual stimulation was estimated by comparing the intensity of the MR signal observed during visual stimulation to the signal observed during a control period. The results showed that blood volume increased up to 30 percent in the primary visual cortex.

In an important development in the field of functional imaging, Ogawa et al. (1990a, 1990b), and Turner et al. (1991), demonstrated that T_2^* relaxation and the amplitude of MR signal could be altered in animals simply by inducing changes in the oxygenation state of the blood. Changes in the MR signal associated with blood oxygenation, referred to as blood oxygen level dependent (BOLD) contrast, is directly related to the relative concentration of deoxyhemoglobin. Unlike oxyhemoglobin which is diamagnetic and has almost the same magnetic susceptibility as the surrounding cerebral tissue, deoxyhemoglobin is more paramagnetic and therefore acts like an endogenous contrast agent (Pauling and Coryell, 1936; Ogawa and Lee, 1990; Ogawa et al., 1990a, 1990b). Therefore, as the relative concentration of deoxyhemoglobin increases, local T_2^* relaxation is enhanced and the intensity of the observed MR signal decreases. In contrast, an increase in the MR signal is indicative of a relative decrease in the concentration of deoxyhemoglobin (Ogawa and Lee, 1990; Ogawa et al., 1990a; 1990b).

The first published reports of the use of BOLD contrast fMRI in humans showed that the MR signal in the visual cortex increased significantly during photic stimulation (Kwong et al., 1992; Ogawa et al., 1992). Following these initial investigations, BOLD contrast fMRI has proven to be an effective non-invasive method for tracking changes in blood flow and oxygenation during cognitive activity or stimulation in humans. The

change in deoxyhemoglobin during neural stimulation is thought to result from the uncoupling of local blood flow and oxygen utilization. Perhaps the most widely cited evidence for this is a PET study of visual activation which demonstrated that while local blood flow and glucose utilization increased in active regions by more than 50%, oxygen consumption increased only by about 5% (Fox et al., 1986). The large influx of richly oxygenated blood into vessels surrounding active neurons combined with only a small increase in oxygen extraction, results in a decline in the relative concentration of deoxyhemoglobin in stimulated brain regions. As a result, T_2* relaxation is delayed, and the intensity of the MR signal sampled from voxels in the region surrounding active neurons will be increased relative to the signal measured during a control period (Kwong et al., 1992; Ogawa et al., 1992; Turner et al., 1993)

1.5. Reliability of fMRI

Reliability, defined as the extent to which a test yields the same result on repeated trials, is essential for the useful interpretation functional neuroimaging studies. Reproducibility across sessions may be particularly important due to the potential clinical research applications that may include comparing patients before and after treatment, or under different experimentally controlled conditions. To date, most reliability studies have focussed on quantifying test-retest reproducibility (Ramsey et al., 1996; Yetkin et al., 1996; Rombouts et al., 1997, 1998; Miki et al., 2000).

1.5.1. Reproducibility of size and location of fMRI activation

Ratios of test-retest reproducibility have been used to describe the relative consistency of data acquired from two trials under identical conditions. For example, Rombouts et al., (1997) devised a ratio to assess the test-retest reproducibility of the

overall number of active voxels throughout the whole brain (difference in number of activated voxels from two sessions, to the total number of voxels activated in either session). The reproducibility of the exact voxel coordinates from two test sessions was evaluated using a similar ratio (the number of voxels that were active during both the first and second trials, to the total number of voxels classified as active in either trial) (Rombouts et al., 1997). These reproducibility ratios have been used to describe the reproducibility of activation detected in trials within the same session, and in separate sessions. For example, in a test-retest study with a sequential motor task, the average extent of voxel coordinate overlap within the sensorimotor area was only about 20% across sessions, and 29.5% within the same session (Ramsey et al., 1996).

Test-retest reproducibility ratios have shown that the size of activation is more consistent than the precise location of the activity during visual stimulation (Rombouts et al., 1997, 1998; Miki et al., 2000). However, since the hemodynamic response associated with BOLD contrast fMRI is not a discrete response, it is reasonable to expect that the precise voxel coordinates will vary to some degree. In fact, Yetkin et al., (1996) confirmed that while the precise overlap of voxel coordinates associated with a repetitive motor task and visual stimulation were quite inconsistent, each iteration of a task usually activated voxels located in the same anatomical region of the brain.

1.5.2. Regional patterns of variability

Changes detected with fMRI in the primary sensorimotor cortex have been repeatedly shown to be more consistent than those detected in secondary motor regions. Mattay et al., (1996) measured the relative proportion of voxels that were activated in subjects who performed a pre-learned sequence of finger movements during three

identical trials in one scanning session. The relative proportion of voxels that were activated during all three trials was 70% in the primary sensorimotor cortex, 60% in SMA, 55% in cerebellum, 22% in premotor cortex, and 44% in parietal cortex.

In a more recent study, Scholz et al., (2000) assessed both within and between subject variability of motor activity in the basal ganglia, motor cortex, and SMA. Twenty-two subjects each performed specific motor tasks (self-paced alternating finger tapping and toe wiggling, writing, cued finger tapping, forearm pronation/ supination, and saccadic eye movements) on two occasions. The mean percent deviation between subjects (the standard deviation of the number of activated voxels divided by the total number of activated voxels) over all of the motor tasks was substantially smaller in the primary motor cortex (23%) than the SMA (55.1%), or basal ganglia (56.6%). As expected, the mean percent deviations within subjects were significantly smaller than between subjects, decreasing substantially to 7.2% in the motor cortex, 21.5% in the SMA, and 26.4% in the basal ganglia. Alternating finger and toe movements were associated with the least overall variability while the forearm pronation task was associated with the most variability.

Reproducibility maps, in which a value is assigned to each voxel that represents the number of experiments or scanning sessions in which that voxel was classified as active, have also been used to provide an indication of the regional reproducibility of activation. This was demonstrated in an elegant study by Tegeler et al. (1999) who produced reproducibility maps from eight subjects who performed a sequence of finger movements three times in a single scanning session. Each voxel in the reproducibility map was assigned a value from 1 to 3 (1 = non-reproducible voxels active only in a

single run, 2 = moderately reproducible voxels active in two runs, and 3 = highly reproducible voxels active in all three runs). Highly reproducible voxels were found in the sensorimotor cortex, SMA and the cerebellum. Moderately reproducible activity was primarily located in the regions surrounding highly reproducible voxels. Overall, while motion correction increased the proportion of highly reproducible voxels in all regions of the brain, the location and number of active voxels in the primary sensorimotor cortex were most reproducible, followed by the cerebellum, and finally the SMA.

The fact that the primary sensorimotor cortex was more consistently active than subcortical or premotor regions during all types of motor tasks, is not surprising given the dominant role of this region in the control of voluntary movement. Furthermore, the BOLD responses observed in primary cortical regions are typically more robust than that from secondary or subcortical structures.

1.5.3. Probabilistic models of variance

While BOLD contrast fMRI is sensitive to blood flow and oxygen utilization associated with neuronal stimulation, the actual activity of individual neurons cannot be measured non-invasively. Since the true neuronal activity associated with the BOLD contrast signal is unknown, it is difficult to model the true probability of variability in fMRI. While several studies have developed unique statistical models to address this problem (Genovese et al., 1997; Noll et al., 1997; and Huu Le and Hu, 1997), these paradigms are too specialized for a typical imaging laboratory to implement on a regular basis. For example, Genovese et al., (1997) and Noll et al., (1997) modeled true neuronal activation using a receiver operator curve which was used to classify each voxel as i) either truly active or truly inactive, and ii) classified active or classified inactive.

Reliability was assessed by estimating the probability that a truly active voxel is classified active, and the probability that a truly inactive voxel is classified active, to assess the number of voxels that were truly activated. It is unclear however, if and how this statistical model would account for the natural physiological fluctuations in human subjects.

1.5.4. Random effects analysis

An alternative to describing and quantifying variability in fMRI data, is to implement analyses that are highly sensitive to variability in the data. Indeed, random effects analysis is considered an optimal method of summarizing multisubject or multisession fMRI data (Holmes et al., 1998), and has been used as an indication of the overall reliability of activation (McGonigle et al, 2000).

Traditional fixed effects analysis of fMRI is based on a single error component that models the variance of the BOLD response within the session or time series (Friston et al., 1995). This is effective for a single subject analysis since scan to scan variance is the only source of variance. However, when multiple subjects are analyzed, the BOLD responses from each subject are simply averaged together to create one time series that summarizes the data from the group. Although the data now includes both scan to scan variance and between subject variance, the analysis is only sensitive to within-session variance (Friston et al., 1995). While a fixed effects analysis effectively assesses the average activity within a group, the results could be biased by signal that is atypical of the group. For example, an unusually strong response in one session or within one subject may dominate the average response across sessions. Therefore, the average

response at that voxel would not be indicative of the typical or consistent activity of the group (Holmes et al., 1998; McGonigle et al., 2000).

In contrast, random effects analysis of a multisubject or multisession fMRI data set, models both within-session and between-session components of variance. Random effects analysis is therefore particularly sensitive to the consistency of responses within a fMRI data set (Holmes et al., 1998). Therefore, if the results from a group of subjects were completely inconsistent and unreliable, random effects analysis would show that there were no significantly active voxels within that data set. A recent study compared the results from fixed effect and random effect analysis of 33 fMRI sessions, and demonstrated that many voxels that showed an average activation response did not survive a random effects analysis (McGonigle et al., 2000). Random effects analysis thus appears to be a meaningful and practical means of evaluating the consistency of data across multiple subjects or sessions.

1.6. General summary & research objectives

BOLD contrast FMRI has been shown to provide valuable information about changes in brain activation associated with the motor impairments in patients with PD (Sabatini et al., 2000; Haslinger et al., 2001). In addition to confirming the results of earlier PET studies (Playford et al., 1992; Jenkins et al., 1992; Jahanashahi et al., 1995; Samuel et al., 1997a), fMRI studies have provided more detailed localization of relatively increased and decreased motor activity in PD patients (Sabatini et al., 2000; Haslinger et al., 2001). Since the true neuronal activity underlying BOLD contrast cannot be measured non-invasively, studies examining the validity and reliability of fMRI have focused on describing the reproducibility of activation across sessions

(Yetkin et al., 1994; Mattay et al., 1996; Ramsey et al., 1996; Rombouts et al., 1997, 1998; Tegeler et al., 1999; McGonigle et al., 2000; Miki et al., 2000; Scholtz et al., 2000). Indeed, a comprehensive exploration of fMRI data will not only identify potential limitations of an experimental design, but will also facilitate the interpretation of observed activation.

This thesis is comprised of two studies designed to characterize the feasibility of BOLD contrast fMRI at a static magnetic field strength of 3 Tesla (3T), both in healthy volunteers and in patients with early PD. The primary objective of the first study was to describe the reproducibility of BOLD contrast fMRI associated with a repetitive motor task. The results of this study confirmed that BOLD contrast fMRI at 3T is a valid and sensitive tool for localizing cortical activity associated with repetitive movement. In addition, this project demonstrated that there was no difference in the reproducibility of data acquired from multiple subjects and data acquired from a single subject tested repeatedly.

The primary objective of the second study was to compare cortical activity detected using BOLD contrast fMRI at 3T in patients with early PD and age-matched control subjects. The results demonstrated that consistent differences between PD patients and control subjects can be detected using a repetitive motor task. While the random effects analysis was inconclusive in the second project due to the low number of subjects, in both studies comparisons of the independent subject data to the results of fixed effects and random effects analyses, indicated that the average group response may not be representative of typical activity across subjects and sessions.

1.7. References

Albin RL, Young AB, Penney JB. The functional anatomy of basal ganglia disorders. Trends Neurosci 1989; 12: 366-75.

Alexander GE, Crutcher MD. Functional architecture of basal ganglia circuits; neuronal substrates of parallel processing. Trends Neurosci 1990; 13: 266-71.

Belliveau JW. Real time proton susceptibility contrast imaging of cerebral physiology. Proc Soc Magn Reson Med 1988; p.222.

Belliveau JW, Kennedy DN, McKinstry RC, Buchbinder BR, Weisskoff RM, Cohen MS, Vevea JM, Brady TJ, Rosen BR. Functional mapping of the human visual cortex by magnetic resonance imaging. Science 1991; 254: 716-19.

Benecke R, Rothwell JC, Dick JPR, Day BL, Marsden CD. Disturbance of sequential movements in patients with Parkinson's disease. Brain 1987; 110: 361-79.

Bluml S, Kopyov O, Jacques S, Ross BD. Activation of neurotransplants in humans. Exp Neurol 1999; 158: 121-25.

Boecker H, Dagher A, Ceballos-Baumann AO, Passingham RE, Samuel M, Friston KJ, Poline JB, Dettmers C, Conrad B, Brooks DJ. Role of the human rostral supplementary motor area and the basal ganglia in motor sequence control. J Neurophysiol 1998; 79: 1070-80.

Brinkman C. Supplementary motor area of the monkey's cerebral cortex: short- and long-term deficits after unilateral ablation and the effects of subsequent callosal section. J Neurosci 1984; 4: 918-29.

Brown MA, Semelka RC. MRI: Basis principles and applications, 2nd ed. New York: Wiley-Liss, 1999.

Bushong SC. Magnetic resonance imaging: physical and biological principles, 2nd ed. St, Louis: Mosby-Year Book Inc., 1996.

Cao Y, D'Olhaberriage L, Vikingstad EM, Levine SR, Welch KMA. Pilot study of functional MRI to assess cerebral activation of motor function after poststroke hemiparesis. Stroke 1998; 29: 112-22.

Ceballos-Baumann AO, Obeso JA, Vitek JL, DeLong MR, Bakay R, Linazasoro G, Brooks DJ. Restoration of thalamocortical activity after posteroventral pallidotomy in Parkinson's disease. Lancet 1994; 344: 814.

Ceballos-Baumann AO, Boecker H, Bartenstein P, VonFalkenhayn I, Riescher H, Conrad B, Moringlane JR, Alesch F. A positron emission tomographic study of subthalamic nucleus stimulation in Parkinson's disease. Arch Neurol 1999; 56: 997-1003.

Chen YC, Thaler D, Nixon PD, Stern CE, Passingham RE. The functions of the medial premotor cortex II. The timing and selection of learned movements. Exp Brain Res 1995; 102: 461-73.

Chollet F, Di Piero V, Wise RJ, Brooks DJ, Dolan RJ, Frackowiak RS. The functional anatomy of motor recovery after stroke in humans; A study with positron emission tomography. Ann Neurol 1991; 29: 63-71.

Cramer SC, Nelles G, Bensom R, Kaplan J, Parker R, Kwong K, Kennedy D, Finklestein SP, Rosen BR. A functional MRI study of subjects recovered from hemiparetic stroke. Stroke 1997; 28: 2518-27.

Davis KD, Taub E, Houle S, Lang AE, Dostrovsky JO, Tasker RR, Lozano AM. Globus pallidus stimulation activated the cortical motor system during alleviation of parkinsonian symptoms. Nat Med 1997; 3: 671-74.

Deecke L, Scheid P, Kornhuber HH. Distribution of readiness potential, pre-motion positivity, and motor potential of the human cerebral cortex preceding voluntary finger movements. Exp Brain Res 1969; 7: 158-68.

Deecke L, Englitz HG, Kornhuber HH, Schmitt G. Cerebral potentials preceding voluntary movement in patients with bilateral or unilateral Parkinson Akinesia. Prog Clin Neurophysiol 1977; 1: 151-63.

Deiber MP, Passingham RE, Colebatch JG, Friston KJ, Nixon PD, Frackowiak RS. Cortical areas and the selection of movement; a study with positron emission tomography. Exp Brain Res 1991; 84: 393-402.

Deiber MP, Ibanez V, Sadato N, Hallet M. Cerebral structures participating in motor preparation in humans: a positron emission tomography study. J Neurophysiol 1996; 75: 233-47.

Deiber MP, Ibanez V, Honda M, Sadato N, Raman R, Hallet M. Cerebral processes related to visuomotor imagery and generation of simple finger movements studied with positron emission tomography. Neuroimage 1998; 7: 73-85.

Deiber MP, Honda M, Ibanez V, Sadato N, Hallet M. Mesial motor areas in self-initiated versus externally triggered movements examined with fMRI: Effect of movement type and rate. J Neurophysiol 1999; 81: 3065-77.

DeLong MR. Primate models of movement disorders of basal ganglia origin. Trends Neurosci 1990; 13: 381-85.

Dick JPR, Benecke R, Rothwell JC, Day BL, Marsden CD. Simple and complex movements in a patient with infarction of the right supplementary motor area. Mov Disord 1986; 1: 255-66.

Dick JP, Cantello R, Buruma O, Gioux M, Benecke R, Day BL, Rothwell JC, Thompson PD, Marsden CD. The bereitschaftspotential, l-dopa, and Parkinson's disease. Electroencephalogr Clin Neurophysiol 1987; 66: 264-74.

Dick JP, Rothwell JC, Day BL, Cantello R, Buruma O, Gioux M, Benecke R, Berardelli A, Thompson PD, Marsden CD. The Bereitschaftspotential is abnormal in Parkinson's disease. Brain 1989; 112: 233-44.

DiSalle F, Formisano R, Linden DE, Goebel R, Bonavita S, Pepino A, Smaltino F, Tedeschi G. Exploring brain function with magnetic resonance imaging. Eur J Radiol 1999; 30: 84-94.

Forster BB, MacKay AL, Whittall KP, Kiehl KA, Smith AM, Hare RD, Liddle PF. Functional magnetic resonance imaging: the basics of blood-oxygen-level dependent (BOLD) imaging. Can Assoc Radiol J 1998; 49: 320-29.

Fox PT, Raichle ME. Focal physiological uncoupling of cerebral blood flow and oxidative metabolism during somatosensory stimulation in human subjects. Proc Natl Acad Sci USA 1986; 83: 1140-44.

Friston KJ, Holmes AP, Worsley KJ, Poline JB, Frith CD, Frackowiak RSJ. Statistical parametric maps in functional imaging: a general linear approach. Hum Brain Mapp 1995; 2: 189-210.

Genovese CR, Noll DC, Eddy WF. Estimating test-retest reliability in functional MR imaging. I. Statistical methodology. Magn Res Mes 1997; 38: 497-507.

Gentilucci M, Bertolani L, Benuzzi F, Negreotti A, Pavesi G, Gangitano M. Impaired control of an action after supplementary motor area lesion: a case study. Neuropsychologia 2000; 38: 1398-1404.

Georgiou N, Bradshaw JL, Iansek R, Phillips JG, Mattingley JB, Bradshaw JA. Reduction in external cues and movement sequencing in Parkinson's disease. J Neurol Neurosurg Psychiatry 1994; 57: 368-70.

Godschalk M, Lemon RN, Nijs HG, Kuypers HGJM. Behaviour of neurons in monkeys per-arcuate and precentral cortex before and during visually guided arm and hand movements. Exp Brain Res 1981; 44: 113-16.

Grafton ST, Waters C, Sutton J, Lew MF, Couldwell W. Pallidotomy increases activity of motor association cortex in Parkinson's disease: a positron emission topographic study. Ann Neurol 1995; 37: 776-83.

Halsband U, Matsuzaka Y, Tanji J. Neuronal activity in the primate supplementary, pre-supplementary and premotor cortex during externally and internally instructed sequential movements. Neurosci Res 1994; 20: 149-55.

Haacke M. Magnetic resonance imaging: physical principles and sequence design. New York: J. Wiley and Sons, 1999.

Haslinger B, Erhard P, Kampfe N, Boecker H, Rummeny E, Schwaiger M, Conrad B, Ceballos-Baumann AO. Event-related functional magnetic resonance imaging in Parkinson's disease before and after levodopa. Brain 2001; 124: 558-70.

Holmes AP, Friston KJ. Generalisability, random effects and population inference. Neuroimage 1998; 7: 124.

Humberstone M, Sawle GV, Clare S, Hykin J, Coxon R, Bowtell R, Macdonald IA, Morris PG. Functional magnetic resonance imaging of single motor events reveals human presupplementary motor area. Ann Neurol 1997; 42: 632-37.

Huu Le T, Hu X. Methods for assessing accuracy and reliability in functional MRI. NMR in Biomed 1997; 10: 160-64.

Jack CR, Thompson RM, Butts RK, Sharbrough FW, Kelly PJ, Hanson DP, Riederer SJ, Ehman RL, Hangiandreou NJ, Cascino GD. Sensory motor cortex: correlation of presurgical mapping with functional MR imaging and invasive cortical mapping. Radiology 1994; 190: 85-92.

Jahanshahi M, Jenkins IH, Brown RG, Marsden CD, Passingham RE. Brooks DJ. Self-initiated versus externally triggered movements. I. An investigation using measurement of regional cerebral blood flow with PET and movement-related potentials in normal and Parkinson's disease subjects. Brain 1995; 118: 913-33.

Jenkins IH, Fernandez W, Playford ED, Lees AJ, Frackowiak RSJ, Passingham RE, Brooks DJ. Impaired activation of the supplementary motor area in Parkinson's disease is reversed when akinesia is treated with apomorphine. Ann Neurol 1992; 32: 749-57.

Kwong KK, Belliveau JW, Chesler DA, Goldberg IE, Weisskopf RM, Poncelet BP, Kennedy DN, Hoppel BE, Cohen MS, Turner R, Cheng HM, Brady TJ, Rosen BR. Dynamic magnetic resonance imaging of human brain activity during primary sensory stimulation. Proc Natl Acad Sci USA 1992; 89: 5675-79.

Laplane D, Talairach J, Meininger V, Bancaud J, Orgaogozo JM. Clinical consequences of corticectomies involving the supplementary motor area in man. J Neurol Sci 1977; 34: 301-14.

Lee KM, Chang KG, Roh JK. Subregions within the supplementary motor area activated at different stages of movement preparation and execution. Neuroimage 1999; 9: 117-23.

Luppino G, Matelli M, Camarda R, Rizzolatti G. Corticocortical connections of area F3 (SMA-proper) and area F6 (pre-SMA) in the macaque monkey. J Comp Neuol 1993; 338: 114-40.

Matsuzaka Y, Aizawa H, Tanji J. A motor area rostral to the supplementary motor area (presupplementary motor area) in the monkey: neuronal activity during a learned motor task. J Neurophysiol 1992; 68: 653-62.

Mattay VS, Frank JA, Santha AKS, Pekar JJ, Duyn JH, McLaughlin AC, Weinberger DR. Whole-brain functional mapping with isotropic MR imaging. Radiology 1996; 201: 399-404.

Mattay VS, Weinberger DR. Organization of the human motor system as studied by functional magnetic resonance imaging. Eur J Radiol 1999; 30: 105-14.

McGonigle DJ, Howseman AM, Athwal BS, Friston KJ, Frackowiak RSJ, Holmes AP. Variability in fMRI: an examination of intersession differences. Neuroimage; 2000: 11: 708-34.

Miki A, Raz J, Van Erp TGM, Liu CSJ, Haselgrove JC, Liu GT. Reproducibility of visual activation in functional MR imaging and effects of postprocessing. Am J Neuroradiol 2000; 21: 910-15.

Mushiake H, Inase M, Tanji J. Selective coding of motor sequence in the supplementary motor area of the monkey cerebral cortex. Exp Brain Res 1990; 82: 208-10.

Noll DC, Genovese CR, Nystrom LE, Vazquez AL, Forman SD, Eddy WF, Cohen JD. Estimating test-retest reliability in functional MR imaging. II. Application to motor and cognitive activation studies. Magn Res Med 1997; 38: 508-17.

Ogawa S, Lee TM. Magnetic resonance imaging of blood vessels at high fields: in vivo and in vitro measurements and image simulation. Mag Reson Med 1990; 16: 9-18.

Ogawa S, Lee TM, Nayak AS, Glynn P. Oxygenation-sensitive contrast in magnetic resonance image of rodent brain at high magnetic fields. Magn Reson Med 1990a; 14: 68-78.

Ogawa S, Lee TM, Kay AR, Tank DW. Brain magnetic resonance imaging with contrast dependent on blood oxygenation. Proc Natl Acad Sci USA 1990b; 87: 9868-72.

Ogawa S, Tank DW, Menon R, Ellermann JM, Kim SG, Merkle H, Ugurbil K. Intrinsic signal changes accompanying sensory stimulation: functional brain mapping with magnetic resonance imaging. Proc Natl Acad Sci USA 1992; 89: 5951-55.

Ogawa S, Menon RS, Kim SG, Ugurbil K. On the characteristics of functional magnetic resonance imaging of the brain. Ann Rev Biophys Biomol Struct 1998; 27: 447-74.

Pandya DN, Yeterian EH. Architecture and connections of cortical association areas. In: Peters A, Jones EG, editors. Cerebral cortex, Vol. 4. New York: Plenum Press, 1985. p.3-61.

Pauling L, Coryell CD. The magnetic properties and structure of hemoglobin, oxyhemoglobin and carbomonoxyhemoglobin. Proc Natl Acad Sci USA 1936; 22: 210-16.

Passingham RE. Premotor cortex: sensory cues and movement. Behav Brain Res 1985; 18: 175-85.

Petrides M. Motor conditional associative-learning after selective prefrontal lesions in the monkey. Behav Brain Res 1982; 5: 407-13.

Piccini P, Lindvall O, Bjorklund A, Brundin P, Hagell P, Ceravolo R, Oertel W, Quinn N, Samuel M, Rehncrona S, Widner H, Brooks DJ. Delayed recovery of movement-related cortical function in Parkinson's disease after striatal dopaminergic grafts. Ann Neurol 2000; 48: 689-95.

Pineiro R, Pendlebury S, Johansen-Berg H, Matthews PM. Functional MRI detects posterior shifts in primary sensorimotor cortex activation after a stroke: evidence of local adaptive reorganization? Stroke 2001; 32: 1134-39.

Playford ED, Jenkins IH, Passingham RE, Nutt J, Frackowiak RSJ, Brooks DJ. Impaired mesial frontal and putamen activation in Parkinson's disease: a positron emission tomography study. Ann Neurol 1992; 32: 151-61.

Posse S, Muller-Gartner HW, Dager SR. Functional magnetic resonance studies of brain activation. Sem Clin Neurophys 1996; 1: 76-88.

Puce A, Constable RT, Luby ML, McCarthy G, Nobre AC, Spencer DD, Gore JC, Allison T. Functional magnetic resonance imaging of sensory and motor cortex: comparison with electrophysiological localization. J Neurosurg 1995; 83: 262-70.

Pujol J, Conesa G, Deus J, Vendrell P, Isamat F, Zannoli G, Marti-Vilalta JL, Capdevila A. Presurgical identification of the primary sensorimotor cortex by functional magnetic resonance imaging. J Neurosurg 1996; 84: 7-13.

Pujol J, Conesa G, Deus J, Lopez-Obarrio L, Isamat F, Capdevila A. Clinical application of functional magnetic resonance imaging in presurgical identification of the central sulcus. J Neurosurg 1998; 88: 863-69.

Raichle ME. Behind the scenes of functional brain imaging: a historical and physiological perspective. Proc Natl Acad Sci USA 1998; 95: 765-72.

Ramsey NF, Tallent K, Van Gelderen P, Frank JA, Moonen CTW, Weinberger DR. Reproducibility of human 3D fMRI brain maps acquired during a motor task. Hum Brain Mapp 1996; 4: 113-21.

Rascol O, Sabatini U, Chollet F, Celsis P, Monstastruc JL, Marc-Vernes JP, Rascol A. Supplementary and primary sensory motor area activity in Parkinson's disease. Regional cerebral blood flow changes during finger movements and effects of apomorphine. Arch Neurol 1992; 49: 144-48.

Rascol O, Sabatini U, Chollet F, Fabre N, Senard JM, Montastruc JL, Celsis P, Marc-Vergnes JP, Rascol A. Normal activation of the supplementary motor area in patients with Parkinson's disease undergoing long-term treatment with levodopa. J Neurol Neurosurg Psychiatry 1994; 57: 567-71.

Rascol O, Sabatini U, Fabre N, Brefel C, Loubinoux I, Celsis P, Senard JM, Montastruc JL, Chollet F. The ipsilateral cerebellar hemisphere is overactive during hand movements in akinetic parkinsonian patients. Brain 1997; 120: 103-10.

Rizzolatti G, Luppino G, Matelli M. The classic supplementary motor area is formed by two independent areas. Adv Neurol 1996; 70: 45-56.

Rombouts SARB, Barkhof F, Hoogenraad FGC, Spenger M, Valk J, Scheltens P. Test-retest analysis with functional MR of the activated area in the human visual cortex. Am J Neuroradiol 1997; 18: 1317-22.

Rombouts SARB, Barkhof F, Hoogenraad, FGC, Sprenger M, Scheltens P. Within-subject reproducibility of visual activation patterns with functional magnetic resonance imaging using multislice echo planar imaging. Magn Reson Imag 1998; 16: 105-13.

Sabatini U, Boulanouar K, Fabre N, Martin F, Carel C, Colonnese C, Bozzao L, Berry I, Montastruc JL, Chollet F, Rascol O. Cortical motor reorganization in akinetic patients with Parkinson's disease. A functional MRI study. Brain 2000; 123: 394-403.

Samuel M, Ceballos-Baumann AO, Blin J, Uema T, Boecker H, Brooks DJ. Evidence for lateral premotor and parietal overactivity in Parkinson's disease during sequential and bimanual movements: A PET study. Brain 1997a; 120: 963-76.

Samuel M, Ceballos-Baumann AO, Turjanski N, Boecker H, Gorospe A, Linazasoro G, Holmes AP, DeLong MR, Vitek JL, Thomas DG, Quinn NP, Obeso JA, Brooks DJ. Pallidotomy in Parkinson's disease increases SMA and prefrontal activation during performance of volitional movements: An $H_2{}^{15}O$ PET study. Brain 1997b; 120: 1301-13.

Samuel M, Williams SCR, Leigh PN, Simmons A, Chakraborti S, Andrew CM, Friston KJ, Goldstein LH, Brooks DJ. Exploring the temporal nature of hemodynamic responses of cortical motor areas using functional MRI. Neurology 1998; 51: 1567-75.

Schell GR, Strick PL. The origin of thalamic inputs to the arcuate premotor and supplementary motor areas. J Neurosci 1984; 4: 539-60.

Scholz VH, Flaherty AW, Kraft E, Keltner JR, Kwong KK, Chen YI, Rosen BR, Jenkins BG. Laterality, somatotopy and reproducibility of the basal ganglia and motor cortex during motor tasks. Brain Res 2000; 879: 204-15.

Shibasaki H, Barrett G, Halliday E, Halliday AM. Components of the movement related cortical potential and their scalp topography Electroencephalogr Clin Neurophysiol 1980; 49: 213-26.

Stein JF, Glickstein M. Role of the cerebellum in visual guidance of movement. Physiol Rev 1992; 72: 967-1017.

Tanji J, Shima K. Role for supplementary motor area cells in planning several movements ahead. Nature 1994; 371: 413-16.

Tegeler C, Strother SC, Anderson JR, Kim SG. Reproducibility of BOLD-based functional MRI obtained at 4T. Hum Brain Mapp 1999; 7: 267-83.

Tomczak RJ, Wunderlich AP, Wang Y, Braun V, Antoniadis G, Gorich J, Richter HP, Brambs HJ. FMRI for preoperative neurosurgical mapping of motor cortex and language in a clinical setting. J Comput Assist Tomogr 2000; 24: 927-34.

Turner R, LeBihan D, Moonen CT, Despres D, Frank J. Echo planar time course MRI of cat brain oxygenation changes. Magn Reson Med 1991; 22: 159-66.

Turner R, Jezzard P, Wen H, Kwong KK, Le Bihan D, Zeffiro T, Balaban RS. Functional mapping of the human visual cortex at 4 and 1.5 Tesla using deoxygenation contrast EPI. Mag Reson Med 1993; 29: 277-79.

Turner R, Howseman A, Rees GE, Josephs O, Friston K. Functional magnetic resonance imaging of the human brain: data acquisition and analysis. Exp Brain Res 1998; 123: 5-12.

Tyszka JM, Grafton ST, Chew W, Woods RP, Colletti PM. Parceling of mesial frontal motor areas during ideation and movement using functional magnetic resonance imaging at 1.5 tesla. Ann Neurol 1994; 35: 746-49.

Van Oostende S, Van Hecke P, Sunaert S, Nuttin B, Marchal G. FMRI studies of the supplementary motor area and the premotor cortex. Neuroimage 1997; 6: 181-90.

Villringer A, Rosen BR, Belliveau JW, Ackerman JL, Lauffer RB, Buxton RB, Chao YS, Wedeen VJ, Brady TJ. Dynamic imaging with lanthanide chelates in normal brain: contrast due to magnetic susceptibility effects. Magn Reson Med 1988; 6: 164-74.

Weiller C, Chollet F, Friston KJ, Wise RJ, Frackowiak RSJ. Functional reorganization of the brain in recovery from striatocapsular infaction in man. Ann Neurol 1992; 31: 463-72.

Yetkin FZ, McAuliffe TL, Cox R, Haughton VM. Test-retest precision of functional MR in sensory and motor task activation. Am J Neuroradiol 1996; 17: 95-98.

Yousry TA, Schmid UD, Jassoy AG, Schmidt D, Eisner WE, Reulen HJ, Reiser MF, Lissner J. Topography of the cortical motor hand area: prospective study with functional MR imaging and direct motor mapping at surgery. Radiology 1995; 195: 23-29.

Zimmerman A, Gibby WA, Carmody RF (eds.). Neuroimaging: clinical and physical principles. New York: Springer, 2000.

2. FUCTIONAL MAGNETIC RESONANCE IMAGING OF CORTICAL MOTOR ACTIVITY AT 3 TESLA

2.1. Introduction

The primary objective of this study was to characterize the feasibility and reproducibility of blood oxygen level dependent (BOLD) contrast functional magnetic resonance imaging (fMRI) activity associated with a repetitive motor task. fMRI studies rely on detecting small changes in the BOLD contrast signal that are associated with a specific cognitive task or sensory stimulation. In addition to variability introduced by the experimental design, there are several other sources of variability that cannot be controlled. These include undetectable change in scanner or hardware performance, as well as small natural fluctuations in individual metabolism and physiology (reviewed by Turner et al., 1998). Recent studies examining the reliability of fMRI data primarily focused on characterizing test-retest reproducibility (Ramsey et al., 1996; Yetkin et al., 1996; Rombouts et al., 1997, 1998; Tegeler et al., 1999; Miki et al., 2000; Scholz et al., 2000).

It is unclear however, if activation over two or even three sessions is an accurate indication of the consistency of the results. Furthermore, aside from the subjective calculation of test-retest reproducibility ratios, it is not known if intra-subject and inter-subject variability actually differentially influence the location, spatial extent or amplitude of the BOLD response within a representative set of data. Variability of a larger data set may be particularly important in fMRI studies at higher magnetic field strengths where problems with hardware instabilities and image distortions have a larger impact on the data (Edelman et al., 1994; Jezzard and Clare 1999).

One method for identifying reliable responses within a set of data is random effects analysis, which models the variability both within sessions and between sessions (Holmes et al., 1998). A random effects analysis is useful since unlike test-retest reliability studies, it can be easily implemented into the analysis of every data set. However a limitation of random effects analysis, is that information about significant between session variability will be lost unless each set of data is first analyzed individually. For example, as demonstrated by McGonigle et al., (2000), while a random effects analysis will identify areas that are typically active within a group of subjects, the results will not identify and localize regions of highly variable activity. Information about the presence of significant variability is an important consideration when interpreting and describing observed differences in activity between groups. This is of particular interest when evaluating the feasibility of an experiment, as inconsistent regional activity may indicate a problem with methods, equipment or experimental task (Jezzard and Song 1996).

In order to verify the validity and specificity of fMRI data in the present study, a motor task was performed once with the right hand and once with the left hand. Activation in the contralateral primary motor cortex was consistently detected in every independently analyzed session in the individual data set, and every subject in the group data set. There was no evidence that data acquired from the same subject tested in ten independent sessions was more reproducible than data acquired from ten different subjects. In addition, there were no significant differences in the mean spatial extent or amplitude of BOLD response between the two groups of individually analyzed data. However, the results of this study demonstrated that in contrast to a fixed effects analysis

which resulted in atypically robust activity, a random effects analysis was a more effective method of summarizing multi-subject or multi-session fMRI data. Overall, it is evident that detecting motor activity associated with repetitive finger tapping at 3T is not only feasible, but as the activation across subjects and sessions was both strong and relatively stable, this task could be used to verify the effectiveness of more complex experimental protocols.

2.2 Methods

2.2.1. Subjects

Ten healthy right-handed subjects (six male, four female, mean age 25.6 ± 1.2 years) were tested in independent scanning sessions over a period of several months. One additional healthy subject (male, age 26 years) volunteered to be tested in ten sessions over a period of several months. A brief medical history interview conducted prior to testing confirmed that the healthy volunteers had no history of neurological or psychiatric disease. Informed consent was obtained from all volunteers. This study received ethical approval from Health Research Ethics Committee of the Faculty of Medicine.

2.2.2. Motor task

Although each scanning session was implemented on separate days, the motor task, data acquisition and analysis were kept constant in order to ensure that the experimental conditions were as similar as possible. The motor task involved repeatedly moving the tip of the index finger to the tip of the thumb. Each subject was trained prior to the scanning session to perform the finger tapping at a rate of approximately 1 Hz, with intermediate amplitude. Although the motor task was self-paced in order to avoid

confounding effects associated with external pacing cues, subjects were instructed to tap at a consistent frequency in order to keep differences in movement execution to a minimum. The frequency of tapping was selected to ensure that all subjects, including patients could perform the task accurately and with minimal fatigue. Subjects were also instructed to keep their eyes closed at all times, to remain motionless, and to avoid thinking about upcoming movements as much as possible during the rest period. Subjects were observed from the control room during the experimental session to identify any difficulties with the task or change in performance.

2.2.3. Experimental Design

Each scanning session consisted of two imaging runs, one with the right hand finger tapping, and one with left hand finger tapping. The order of right and left hand finger tapping within the scanning sessions was balanced across subjects. Each imaging run was organized as a block design experiment with four repeating cycles of alternating rest and activation (Figure 2-1), each lasting 20 seconds. A brief verbal signal was provided through the headphones to at the beginning of each rest and activation period. The brain was imaged every 2 seconds, 20 times during each rest and activation block, producing a image time series of 80 images. The total scanning time of each imaging run was therefore160 seconds.

2.2.4. fMRI data acquisition

All images were acquired using a Magnex 3T magnet equipped with actively shielded gradients, a SMIS operating system, and a quadrature birdcage resonator for RF transmission and reception. Subjects were positioned in a supine position within the scanner. A supportive head restraint and optional padding surrounding the head was

Figure 2-1. *FMRI experimental design*

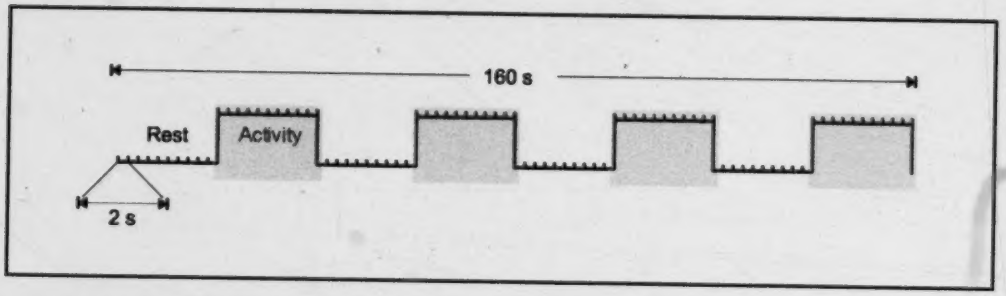

Figure 2-1. Schematic representation of the fMRI experimental design. An imaging run consists of 4 repeatingcycles of 10 scans (20s) activity, beginning with a rest period. Each scanning run therefore lasts for a total of 160 s.

used to minimise unintentional head movement. A non-magnetic headphone and speaker system was used for communication between the subjects in the scanner and the experimenter in the control room.

Each imaging run began with the acquisition of T_1-weighted structural images of the brain (repetition time, TR=250ms; echo time, TE=11ms; 256x256, FOV 225mm) in the transverse, sagittal, and coronal planes. These images were used as a template to position the slices used for functional images. Functional images were acquired using an echo planar imaging (EPI) gradient echo sequence (TR=2000 ms; TE=25 ms; 128x128, FOV 240mm). Each of the 80 functional EPI images acquired during the imaging run included twenty slices oriented in the transverse direction (5 mm thick, separated by 5 mm, 3mm x 3mm x 5mm voxels). Shimming (the process of locally adding and removing magnetization in order to optimize the uniformity of the external magnetic field) was performed manually prior to initiation of the imaging run. In addition, during each imaging run ten additional EPI 'dummy' scans were acquired and discarded prior to the first image in the functional time series to allow for stabilization of the MR signal. Following the completion of the first imaging run, where tapping was performed with either the left or right hand, the process was repeated using the other hand.

2.2.5. Data pre-processing

The functional images were preprocessed and analyzed using Statistical Parametric Mapping (SPM99) software (*Wellcome Department of Cognitive Neurology, London UK; http:/www.fil.ion.ucl.ac.uk/spm*).

As small amounts of head movement are difficult to avoid during scanning sessions, the first step in the analysis of an image time series is to correct for

unintentional head movement (Friston et al., 1996). The correction of head movement is especially important when the experimental task may be correlated with head movement, as changes in signal associated with head movement may therefore appear as task related brain activity (Hajnal et al., 1994; Field et al., 2000). In addition, in all scanning sessions head movement will add additional signal variance, decreasing the sensitivity of the analysis to true task related brain activity (Friston et al., 1996). Head movement correction was implemented by applying spatial translations and rotations along the x, y, and z axes to realign each of the 80 images in the fMRI time series to the first image in the time series (Friston et al., 1996).

Spatial normalization further corrects for difference in the global size and shape of the functional images by co-registering each image to a standard template image (Friston et al., 1995a; Ashburner et al., 1999). The functional images obtained from each individual in this study were co-registered to the EPI template image that is included with SPM99 (Figure 2-2). The EPI template was created at the Montreal Neurological Institute (MNI), and is the same size and shape as the templates used in SPM for displaying activation. Spatial normalization facilitates the comparison of data between subjects and groups by minimizing differences in the size and shape of cerebral anatomy. In addition, spatial normalization allows the results to be accurately reported in co-ordinates of a standard stereotactic space (Friston et al., 1995a).

In addition to changes in the BOLD MR signal associated with neuronal activation, both thermal changes and cardiac and respiratory cycles can introduce additional fluctuations in signals, or noise, that can interfere with the detection of the true BOLD activation signal (reviewed by Turner et al., 1998). While this noise can be

Figure 2-2. *EPI template image (SPM 99) and spatially normalized EPI images*

Figure 2-2. Coronal (A), saggital (B), and transverse (C) views of the EPI template image and the EPI images after being spatially normalized to that template.

problematic, smoothing the data by locally averaging the data with a Gaussian function has been shown to enhance or increase the strength of the true signal, relative to the signal associated with noise (Friston et al., 2000). While the increase in signal to noise from smoothing is at the expense of spatial resolution, assessing images using statistical parametric maps also requires that the data is sufficiently smooth to meet the assumptions of the Theory of Gaussian fields (Friston et al., 1995c; Worsely et al., 1995).

In this study each image was spatially smoothed with an 8-mm full width at half maximum (FWHM) Gaussian kernel. 8-mm FWHM has been shown to be particularly effective for detecting robust activity within the primary cortical regions and is considered an acceptable trade-off between sensitivity and spatial resolution (Friston et al., 2000). The time series was also temporally smoothed with a high pass filter and a low pass filter. In addition to minimizing low frequency drifts and high frequency noise in the time series, temporally smoothing the time series provides a known temporal autocorrelation function that is modelled at the estimation stage of analysis (Friston et al., 1995b; Worsely and Friston, 1995). The MR signal of each image in the time series was also proportionally scaled to ensure that the signal of each had the same global mean voxel value.

2.2.6. Statistical analysis

Statistical inference in SPM99 (Friston et al., 1995c; Worsely et al., 1995) is based on the use of the general linear model to perform an independent statistical test for every voxel in an image. The general linear model, also known as regression analysis, is

a model that explains the variation of the observed variable (Y) in terms of a linear combination of explanatory variables (α) and an error term (ε):

$$Y = \beta \alpha + \varepsilon$$

In fMRI, there is one observed MR signal (Y) for every scan in the time series (i.e.,80 scans) at that voxel. Each scan or time point in the time series is also associated with a specific explanatory value, α. The explanatory variables are defined by a numerical code or reference function describing the experimental condition to which that point in the time series corresponds. For example, in this study a box car reference function (where values of 0 and 1 were assigned to scans acquired during the rest and activation blocks, respectively) was used to model the experiment. Each observation (Y) in the time series was therefore associated with a value of 1 or 0 depending on whether it occurred while the subject was at rest or while engaged in an activation task. The final parameter in the model, beta (β), is estimated by determining the single value that when multiplied by each of the explanatory variables is the best overall fit for the observed signal time course. Following the estimation of β, the products of the parameter estimate and the reference function at each time point are referred to as the fitted values. At each time point in the time series, the observed variable for that voxel would now have actual values and fitted values. The *t*-statistic for each voxel (parameter estimate, β / sum of the squared difference between the actual and fitted values) is a measure of how well the observed MR signal at that voxel fits the experimental design.

In this study the experiment was modeled with a box-car reference waveform, that was convolved with a temporal delay estimated to approximate delay of the

haemodynamic response. Using the general linear model a *t*-statistic was calculated for each voxel. Voxels with *t*-values that survived a threshold of $p<0.05$, corrected for multiple non-independent comparisons, were classified as significantly active.

The locations of activated clusters were displayed on binary statistical images, referred to as maximum intensity projection images, in which voxels are classified as either active or inactive (Friston et al., 1995c). Activity was also superimposed onto surface renderings of a standard brain that is based on templates developed at the Montreal Neurological Institute (MNI). While all active voxels are collapsed onto a single image plane in the maximum intensity projection display, in a surface rendering the intensity of colour is used as an indication of voxels' location relative to the brain surface. Specifically, intensity of colour decays exponentially with the distance of the active voxel from the surface of the brain. Since information from every voxel in the brain is included with these methods, they are particularly useful for displaying widespread activity.

The MNI space utility, developed at the PET Laboratory at the Institute of the Human Brain (Russian Academy of Sciences, St. Petersburg, Russia) was used to create reports about the localization of SPM99 activation based on the Talairach atlas (Talairach and Tournoux, 1988). The MNI space utility transforms the MNI coordinates which are implemented in SPM99 in mm, into Talairach coordinates using nonlinear transformations. The Talairach coordinates were used as input into the stand-alone version of the Talairach Daemon to get the appropriate Talairach Atlas Labels for each voxel cluster.

2.2.7. Single subject/session analyses

In an effort to fully assess the within subject and between subject variability, the data from each of the ten different subjects and from each of the ten scanning session from the one individual subject were analysed independently. Voxels that survived a probability threshold of $p<0.05$ (corrected for multiple comparisons) were classified as active. In addition to visually assessing the activity, the spatial extent and percent BOLD signal change associated with each motor task was quantified for each subject in the multi-subject group (group data set) and for each session from the additional subject (individual data set). Significant differences between groups were determined using a one way analysis of variance (ANOVA), and post hoc comparisons were made using Bonferroni corrected t-tests. Significance for every analysis was accepted at $p<0.05$.

2.2.8. Multi subject/session analyses

To explore the association between single subject and group activation, a test for significant motor activity within each data set was assessed using both fixed and random effects analysis. The rationale for including both types of analysis was to determine if there was a difference between the average effect and the typical effect within and between each data set. The fixed effects analysis involves using the general linear model as described above. However, the observation at each time point for that voxel is based on the average signal from all of the subjects or sessions. The results therefore provide an indication of the average effect within the group of data (Friston et al., 1995c). A random effects analysis on the other hand, is implemented by entering the contrast images from the individually analyzed data into a one-sample t-test. Since the one sample t-test specifically models between subject or session variance, a random effects analysis identifies the typical activity across multiple subjects or sessions. Random

effects analysis therefore accounts for significant variability between sessions by removing related activity from the statistical parametric map (Holmes et al., 1998). In both the fixed effects and random effects analyses, voxels that survived a threshold of $p<0.05$ were classified as active.

2.3 Results

While subjects in both data sets were tested in independent sessions, it was assumed that the results of multiple tests of the same subject would be a relatively effective estimation of variability of responses associated with intra-subject variability. In contrast, the results from a group of multiple young healthy subjects would be influenced more by inter-subject variability.

2.3.1. Task performance

Following detailed instructions and a brief practice session, all subjects were able to perform the tapping task with ease. Although the task was repetitive and the scanning runs were relatively short, during every scanning run both the rate and amplitude of finger tapping were observed from the control room to ensure that every subject consistently performed the task according to the given instructions. As expected, there were no observed variations in task performance.

2.3.2. Single subject/session analyses

In order to characterize the reproducibility of activation associated with right and left hand finger tapping, data from each subject in the group data set and each sessions in the individual data set were first assessed independently using standard single subject analysis based on the general linear model (Friston et al., 1995c). Voxels that survived a threshold of $p<0.05$ are shown displayed on maximum intensity projection

images for each of the ten sessions acquired from the individual subject (Figure 2-3), and each of the ten different subjects (Figure 2-4). Figure 2-5 shows an example of the BOLD signal change of the peak voxel in the primary motor cortex over a time series of alternating blocks of rest and repetitive finger tapping.

2.3.2.1. Primary somatosensory and motor cortex activation

Upon visual inspection, it is evident that although the size and focal location of activation varied, the largest and most dominant cluster of active voxels in every independently analyzed subject and session was relatively well localized to the frontal and parietal regions surrounding the central sulcus. This included both the precentral gyrus, known as the motor cortex which is primarily involved in the control of voluntary movement, and the postcentral gyrus which is the site of the somatosensory cortex involved more with processing sensory and proprioceptive information.

Although the somatosensory and motor cortices have relatively well defined independent functions, sensation and proprioception are closely linked to voluntary movement. In fact one of the primary sources of input of the motor cortex is from the primary somatosensory cortex. In addition, both the motor cortex and somatosensory cortex form pathways that mediate the opposite side of the body (Nyberg-Hansen et al., 1965). As expected, the results show that cortical activity was lateralized to the cerebral hemisphere contralateral to the hand that was performing the motor task.

While it is evident that the experimental parameters implemented in this study are effective for detecting contralateral cortical motor activity, during both right and left hand tapping the cluster of contiguously active voxels often extended over several gyri and sulci within the frontal, parietal and even into the temporal regions in some sessions.

Figure 2-3. *MIP images of activity associated with right and left hand finger tapping from each session in the individual data set*

A. Right Hand Finger Tapping

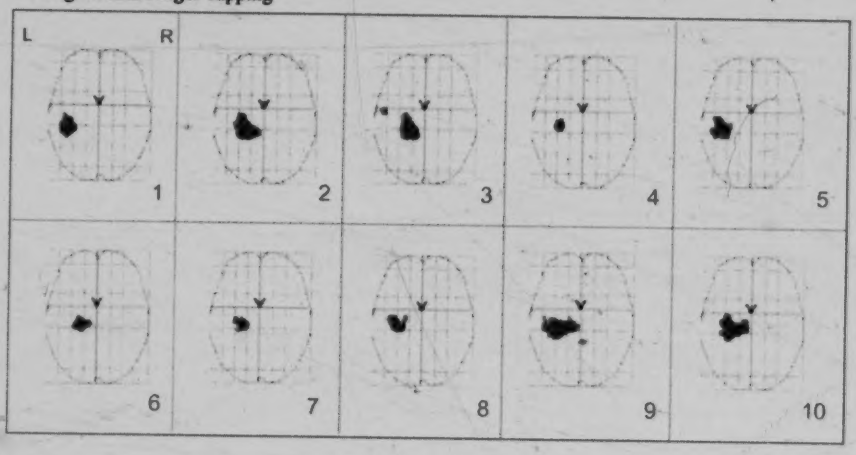

B. Left Hand Finger Tapping

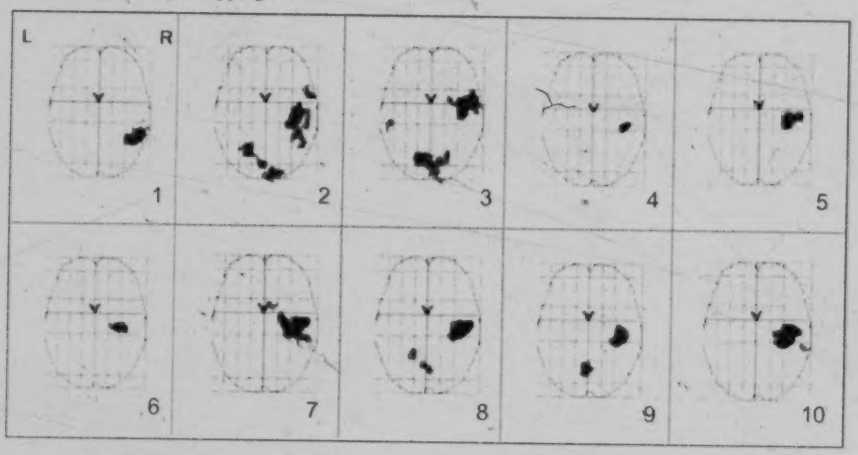

Figure 2-3. Maximum intensity projection (MIP) images showing active voxels associated with right (A) and left (B) hand finger tapping in each of the ten sessions labelled 1 through 10 in the individual data set. Active voxels were significant at $p<0.05$.

Figure 2-4. *MIP images of activity associated with right and left hand finger tapping from each subject in the group data set*

A. Right Hand Finger Tapping

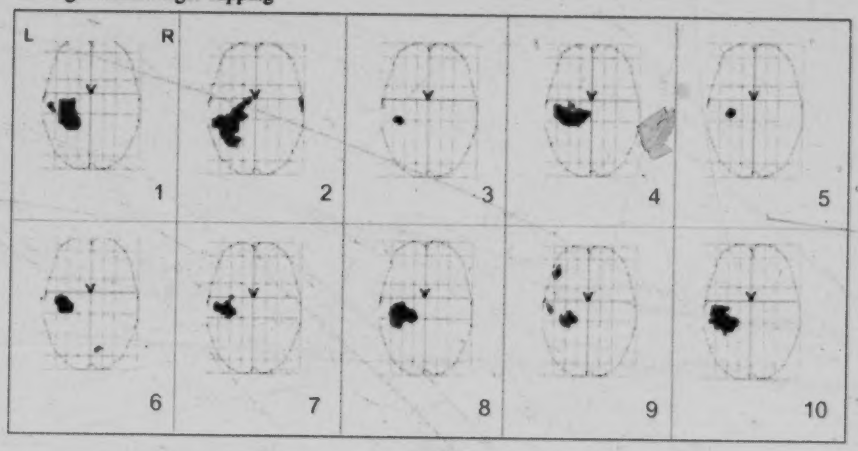

B. Left Hand Finger Tapping

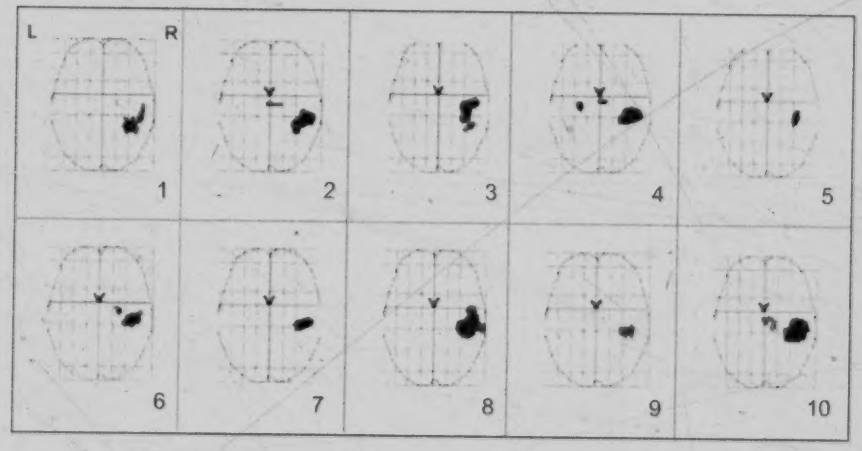

Figure 2-4. Maximum intensity projection (MIP) images showing active voxels associated with right (A) and left (B) hand finger tapping in each of the ten subjects labelled 1 through 10 in the group data set. Active voxels were significant at $p<0.05$.

Figure 2-5. *The change in BOLD signal associated with a time series of alternating blocks of rest and repetitive finger tapping*

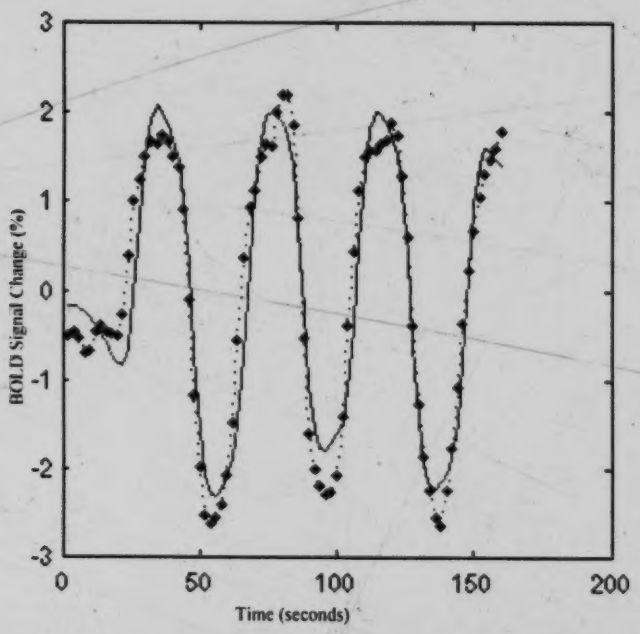

Figure 2-5. A plot showing the typical percent change in BOLD signal relative to the global whole brain mean in the peak voxel in a time series consisting of alternating blocks or rest and repetitive finger tapping modelled with a box car reference function. The solid and dashed lines represent the fitted and adjusted data respectively.

More refined pre-processing and perhaps more specific motor tasks may be necessary to isolate more defined localization of activity within the motor cortex.

2.3.2.2. Other regions of activity

Although in the individual and group data sets the majority of active voxels were observed in the contralateral motor and somatosensory cortices, smaller clusters of active voxels were detected in other regions of the brain. However, in both the group and individual data sets, these smaller clusters of active voxels were primarily associated with left hand finger tapping. For example, within the individual data set, clusters of active voxels were observed bilaterally in the cerebellum in four out of the ten sessions, but only during left hand finger tapping. While the cerebellum is involved in the control of movement, it is unclear why activity was only detected in the individual data set and only during left hand tapping. It is important to note that there is no evidence of longitudinal trends across the ten sessions of the individual data set, indicating that habituation or practice effects were not a factor.

Within the group data set, in addition to robust activity in the frontal and parietal regions, in three subjects additional smaller clusters of active voxels were observed in the supplementary motor area and anterior cingulate gyrus, but once again only during left hand tapping. While this activity cannot be specifically attributed to a particular performance or physiological factor, these regions were previously shown to be involved in higher order motor planning and are preferentially associated with more complex motor tasks (Rao et al., 1993; Shibasaki et al., 1993; Boecker et al., 1998).

Although the motor tasks in this study were relatively simple, the presence of additional foci of activation associated with left hand tapping is consistent with several

fMRI studies which demonstrated that task performance with the non-dominant hand is often associated with additional ipsilateral cortical activity (Kim et al., 1993; Solodkin et al., 2001). It is important to note however, that the objective of including both right and left hand tapping was simply to provide a comprehensive assessment of the validity and specificity of the data. Since every subject in this study was right handed, activation differences between right and left hand tapping can therefore not be solely attributed to hand dominance.

2.3.2.3. Consistency of motor activation

Upon subjective visual inspection there is no evidence of substantial differences in the overall consistency of activity between the group and individual data sets. Despite some small regions of sporadic activity, overall the anatomical location of activity was consistent across subjects and across sessions. While in both data sets the location of activity associated with left hand tapping was more variable than right hand tapping, overall the results demonstrate that BOLD contrast fMRI at 3T is a valid and sensitive tool for localizing cortical activity associated with repetitive finger tapping movement.

2.3.2.4. Spatial extent of activation

Although variability in the spatial extent or size of the activity across subjects and sessions is evident through visual inspection, the spatial extent of fMRI activation was assessed more specifically by quantifying both the total number of significantly active voxels throughout the whole brain (total voxel count), and within a sensorimotor region of interest which included both the contralateral primary somatosensory and motor cortex (regional voxel count). Due to the low spatial resolution of EPI images, the regional voxel count included all contiguous voxels within the dominant cluster of active

voxels in the precentral and postcentral gyri, and therefore in some cases also included voxels from adjacent frontal and parietal gyri.

As shown in Figure 2-6, within the individual data set both the mean number of active voxels throughout the whole brain and within the contralateral sensorimotor region were larger during finger tapping with the left hand compared to the right hand. In contrast, within the group data set both the mean number of active voxels throughout the whole brain and within the contralateral sensorimotor region were greater during finger tapping with the right hand compared to the left hand. Overall however, an ANOVA at $p<0.05$ showed no significant differences between the total and regional voxel counts between the right and left hand tapping within or between the group and individual subject data sets.

Despite the fact that there were no significant differences in the mean total and regional voxel counts within each data set, the voxel counts associated with right and left hand tapping from the independently analyzed data from each subject in the group data set and each session in the individual data set were quite variable. For example, within the individual data set, the total number of active voxels observed during right hand finger tapping ranged from 55 to 539 voxels (mean 283.0 ± 53.8), while the size of activation in the contralateral sensorimotor region ranged from 55 to 477 voxels (mean 263.7 ± 47.6). During left hand finger tapping the total number of active voxels ranged from 33 to 1034 voxels (mean 469.0 ± 103.5) and the size of activation in the contralateral sensorimotor region ranged from 33 to 589 voxels (mean 332.6 ± 58.0).

Within the group data set the total number of active voxels associated with right

Figure 2-6. *The mean spatial extent of activity associated with right and left hand finger tapping in the individual and group data sets.*

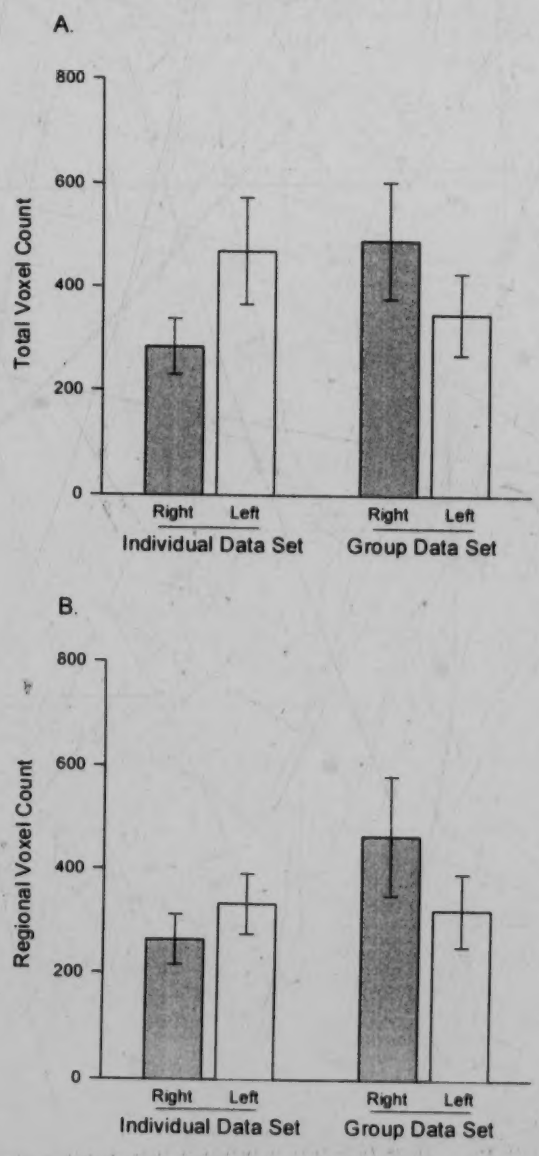

Figure 2-6. The mean size of activity within the whole brain (A) and within the sensorimotor region (B), associated with right (grey bars) and left (white bars) hand finger tapping in the individual and group data sets were not significantly different at $p<0.05$. [Error bars represent the standard error (SE)].

hand finger tapping ranged from 31 to 1024 voxels (mean 489.8 ± 113.0), while the size of the activation within the sensorimotor region ranged from 31 to 987 voxels (mean 465.2 ± 115.3). During left hand tapping the total number of active voxels within the group data set ranged from 60 to 898 voxels (mean 347.1 ± 79.2) and the size of activation within the sensorimotor region ranged from 60 to 809 voxels (mean 322.0 ± 69.8).

It is important to note that the range of voxels counts in the group and individual data were both influenced by a few atypical observations within each data set, indicating that the presence of unexpected or atypical activation was equally prominent in the group and individual data sets. In addition to demonstrating that the spatial extent of activity is just as reproducible in a data set made up of different subjects as in a data set comprised of the same subject, these results also verify that the mean extent of activity in each data set is comparable. This suggests that the relative presence of intra and inter-subject variance did not differentially influence the reproducibility of the spatial extent of activity.

2.3.2.5. Amplitude of BOLD response

In contrast to the spatial extent of activity, the degree of change in BOLD signal associated with the activation task is not immediately obvious by visual inspection. Since the data was statistically thresholded at the same level, there was little variability in the observed t-values within each data set. However, the statistical value at every voxel is a function of both the size and residual error of BOLD signal change associated with the activation task (Friston et al., 1995c). As such, regardless of the statistical value,

the actual amplitude of BOLD signal change associated with the activation task, which can be influenced by individual anatomy and physiology, fluctuations in the neurovascular response, and signal to noise ratio, can still vary between subjects and sessions (Arguirre et al., 1998).

The BOLD MR signal change associated with the activation task is conventionally identified from the beta parameter estimated with the general linear model during at the statistical analysis stage (Friston et al., 1995c). Since the signal from each voxel is scaled to a common global mean value of 100, the estimated size of BOLD effects is typically described as the percent MR signal change relative to the global mean intensity.

As shown in Figure 2-7, the mean BOLD response associated with right hand finger tapping in the individual data set (mean 3.8% ± 0.4), was significantly higher than the mean BOLD response associated with left hand tapping (mean 2.5% ± 0.3), as well as both right (mean 2.2% ± 0.3), and left (mean 2.3% ± 0.2) hand tapping in the group data set. Interestingly however, the estimated BOLD signal change from the individual data set was also variable, especially during right hand finger tapping in which the estimated BOLD response ranged from 1.9% to 5.3% of the global mean response. The BOLD response associated with left hand finger tapping also ranged substantially from 1.3% to 4.5%. In contrast, within the group data set, the range of estimated BOLD signal change associated with right and left hand finger tapping was comparatively small. For example, within the group data set the estimated BOLD response associated with hand finger tapping ranged from 1.2% to 3.8% of the mean global signal. Similarly, the BOLD response associated with left hand finger tapping ranged from

Figure 2-7. *The mean estimated BOLD signal change associated with right and left hand tapping in the individual and group data sets*

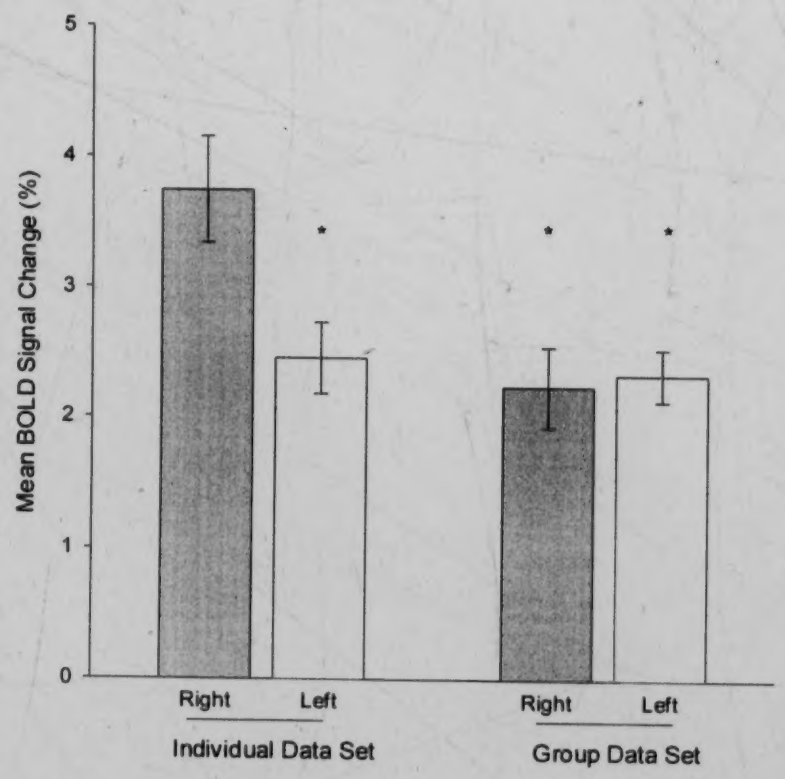

Figure 2-7. The estimated mean BOLD signal change (% signal change relative to global mean) during right (grey bars) and left (white bars) hand finger tapping in the individual and group data sets. * Denotes significance compared to the right hand tapping condition in the individual data set at $p<0.05$. [Error bars represent the standard error (SE)].

1.0% to 3.3% of the mean global signal.

This suggests that the intensity of the BOLD signal change can vary substantially between scanning sessions even within the same subject. While this may be indicative of imaging instabilities or problems with the signal to noise ratio, overall in both the group and individual data sets the range of BOLD contrast fMRI signal change during the motor task was within the range reported by previous EPI studies (reviewed by Turner et al., 1998).

2.3.3. Multi subject/session analyses

To explore the association between single subject and group activation, a test for significant motor activity within each data set was assessed using both fixed and random effects analysis. The anatomical location, cluster size, and Talairach coordinates (Talairach and Tournoux, 1988) of activation observed following fixed and random effects analyses of activity associated with right hand (Table 2-1) and left hand (Table 2-2) finger tapping in the individual data set are listed. Activation detected using fixed and random effects analysis of right and left hand tapping in the group data set are listed in Table 2-3.

A comparison of voxels that survived a probability threshold of $p<0.05$ following fixed and random effects analyses of both right and left hand finger tapping within the individual data set (Figure 2-8), and the group data set (Figure 2-9) are displayed on maximum intensity projection images. In addition, the results of fixed and random effects analyses from each group associated with right hand finger tapping (Figure 2-10) and left hand finger tapping (Figure 2-11), have been superimposed onto surface renderings of a standard brain.

Table 2-1. *Anatomical localization of activity associated with right hand finger tapping in the individual data set*

Analysis	Area	Cluster Size	Talairach Coordinates		
			x	*y*	*z*
Fixed Effects	Left Superior Temporal Gyrus	667	-64	-38	10
	Left Lentiform Nucleus				
	Left Insula				
	Left Postcentral Gyrus				
	Left Inferior Parietal Lobule				
	Left/ Right Cerebellum, Anterior Lobe	476	-13	-32	-10
	Left Parahippocampal Gyrus				
	Left Pre/Post Central Gyrus	335	-36	-30	65
	Right/Left Occipital Lobe	153	4	-92	-5
	Left Thalamus	94	-13	-13	15
	Left Superior/Middle Temporal Gyrus	61	-53	8	-10
	Left Inferior Frontal Gyrus				
	Left Precentral Gyrus				
	Right Thalamus	60	15	-6	15
Random Effects	Left Precentral Gyrus	40	-24	-19	75

Table 2-1. Cortical regions showing significant ($p<0.05$) activity associated with right hand finger tapping in the individual data set assessed using fixed and random effects analysis. The anatomical labels and cluster size corresponding to the peak voxel Talairach coordinates (Talairach and Tournoux, 1988) are reported. In cases where an active cluster included significantly active voxels in more than one cortical region, these additional regions are also listed under that cluster. The order of listing represents the relative size of activity.

Table 2-2. *Anatomical localization of activity associated with left hand finger tapping in the individual data set*

Analysis	Area	Cluster Size	Talairach Coordinates		
			x	*y*	*z*
Fixed Effects	Right Precentral/Postcentral Gyrus	1035	39	-19	50
	Right Superior/Middle Frontal Gyrus				
	Right Inferior Parietal Lobule				
	Right Insula	861	32	-13	5
	Right Superior Temporal Gyrus				
	Right Lentiform				
	Right/Left Cerebellum, Anterior Lobe	296	2	-49	0
	Right Occipital Lobe				
	Right Anterior Cingulate Gyrus	128	8	-9	50
	Right Inferior Parietal Lobule	84	56	-28	20
	Right Postcentral Gyrus				
	Right Superior Temporal Gyrus				
	Left Inferior Parietal Lobule	67	-53	-34	20
	Left Superior Temporal Gyrus				
	Left Postcentral Gyrus				
	Left Lentiform Nucleus	59	-26	-8	0
	Left Precentral Gyrus	44	-24	-21	75
	Right Middle Occipital Gyrus	43	17	-92	10
	Left Postcentral Gyrus	35	-51	-19	25
	Right Superior/Middle Temporal Gyrus	33	53	-47	10
	Right Occipital Lobe, Cuneus	25	9	-73	15
	Left Supramarginal Gyrus	20	-58	-56	25
	Left Superior Temporal Gyrus				
Random Effects	Right Precentral/Postcentral Gyrus	187	45	-17	65
	Right Inferior Parietal Lobule				
	Right Superior Temporal Gyrus	42	60	-8	5
	Right Postcentral Gyrus				
	Right Precentral/Postcentral Gyrus	30	39	-19	50
	Right Cerebellum, Anterior Lobe	21	4	-53	0

Table 2-2. Cortical regions showing significant ($p<0.05$) activity associated with left hand finger tapping in the individual data set assessed using fixed and random effects analysis. The anatomical labels and cluster size corresponding to the peak voxel Talairach coordinates (Talairach and Tournoux, 1988) are reported. In cases where an active cluster included significantly active voxels in more than one cortical region, these additional regions are also listed under that cluster. The order of listing represents the relative size of activity.

Table 2-3. *Anatomical localization of activity associated with right and left hand finger tapping in the group data set*

Analysis	Area	Cluster Size	Talairach Coordinates		
			x	*y*	*z*
Right Hand Tapping					
Fixed Effects	Left Precentral/Postcentral Gyrus	1691	-30	-26	70
	Left Inferior/Superior Parietal Lobule				
	Left Middle/Superior Frontal Gyrus				
	Left/Right SMA	52	-2	-15	50
	Left Anterior Cingulate Gyrus				
	Right SMA	48	8	-2	60
Random Effects	Left Precentral/Postcentral Gyrus	317	-41	-23	60
	Left Inferior Parietal Lobule				
	Left Superior Parietal Lobule	21	-30	-51	65
Left Hand Tapping					
Fixed Effects	Right Precentral/Postcentral Gyrus	1337	45	-23	60
	Right Inferior Parietal Lobule				
	Right SMA	191	8	-6	55
	Right Anterior Cingulate Gyrus				
	Right Inferior Parietal Lobule	136	58	-26	25
	Right Postcentral Gyrus				
	Right Superior Temporal Gyrus				
	Right Insula	20	49	-4	5
	Right Precentral Gyrus				
Random Effects	Right Precentral/Postcentral Gyrus	568	43	-35	40
	Right Inferior Parietal Lobule				

Table 2-3. Cortical regions showing significant ($p<0.05$) activity associated with right and left hand finger tapping in the group data set assessed using fixed and random effects analysis. The anatomical labels and cluster size corresponding to the peak voxel Talairach coordinates (Talairach and Tournoux, 1988) are reported. In cases where an active cluster included significantly active voxels in more than one cortical region, these additional regions are also listed under that cluster. The order of listing represents the relative size of activity.

Figure 2-8. *Fixed and random effects analysis of activity associated with right and left hand finger tapping across sessions in the individual data set*

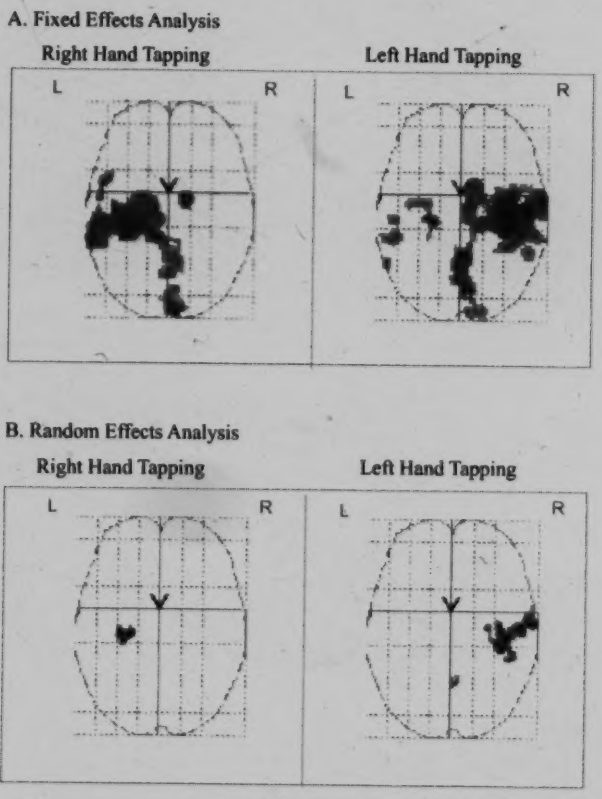

Figure 2-8. Maximum intensity projection (MIP) images showing the difference in activation associated with right and left hand finger tapping following a within group analysis of the data from the ten sessions in the individual data set using fixed effects analysis (A) and random effects analysis (B). Active voxels were significant at $p<0.05$.

Figure 2-9. *Fixed and random effects analysis of activity associated with right and left hand finger tapping across sessions in the group data set*

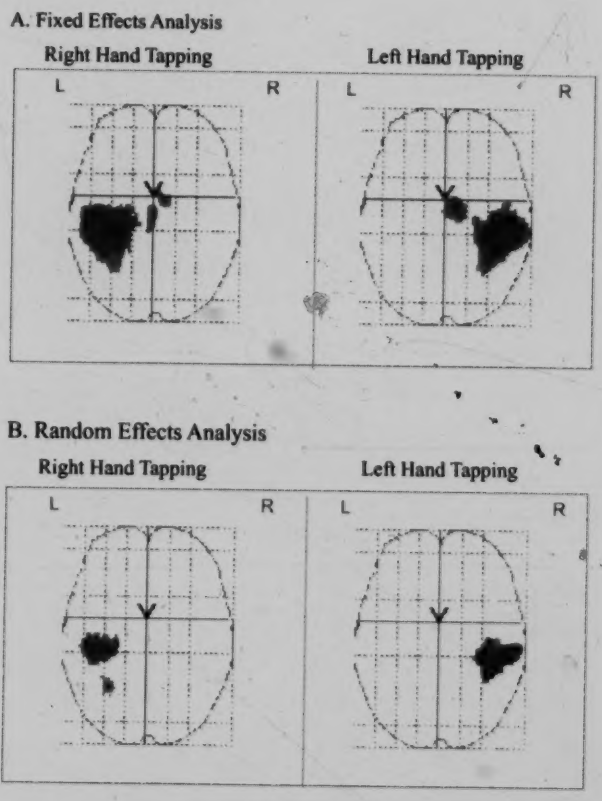

Figure 2-9. Maximum intensity projection (MIP) images showing the difference in activation associated with right and left hand finger tapping following a within group analysis of the data from the ten subjects in the group data set using fixed effects analysis (A) and random effects analysis (B). Active voxels were significant at $p<0.05$.

Figure 2-10. *Fixed and random effects analysis of activity associated with right hand finger tapping in the individual and group data sets*

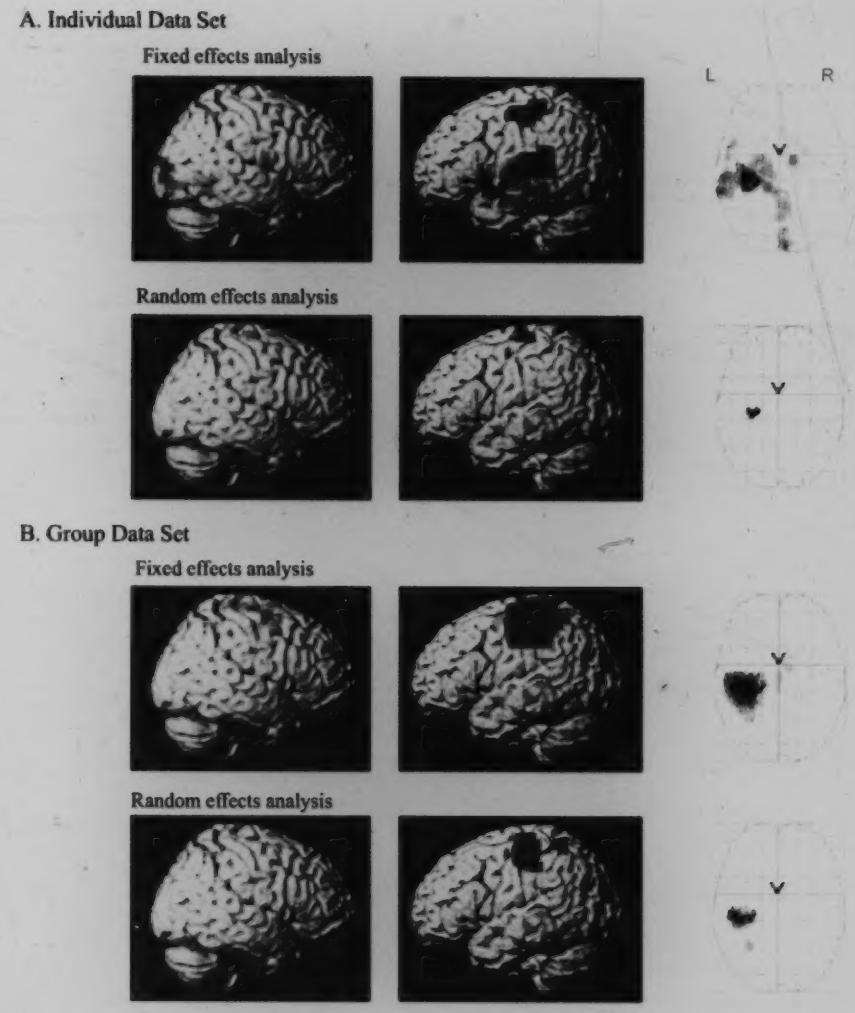

Figure 2-10. Activation associated with right hand finger tapping in the individual data set (A) and the group data set(B). Active voxels in each data set assessed using fixed and random effects analysis are shown superimposed ono surface renderings of the right and left hemispheres of a standardized brain with the corresponding MIP images. Surface rendering colour intensity was derived from the statistical value multiplied by an exponential decay function based on the distance of the active voxel from the surface of the brain.

Figure 2-11. *Fixed and random effects analysis of activity associated with left hand finger tapping in the individual and group data sets*

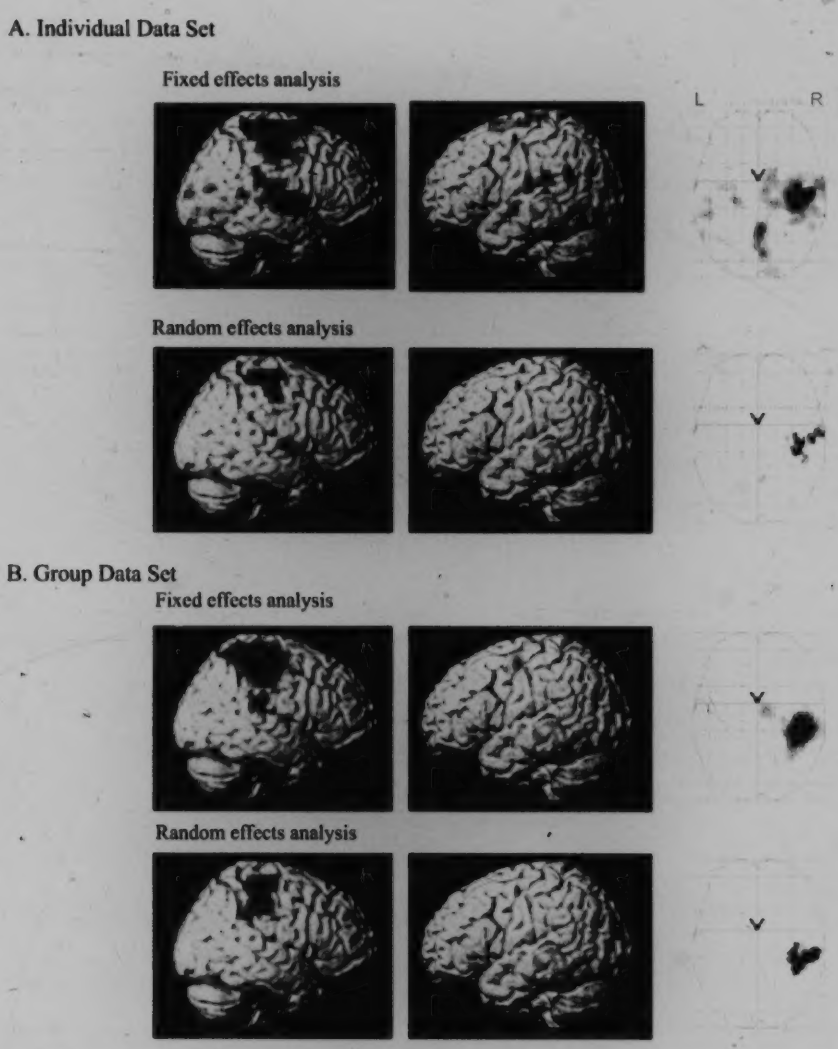

Figure 2-11. Activation associated with left hand finger tapping in the individual data set (A) and the group data set (B). Active voxels in each data set assessed using fixed and random effects analysis are shown superimposed onto surface renderings of the right and left hemispheres of a standardized brain with the corresponding MIP images. Surface rendering colour intensity was derived from the statistical value multiplied by an exponential decay function based on the distance of the active voxel from the surface of the brain.

While the results of each type of within group analysis are described in more detail in the following sections, in both fixed and random effects analyses, robust activity was observed in the contralateral precentral and postcentral gyri. This is consistent with the results from the single subject and session analyses, providing additional confirmation that BOLD contrast fMRI at 3T is a valid and sensitive tool for localizing cortical activity associated with repetitive finger tapping.

2.3.3.1. Fixed effects analyses

The traditional fixed effects analysis of the multi-subject and multi-session data sets was implemented in a similar manner as the single subject analysis. However, the data from every subject and session within the group was included in the estimation of the general linear model (Friston et al., 1995c). As such, the results from the fixed effects analysis are indicative of the average activity associated with the comparison. It is important to note that the results of the fixed effects analyses are generated based only on the average activity at each voxel, with no regard to the consistency of that response across subjects or sessions (Holmes et al., 1998).

Compared to the previously reported results of the independent analyses of right and left hand tapping in each of the ten sessions of the individual data set, as shown in Figure 2-8, the fixed effects analysis of the average activity across these ten sessions revealed much more widespread cortical activity. In addition to active voxels in the lateral and medial regions of the left frontal cortex and the left inferior parietal lobules, right hand finger tapping was also associated with large clusters of active voxels in the left lentiform nucleus, insula, and both the superior and middle temporal lobules, the right thalamus, and bilaterally in the cerebellum and occipital cortex. While left hand

finger tapping was associated with similar pattern of activation in the contralateral and posterior regions, additional activity was also detected in the ipsilateral precentral and postcentral gyri, inferior parietal lobule, superior temporal lobule, supramarginal gyrus, and lentiform nucleus.

Within the group data set, the fixed effects analysis of right and left hand tapping (Figure 2-9) showed large clusters of active voxels in the region surrounding the contralateral precentral and postcentral gyri. During right hand finger tapping, this dominant cluster of active voxels extended to the left inferior and superior parietal lobules, as well as the middle and superior frontal gyri. Additional clusters of active voxels associated with right hand finger tapping within the group data set were also detected in the left anterior cingulate gyrus, and bilaterally in the SMA. A similar pattern of activity was observed during left hand finger tapping within the group data set, with the dominant cluster of active voxels including voxels in the right precentral and postcentral gyri, inferior parietal lobule, superior temporal lobule and insula, along with a smaller cluster of active voxels in the right SMA.

While averaging observed responses has traditionally been a common method of summarizing and compare group imaging data, the results of this study show that a large number of voxels that were not significantly active in any of the independently analyzed data reached significance when the average group response was assessed with a fixed effects analysis. This demonstrates that the average responses within each data set were not representative of the typical activity across all subjects and sessions.

2.3.3.2. Random effects analyses

In contrast to fixed effects analysis, a random effects analysis is highly sensitive

to between subject or session variability. While interest in random effects analysis is relatively new in the field of functional neuroimaging, random effects analysis is useful for identifying consistent, rather than overall average, activity across subjects or sessions in a within group analysis (Holmes et al., 1998).

As shown in the comparison of fixed and random effects analysis of the individual data set (Figure 2-8) and the group data set (Figure 2-9), differences between fixed and random effects analysis are obvious. In each case, the random effects analysis is much more conservative. Specifically, in the individual data set the total number of active voxels within the whole brain associated with right hand finger tapping declined from 1846 after a fixed effects analysis, to only 40 after the random effects analysis. The respective voxel counts associated with left hand finger tapping also declined from 2730 to 80. In the group data set, a similar decline was observed as voxel counts declined from 1684 to 568 during right hand finger tapping, and from 1791 to 338 during left hand finger tapping.

Furthermore, compared to the fixed effects analyses, following a random effects analysis the activation associated with finger tapping in both the individual and group data sets was generally confined to the contralateral frontal and parietal regions. For example, in both the individual and group data sets activation associated with right hand finger tapping was observed in the left precentral gyrus, with additional activity in the left postcentral gyrus and inferior and superior parietal lobules in the group data set. Activity associated with left hand finger tapping was observed in the right precentral and postcentral gyri, and inferior parietal lobules in both the individual and group data sets, while activity was also detected in the superior temporal lobule and the anterior lobe of

the right cerebellum in the individual data set.

The relationship between the independently analyzed data to the fixed and random effects analysis of the group activity within each data set demonstrate the potential limitations of using a traditional fixed effects analysis to summarize group data. It is evident that unlike the fixed effects analysis, the results of the random effects analyses were representative of the typical activity within each group. Overall however, it is evident that strong motor activity in the primary cortical region was observed at every level of analysis.

2.4 Discussion

The results of this study provide valuable information regarding the feasibility and stability of fMRI of motor activity observed using a 3T imaging system. First, the results of this study demonstrated localization of cortical activity that was consistent with the known organization of the motor system, and previous functional neuroimaging studies (reviewed by Mattay and Weinberger, 1999). Second, while the spatial extent and amplitude of the BOLD response varied to a certain degree, there was no evidence of meaningful differences in either the mean size or amplitude of activation in data acquired from ten different subjects versus data acquired from one subject tested in ten sessions. This suggests that the consistency of activation across individuals and sessions was acceptable. Finally, while we have demonstrated that the technique was sensitive to the task of interest, in both data sets it was obvious that a random effects analysis is the most effective means of summarizing multisession and multisubject activation. This suggests that the results from more traditional fMRI studies that relied on fixed effects methods to average activity across groups should be interpreted with caution.

2.4.1. Activation of the motor cortex

The primary motor cortex has been shown to mediate the control of movement through the descending fibres of the pyramidal tract which terminate on motor neurons in the ventral horn of the spinal cord. Most of these corticospinal fibres decussate in the medulla and therefore innervate motor neurons that control the contralateral side of the body. (Nyberg-Hansen & Rinvik, 1962). The role of the contralateral motor cortex in the control of voluntary movement has been previously explored in PET and fMRI studies which have consistently demonstrated robust activity in the contralateral motor cortex during a variety of motor tasks (reviewed by Mattay and Weinberger, 1999). Furthermore, several studies have verified that the fMRI localization of motor activity acquired in pre-operative patients is consistent with direct surgical mapping of cortical motor activity (Jack et al., 1994; Puce et al., 1995; Yousry et al., 1995; Pujol et al., 1996; 1998; Tomczak et al., 2000).

As anticipated in light of the dominant role of the primary motor cortex in the control of voluntary movement and consistent findings from previous functional imaging studies, we observed strong activation in the contralateral motor cortex at every level of analysis. This indicates that the experimental protocol was effective, and may be useful for testing and verifying future more complex fMRI experimental protocols.

2.4.2. Activation of the somatosensory cortex

In addition to activity in the primary motor cortex, active voxels were also found in the contralateral somatosensory cortex in several subjects and sessions. Since both tactile sensation and proprioception are closely linked to voluntary movement, this finding is not unexpected. In fact, there is evidence that even with highly specific motor

and sensory tasks it is difficult to dissociate activity of the precentral and postcentral gyri. For example, activity in both the contralateral primary somatosensory and motor cortices were reported during continuous tactile stimulation of the palm with no movement (Yetkin et al., 1995). Furthermore, both regions were also active during finger to thumb tapping when subjects touched the fingertip with the thumb, and when the same movements were performed without touching the fingertips (Jansma et al., 1998). Aside from the involvement of somatosensory and proprioceptive feedback in the control of voluntary movement, it is also possible that the inability to distinguish between the adjacent gyri is influenced by the low resolution of echo planar imaging (EPI) fMRI images (Edelman et al., 1994).

2.4.3. Activation of other cortical regions

While the dominant clusters of active voxels in the independently analyzed data were localized to the primary cortical regions, following the fixed effects group analyses smaller clusters of active voxels were also detected in several other regions. This included the SMA and anterior cingulate gyrus, which were shown in previous studies to be preferentially active during more complex sequential movements (Rao et al., 1993; Shibasaki et al., 1993; Boecker et al., 1998).

Since the motor tasks in this study were repetitive, the demands of both movement programming and execution should have been minimal. It is important to note however, that with a few exceptions, additional activity was only detected within each data set following fixed effects analyses of the average response across subjects or sessions. For example, following fixed effects analyses in both data sets, active voxels were distributed throughout the contralateral frontal, parietal, and temporal lobules. In

addition, within the individual data set, activity in the ipsilateral cortex and in the occipital and cerebellar regions, that was detected in only a few sessions, was remarkably strong during both right and left hand tapping following the fixed effects analysis. In contrast, the results of the random effects analysis were more closely representative of the typical activity in each subject or session. As previously demonstrated by McGonigle et al., (2000), this illustrates a limitation of using a traditional fixed effects analysis to summarize multisubject or multisession data.

2.4.4. Variability

While fMRI data is typically used to identify significant differences in the MR signal between distinct tasks or groups, there is a certain degree of unavoidable variability in the MR signal that is unrelated to the experimental question. This variability (reviewed by Turner et al., 1998), can be associated with individual differences in the size and location of various sulci within the brain, as well as small intra-individual fluctuations in neurovascular response. Between scanning sessions there is often additional variability associated with image acquisition and processing procedures (such as re-positioning of subject within the scanner/ signal to noise ratio, head motion, and hardware or system stability).

Although several test-retest studies reported that the size of activation was more reliable than the location of activation, the location of active voxels were defined by the specific x, y, z spatial coordinates of the voxels (Yetkin et al., 1996; Rombouts et al., 1997, 1998, Miki et al., 2000). For example if the location of an active voxel varied by 1 mm along one axis, it was not classified as a replicated response even though the activity from each session was still localized to the same anatomical region. Conclusions based

on this type of reliability assessment are therefore limited, since in most experimental applications fMRI activation is localized to anatomical structures, not specific spatial coordinates. Furthermore, the reproducibility ratios used in these studies only concerned reproducibility between two or three trials with no consideration of chance variability.

In the present study, the independently analyzed data show that while the anatomical localization of activation associated with repetitive finger tapping was relatively consistent, there were obvious variations in the spatial extent of activity between subjects and sessions. In fact, even in data from the same subject, the numbers of active voxels throughout the whole brain and within the sensorimotor region varied substantially across sessions. Since there was no evidence of any change in task performance, differences in activation in the primary cortical regions was likely influenced by either natural fluctuations in individual neurovascular response or technical issues related to data acquisition. These limitations will be explored in more detail in the general discussion.

As expected due to the repetitive nature of the task, in both data sets the most consistent activity was detected in the contralateral primary sensorimotor cortex. However, although in both data sets smaller clusters of activity were occasionally observed in other regions, there was no evidence that the data acquired from ten different subjects was more variable than data acquired from a single subject tested in ten sessions. Furthermore, the results also demonstrate that small differences in the relative variability within each data set did not affect the activity detected when the each data set was analyzed as a group using random effects analyses.

2.4.5. Conclusions

The results of this study have demonstrated the feasibility of investigating motor activity at 3T. In summary, while it is evident that a random effects analysis was the optimal method of summarizing multi-subject or multi-session data, the independent analyses of single subject and single session data provides more detail about the consistency of activation. It is difficult to quantitatively assess the validity and reliability of BOLD contrast fMRI since the true neuronal activity underlying the observed BOLD signal is unknown. However, during both right and left hand tapping robust activity was detected in the contralateral sensorimotor cortex in every subject and session. In addition, there was no evidence that the data acquired from multiple subjects was more variable than data acquired from a single subject tested over several sessions. This suggests that the validity and consistency of the data was acceptable. Recent developments with combined intracellular recording and fMRI in primates (Logothetis et al., 2001), will undoubtedly contribute to our understanding of the neuronal activity associated with BOLD contrast signal, allowing for a more accurate assessment of the quality and precision of fMRI data.

2.5. References

Aguirre GK, Zarahn E, D'Esposito M. The variability of human BOLD hemodynamic responses. Neuroimage 1998; 8: 360-69.

Ashburner J, Friston KJ. Nonlinear spatial normalization using basis functions. 1999; 7: 254-66.

Boecker H, Dagher A, Ceballos-Baumann AO, Passingham RE, Samuel M, Friston KJ, Poline JB, Dettmers C, Conrad B, Brooks DJ. Role of the human rostral supplementary motor area and the basal ganglia in motor sequence control. J Neurophysiol 1998; 79; 1070-80.

Edelman RR, Wielopolski P, Schmitt F. Echo-planar MR imaging. Radiology 1994; 192: 600-12.

Field AS, Yen Y-F, Burdette JH, Elster AD. False cerebral activation on BOLD functional MR images: Study of low-amplitude motion weakly correlated to stimulus. Am J Neuroradiol 2000; 21: 1388-96.

Friston KJ, Ashburner J, Frith CD, Poline JB, Heather JD, Frackowiak RS. Spatial registration and normalization of images. Hum Brain Mapp 1995a; 3: 165-89.

Friston KJ, Holmes AP, Poline JB, Grasby PJ, Williams SCR, Frackowiak RSJ, Turner R. Analysis of fMRI time-series revisited. Neuroimage 1995b; 2: 45-53.

Friston KJ, Holmes AP, Worsley KJ, Poline JB, Frith CD, Frackowiak RSJ. Statistical parametric maps in functional imaging: a general linear approach. Hum Brain Mapp 1995c; 2: 189-210.

Friston KJ, Williams S, Howard R, Frackowiak RSJ, Turner R. Movement related effects in fMRI time series. Mag Res Med 1996; 35: 346-55.

Friston KJ, Josephs O, Zarahn E, Holmes AP, Rouquette S, Poline JB. To smooth or not to smooth. Neuroimage 2000; 12: 196-208.

Hajnal JV, Mayers R, Oatridge A, Schwieso JE, Young JR, Bydder GM. Artifacts due to stimulus correlated motion in functional imaging of the brain. Magn Reson Med 1994; 31: 289-91.

Holmes AP, Friston KJ. Generalisability, random effects and population inference. Neuroimage 1998; 7: 124.

Jack CR, Thompson RM, Butts RK, Sharbrough FW, Kelly PJ, Hanson DP, Riederer SJ, Ehman RL, Hangiandreou NJ, Cascino GD. Sensory motor cortex: correlation of

presurgical mapping with functional MR imaging and invasive cortical mapping. Radiology 1994; 190: 85-92.

Jansma JM, Ramsey NF, Kahn RS. Tactile stimulation during finger opposition does not contribute to 3D fMRI brain activity pattern. Neuroreport 1998; 16: 501-5.

Jezzard P, Song AW. Technical foundations and pitfalls of clinical fMRI. Neuroimage 1996; 4: S63-S75.

Jezzard P, Clare S. Sources of distortion in functional MRI data. Hum Brain Mapp 1999; 8: 80-5.

Kim SG, Ashe J, Hendrich K, Ellermann JM, Merkle H, Ururbil K, Georgopoulos AP. Functional magnetic resonance imaging of motor cortex: hemisphere asymmetry and handedness. Science 1993; 261: 615-17.

Logothetis KS, Pauls J, Augath M, Trinath T, Oeltermann A. Neurophysiological investigation of the basis of the fMRI signal. Nature 2001; 412: 150-57.

Mattay VS, Weinberger DR. Organization of the human motor system as studied by functional magnetic resonance imaging. Eur J Radiol 1999; 30: 105-14.

McGonigle DJ, Howseman AM, Athwal BS, Friston KJ, Frackowiak RSJ, Holmes AP. Variability in fMRI: an examination of intersession differences. Neuroimage 2000; 11: 708-34.

Miki A, Raz J, Van Erp TGM, Liu CSJ, Haselgrove JC, Liu GT. Reproducibility of visual activation in functional MR imaging and effects of postprocessing. Am J Neuroradiol 2000; 21: 910-15.

Nyberg-Hansen R, Rinvik E. Some comments on the pyramidal tract, with special reference to its individual variations in man. Acta Neurol Scand 1965; 39: 1-30.

Puce A, Constable RT, Luby ML, McCarthy G, Nobre AC, Spencer DD, Gore JC, Allison T. Functional magnetic resonance imaging of sensory and motor cortex: comparison with electrophysiological localization. J Neurosurg 1995; 83: 262-70.

Pujol J, Conesa G, Deus J, Vendrell P, Isamat F, Zannoli G, Marti-Vilalta JL, Capdevila A. Presurgical identification of the primary sensorimotor cortex by functional magnetic resonance imaging. J Neurosurg 1996; 84: 7-13.

Pujol J, Conesa G, Deus J, Lopez-Obarrio L, Isamat F, Capdevila A. Clinical application of functional magnetic resonance imaging in presurgical identification of the central sulcus. J Neurosurg 1998; 88: 863-69.

Ramsey NF, Tallent K, Van Gelderen P, Frank JA, Moonen CTW, Weinberger DR. Reproducibility of human 3D fMRI brain maps acquired during a motor task. Hum Brain Mapp 1996; 4: 113-21.

Rao SM, Binder JR, Bandettini PA, Hammeke TA, Yatkin FZ, Jesmanowicz A, Lisk LM, Morris GL, Mueller WM, Estkowski et al. Functional magnetic resonance imaging of complex human movements. Neurology 1993; 43: 2311-18.

Rombouts SARB, Barkhof F, Hoogenraad FGC, Spenger M, Valk J, Scheltens P. Test-retest analysis with functional MR of the activated area in the human visual cortex. Am J Neuroradiol 1997; 18: 1317-22.

Rombouts SARB, Barkhof F, Hoogenraad, FGC, Sprenger M, Scheltens P. Within-subject reproducibility of visual activation patterns with functional magnetic resonance imaging using multislice echo planar imaging. Magn Reson Imag 1998; 16: 105-13.

Scholz VH, Flaherty AW, Kraft E, Keltner JR, Kwong KK, Chen YI, Rosen BR, Jenkins BG. Laterality, somatotopy and reproducibility of the basal ganglia and motor cortex during motor tasks. Brain Res 2000; 879: 204-15.

Shibasaki H, Sadato N, Lyshkow H, Yonekura Y, Honda M, Nagamine T, Sywazono S, Magata Y, Ikeda A, Miyazaki M. Both primary motor cortex and supplementary motor area play an important role in complex finger movement. Brain 1993; 116: 1387-98.

Solodkin A, Hlustik P, Noll DC, Small SL. Lateralization of motor circuits and handedness during finger movements. Eur J Neurol 2001; 8: 425-34.

Talairach P, Tournoux J. A Stereotactic Coplanar Atlas of the Human Brain. 1988; Thieme, Stuttgart.

Tegeler C, Strother SC, Anderson JR, Kim SG. Reproducibility of BOLD-based functional MRI obtained at 4T. Hum Brain Mapp 1999; 7: 267-83.

Tomczak RJ, Wunderlich AP, Wang Y, Braun V, Antoniadis G, Gorich J, Richter HP, Brambs HJ. FMRI for preoperative neurosurgical mapping of motor cortex and language in a clinical setting. J Comput Assist Tomogr 2000; 24: 927-34.

Turner R, Howseman A, Rees GE, Josephs O, Friston K. Functional magnetic resonance imaging of the human brain: data acquisition and analysis. Exp Brain Res 1998; 123: 5-12.

Worsley KJ, Friston KJ. Analysis of fMRI time-series revisited- again. Neuroimage 1995; 2: 173-81.

Worsley KJ, Poline JB, Vandal AC, Friston KJ. Tests for distributed, nonfocal brain activations. Neuroimage 1995; 2: 183-94.

Yetkin FZ, Mueller WM, Hammeke TA, Morris GL, Haughton VM. Functional magnetic resonance imaging mapping of the sensorimotor cortex with tactile stimulation. Neurosurgery 1995; 36: 921-25.

Yetkin FZ, McAuliffe TL, Cox R, Haughton VM. Test-retest precision of functional MR in sensory and motor task activation. Am J Neuroradiol 1996; 17: 95-98.

Yousry TA, Schmid UD, Jassoy AG, Schmidt D, Eisner WE, Reulen HJ, Reiser MF, Lissner J. Topography of the cortical motor hand area: prospective study with functional MR imaging and direct motor mapping at surgery. Radiology 1995; 195: 23-9.

3. FMRI OF MOTOR ACTIVITY IN PATIENTS WITH PARKINSON'S DISEASE AND HEALTHY AGE-MATCHED CONTROL SUBJECTS

3.1. Introduction

The primary objective of the present study was to compare the cortical activity detected using BOLD fMRI at 3T in groups of patients with early Parkinson's disease (PD) and age-matched control subjects during performance of a repetitive motor task with the right and left hands. PD is a progressive neurodegenerative disorder associated with impaired motor ability. Patients with PD experience muscle rigidity and slowness of movement that is particularly severe during self-initiated sequences of movement, while movements that are guided by sensory cues are relatively unimpaired (Benecke et al., 1987; Georgiou et al., 1994).

Functional imaging studies comparing patients with early PD to healthy aged matched control subjects have consistently shown changes in cortical activation associated with the disease. The most prevalent finding has been relative hypoactivity of the SMA in patients during performance of movements that are self-directed or not guided by any visual or auditory sensory cues. This includes sequences of movements that are performed from memory (Rascol et al., 1992, 1994, 1997; Samuel et al., 1997a; Sabatini et al., 2000; Haslinger et al., 2000), and tasks where the direction (Playford et al., 1992) or timing (Jahanashahi et al., 1995) of movements were freely selected by patients.

SMA activity has been shown to return to the level of healthy control subjects in PD patients following pharmacological (Jenkins et al., 1992; Rascol et al., 1992, 1994; Haslinger et al., 2001) and surgical treatment (Ceballos-Baumann et al., 1994, 1999;

Grafton et al., 1995; Davis et al., 1997; Samuel et al., 1997b; Bluml et al., 1999; Piccini et al., 2000). As previously discussed, impaired SMA activation in patients with PD is consistent with the pathology and symptoms of PD. More recently however, several studies have shown that in addition to impaired SMA activity, patients with PD also exhibit relatively increased activity in several regions including the lateral premotor cortex, parietal cortex, cerebellum, bilateral primary motor cortex, and caudal SMA (Rascol et al., 1997; Samuel et al., 1997a; Sabatini et al., 2000; Haslinger at al., 2001). It has been suggested that this hyperactivity in PD patients is associated with functional compensation for disrupted striatal motor pathways. At this time however, the basis for this compensation is not known. It is possible that despite the lack of observable impairments in task performance (i.e., rate or amplitude), there are differences in the cognitive and physiological demands of the task for PD patients and age-matched control subjects.

Previous functional imaging studies of motor activation in PD patients have only looked at activity associated with complex sequential motor tasks, either sequential finger tapping (Rascol et al., 1992. 1994, 1997; Samuel et al., 1997a; Jahanashahi et al., 1995; Sabatini et al., 2000) or freely selected joystick movement (Playford et al., 1992; Haslinger et al., 2001). In addition, it is unclear if abnormal motor activation in PD patients is associated only with tasks performed with the akinetic hand. In an effort to fully characterize cortical activation associated with repetitive motor task in PD patients and age-matched control subjects, the data from each control subject and PD patient in this study were first analyzed individually, followed by both fixed and random effects analyses of group effects. The inclusion of single subject analyses provided insight into

the reproducibility of activity in PD patients and age-matched control subjects, while simultaneously verifying the validity of the data.

3.2. Methods

3.2.1. Subjects

Six right handed patients diagnosed with early PD (four male, two female, mean age 56.5 ± 5.21 years) were studied. Data from one additional PD patient was discarded due to severe motor impairment, while two other patients withdrew from the study prior to scanning due to difficulties unrelated to the disease. The clinical details of the patients that were studied are shown in Table 3.1. All patients were studied in the 'off' condition, and when applicable patients were instructed to ensure that they avoided taking levodopa at least 8 hours prior to their visit to the research centre. At the time of testing observed neurological symptoms in PD patients ranged from undetectable to mild unilateral resting tremor.

Six right handed healthy control subjects (four male, two female, mean age 55.5 ± 3.06 years) were also studied. A brief medical history interview conducted prior to testing confirmed that the healthy control subjects had no history of neurological or psychiatric disease. Informed consent was obtained from all PD patients and control subjects. This study received ethical approval from the Health Research Ethics Committee of the Faculty of Medicine.

3.2.2. Motor task, experimental design, data acquisition, and analyses

The motor task, experimental design, data acquisition, and analysis implemented in this study were described in Sections 2.2. in the previous chapter. In the present study, the data from the each of the six PD patients and control subjects were first

Table 3-1. *Clinical characteristics of patients with Parkinson's disease*

Patient	Age (years)	Disease Duration (years)	Medication	Hoehn & Yahr
1 (F)	72	5.5	none	2
2 (M)	73	4.5	levodopa	2.5
3 (M)	53	4	levodopa	2
4 (M)	50	2	none	1.5
5 (M)	47	5	levodopa	1
6 (F)	44	1.5	none	1

Abbreviations: M = male; F = female.

analyzed independently with a standard single subject analysis. The results of the single subject analyses were assessed first through visual inspection, and in more detail by quantifying the number of active voxels within the whole brain, the number of active voxels within the motor region, and the percent BOLD signal change associated with the task relative to rest. ANOVA with Bonferroni post hoc analysis was used to identify any significant differences in these measures between the group of control subjects and PD patients. In addition, the data from the PD patients and control subjects were analyzed as separate groups using both fixed and random effects models. Finally, the contrast images from each individual analysis was entered into a two-sample t-test to identify significant differences between PD patients and control subjects. Significance for the ANOVA and t-tests were accepted at the level of $p<0.05$.

3.3. Results

3.3.1. Task performance

Following task instructions and a brief practice session all control subjects and PD patients were able to perform the tapping task with ease. During every scanning run the rate and amplitude of finger tapping were observed from the control room to ensure that every subject consistently performed the task according to the given instructions. There were no observed variations in task performance during any of the scanning sessions in PD patients or control subjects.

3.3.2. Head movement

Although it is difficult to specifically measure head movement during a standard fMRI experiment, the estimated image realignment transformations were developed to correct any differences in image location related to head movement (Friston et al., 1996).

While the estimated realignment parameters are actually descriptions of the corrections that were made to realign each image in the time series, the severity of the required correction are indicative of the relative stability of the image location throughout the time series. As such we chose to explore these parameters in order to determine if there were any significant differences in image stability. An ANOVA ($p<0.05$) was used to test for significant differences in the mean and maximum realignment parameters between control subjects and PD patients during left and right hand tapping. As shown in Figure 3-1, there were no significant differences in the mean degree of movement or maximum head movement between tasks or groups. In fact, the mean estimated realignment parameters were similar during finger tapping with the right and left hands in both the control subjects and PD patients. In both groups however, mean estimated realignment parameters were slightly greater when the task was performed with the left hand.

3.3.3. Single subject analyses

Data from each control subject and PD patient was first analyzed independently. Voxels that survived a threshold of $p<0.05$ are shown on maximum intensity projections in Figure 3-2.

3.3.3.1. Location of activity

Upon visual inspection it is evident in each of the PD patients and control subjects that the majority of active voxels were located in the contralateral sensorimotor cortex. As shown in Figure 3-2b, activation associated with right hand tapping in the control subjects was well localized to the precentral and postcentral gyri. In contrast, during left hand tapping most of the control subjects showed additional activity in the

Figure 3-1. *Maximum and mean estimated head movement associated with right and left hand finger tapping in PD patients and control subjects.*

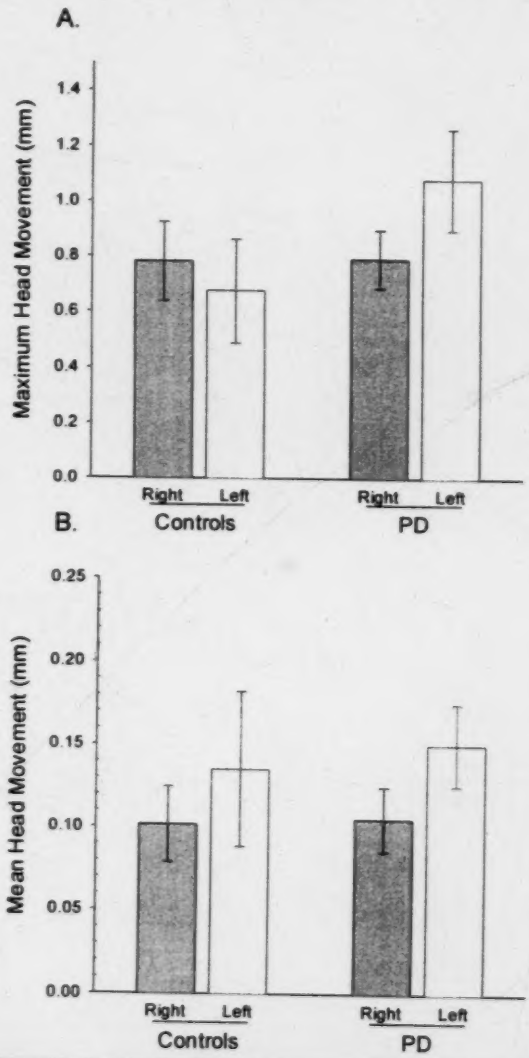

Figure 3-1. The maximum (A) and mean (B) head movement (mm) as estimated from the image realignment parameters associated with right (grey bars) and left (white bars) hand finger tapping were not significantly different in PD patients and controls at $p<0.05$. [Error bars represent the standard error (SE)].

Figure 3-2. *MIP images of activity associated with right and left hand finger tapping from each subject in the PD and control groups*

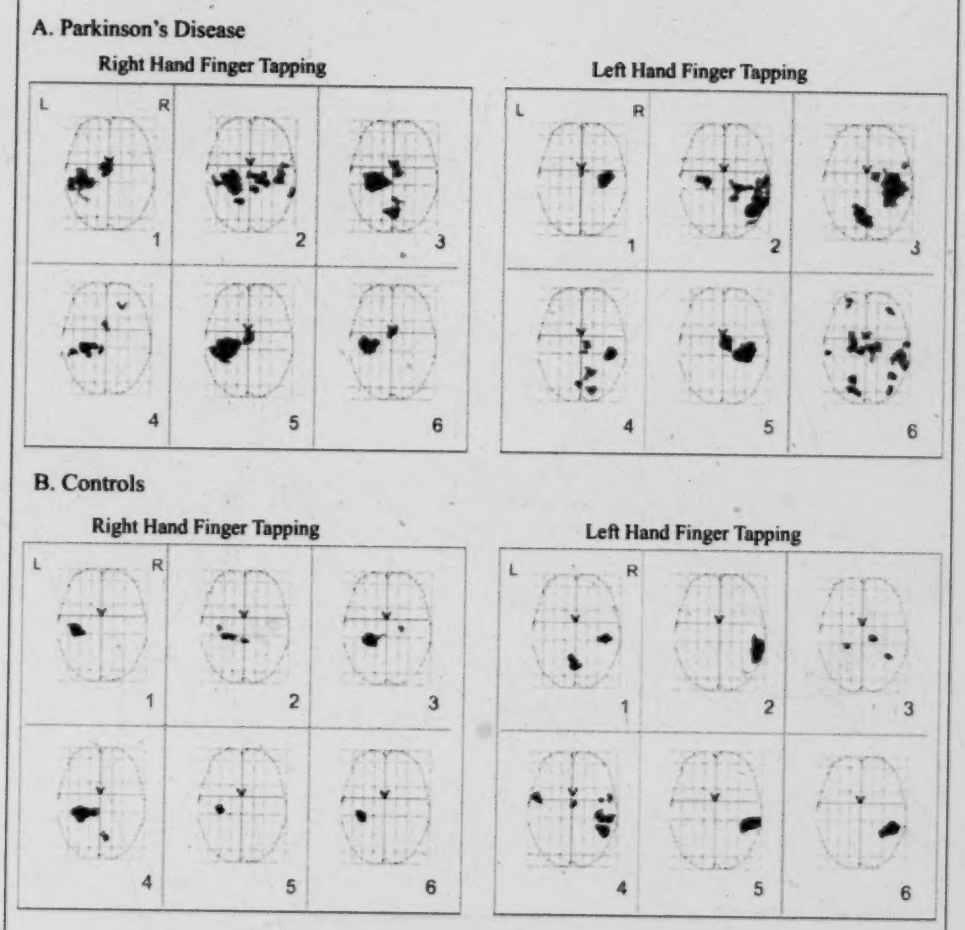

Figure 3-2. Maximum intensity projection (MIP) images showing active voxels associated with right and left hand finger tapping in each of the six PD patients labelled 1 through 6 (A), and each of the six healthy aged matched control subjects labelled 1 through 6 (B). Active voxels were significant at $p<0.05$.

superior temporal gyrus and inferior parietal lobule, while two subjects also showed activity in the SMA and ipsilateral motor cortex.

In the PD patients, activity associated with both right and left hand tapping was more widely distributed throughout the cortex (Figure 3-2a). For example, in addition to large voxel clusters in the sensorimotor cortex, clusters of active voxels in the SMA and anterior cingulate gyrus were detected in every PD patient. In addition, activation in the ipsilateral cortex was found in one subject during right hand tapping and in two subjects during left hand tapping. Cerebellar activity was also observed in some control subjects and PD patients during both right and left hand tapping.

3.3.3.2. Spatial extent of activation

In order to fully characterize the data from single subject analyses in PD patients and control subjects, the mean spatial extent of cortical motor activity in each group was compared (Figure 3-3). Variability in the spatial extent of activity within and between the groups of PD patients and control subjects was assessed by quantifying both the total number of significantly active voxels within the whole brain and within a sensorimotor region of interest which included the contralateral primary somatosensory and motor cortices. Due to the relatively low spatial resolution of EPI images, the regional voxel count also included all active voxels that were contiguous with active voxels in the precentral and postcentral gyri.

Although the majority of active voxels in control subjects were located within the sensorimotor area, there was a rather large range of total and regional voxel counts. Within the group of control subjects the total number of active voxels associated with right hand finger tapping ranged from 28 to 392 voxels (mean 188.3 ± 55.4), while the

Figure 3-3. *The mean spatial extent of activity associated with right and left hand finger tapping in PD patients and control subjects*

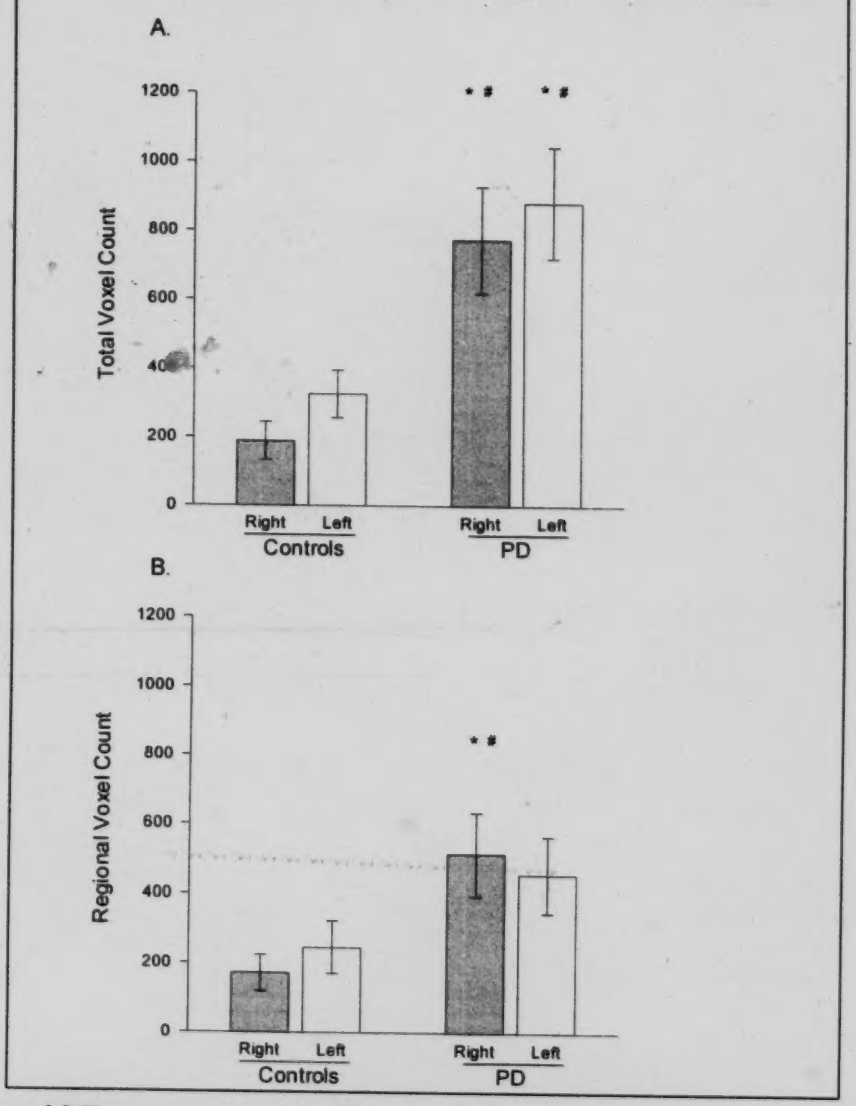

Figure 3-3. The mean size of activity within the whole brain (A) and within the sensorimotor regions (B), associated with right (grey bars) and left (white bars) hand finger tapping were both significantly greater in the group of PD patients compared to controls. In both (A) and (B), mean voxels counts significantly greater than those associated with right hand tapping in controls is indicated by the symbol *, while # denotes voxel counts sigificantly greater than those associated with left hand tapping in controls. Significance was accepted at $p < 0.05$. [Error bars represent the standard error (SE)].

voxel count within the sensorimotor region ranged from 28 to 355 voxels (mean 171.1 ± 52.7). This is consistent with the image appearance, where with a few minor exceptions all active voxels were located in either the precentral or postcentral gyri. During left hand tapping the total number of active voxels ranged from 92 to 491 voxels (mean 325.5 ± 68.6) and the size of activation within the sensorimotor region ranged from 44 to 491 voxels (mean 246.0 ± 75.9).

Within the group PD patients, the total number of active voxels observed during right hand finger tapping ranged from 293 to 1236 voxels (mean 770.8 ± 155.0), while the size of activation in the contralateral sensorimotor region ranged from 135 to 1004 voxels (mean 513.5 ± 119.5). During left hand finger tapping the total number of active voxels ranged from 403 to 1341 voxels (mean 879.5 ± 161.8) and the size of activation in the contralateral sensorimotor region ranged from 159 to 828 voxels (mean 455.5 ± 108.8).

An analysis of variance indicated that there were significant differences between the groups of PD patients and control subjects in both the mean total ($p=0.001$) and regional voxel counts ($p=0.05$) (Figure 3-3). Post-hoc tests verified that the mean total voxel count associated with right hand tapping and left hand tapping in the group of PD patients was significantly greater than the mean total voxel count associated with right ($p=0.003$; $p=0.001$) and left ($p=0.017$; $p=0.004$) hand tapping in the group of control subjects. In addition, the mean regional voxel count associated with right hand tapping in the group of PD patients was significantly greater than the mean regional voxel count associated with both right ($p=0.017$) and left hand tapping ($p=0.043$) in the group of

control subjects. Although the mean regional voxel count associated with left hand tapping in the group of control subjects was also substantially lower than that of the group of PD patients, the difference was not significant at the $p<0.05$ level.

3.3.3.3. Amplitude of BOLD response

To identify all potential sources of data variability across groups, we also examined the mean estimated percent BOLD signal change, associated with finger tapping in each group. As shown in Figure 3-4, in the group of control subjects the mean estimated BOLD response was similar during right and left hand finger tapping. The mean estimated BOLD response associated with right hand finger tapping ranged from 1.0% to 2.8% (mean 1.5% ± 0.3) of the mean global signal, while the response associated with left hand finger tapping ranged from 0.8% to 2.1% (mean 1.3% ± 0.2) of the mean global signal.

In contrast, the mean estimated BOLD response in the group of PD patients was more variable, especially during right hand finger tapping in which the response ranged from 0.7% to 1.9% (mean 1.3% ± 0.2) of the global mean response. The BOLD response associated with left hand finger tapping also ranged from 1.2% to 1.9% (mean 1.6% ± 0.13). While the overall range of estimated BOLD response associated with right and left hand tapping was lower in the group of PD patients relative to control subjects, there were no significant differences in the mean response between groups or tasks.

Figure 3-4. *The mean estimated BOLD signal change associated with right and left hand finger tapping in PD patients and control subjects*

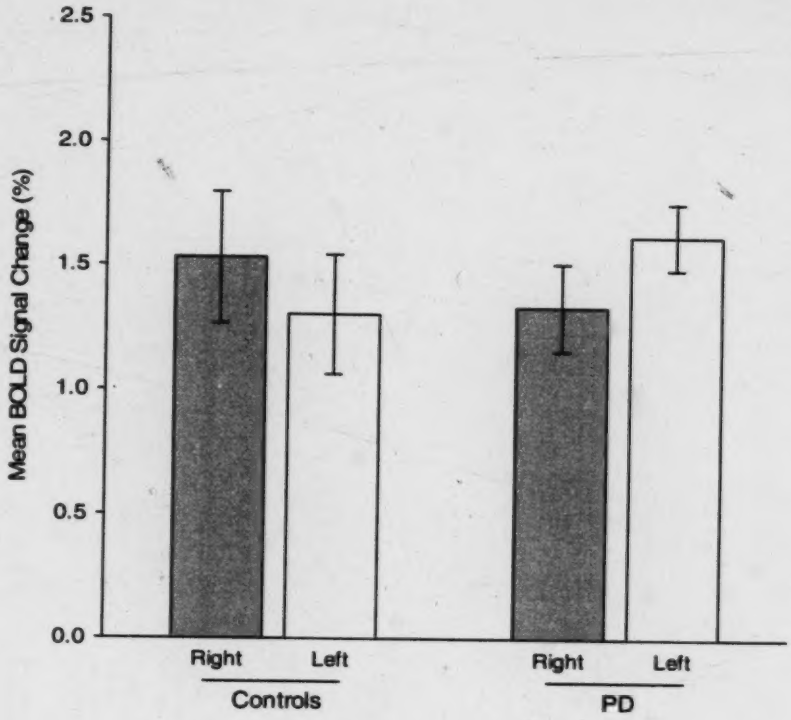

Figure 3-4. The estimated mean BOLD signal change (% signal change relative to global mean) during right (grey bars) and left (white bars) hand finger tapping in PD patients and healthy controls. There were no significant differences between the tasks or groups at $p<0.05$. [Error bars represent the standard error (SE)].

3.3.4. Group analyses

To explore the association between single subject and group activation in the PD patients and control subjects, a test for significant motor activity within each data set was assessed using both fixed and random effects analysis. The anatomical location, cluster size, and Talairach coordinates (Talairach and Tournoux, 1988) of activation observed following fixed and random effects analyses of activity associated with right hand (Table 3-2) and left hand (Table 3-3) finger tapping in the group of PD patients are listed. Activation detected using fixed and random effects analysis of right and left hand tapping in the group of control subjects are listed in Table 3-4.

A comparison of voxels that survived a probability threshold of $p<0.05$ following fixed and random effects analyses of both right and left hand finger tapping within the group of PD patients (Figure 3-5) and control subjects (Figure 3-6) are displayed on maximum intensity projection images. In addition, to directly compare the data of the PD patients and control subjects, the results of fixed and random effects analyses associated with right hand finger tapping (Figure 3-7), and left hand finger tapping (Figure 3-8), are shown superimposed onto surface renderings of a standard brain.

Once again, in both PD patients and control subjects, activity was primarily localized to the cerebral hemisphere contralateral to the hand that was active. This is consistent with the results from the single subject and session analyses, providing additional confirmation that BOLD contrast fMRI at 3T is a valid and sensitive tool for localizing cortical activity associated with repetitive movement. The results of each type of within group analysis are described in more detail in the following sections.

Table 3-2. *Anatomical localization of activity associated with right hand finger tapping in the group of PD patients*

Analysis	Area	Cluster Size	Talairach Coordinates		
			x	*y*	*z*
Fixed Effects	Left Precentral/Postcentral Gryus	7535	-36	-23	55
	Right/Left SMA				
	Right/Left Anterior Cigulate Gyrus				
	Right Precentral/Postcentral Gyrus				
	Left Superior Temporal Gyrus				
	Left Inferior/Superior Parietal Lobule				
	Left Middle/Inferior Frontal Gyrus				
	Right Precentral/Postcentral Gyrus	306	60	-30	30
	Right Inferior Parietal Lobule				
	Right Superior Temporal Gyrus				
	Left Superior/Middle Frontal Gyrus	93	-23	45	35
	Left Middle/Inferior Frontal Gyrus	91	-28	47	-5
	Right Inferior/Superior Parietal Lobule	81	32	-62	45
	Right Supramarginal Gyrus				
	Right Middle Temporal Gyrus	69	36	-62	20
	Right Parietal Lobule, Precuneus				
	Right Lentiform Nucleus	67	28	-13	-5
	Right Parahippocampal Gyrus				
	Right Postcentral Gyrus	43	49	-32	50
	Right Inferior Parietal Lobule				
	Right Inferior Frontal Gyrus	41	43	28	10
	Left Parietal Lobe, Precuneus	40	-13	-75	35
	Left Middle Frontal Gyrus	31	-36	24	30
	Right Lentiform Nucleus	26	26	2	5
	Right Cerebellum, Anterior Lobe	24	6	-51	-10
	Right Paracentral Lobule	22	17	-41	50
Random Effects	Left Precentral/Postcentral Gyrus	50	-30	-24	45
	Left Precentral/Postcentral Gyrus	44	-36	-32	65
	Right/Left Anterior Cingulate Gyrus	33	0	-4	50
	Right Supramarginal Gyrus	23	41	-45	30
	Right Inferior Parietal Lobule				
	Left Inferior Parietal Lobule	23	-39	-47	55
	Left Superior Parietal Lobule	20	-23	-60	55

Table 3-2. Cortical regions showing significant ($p<0.05$) activity associated with right hand finger tapping in the group of PD patients assessed using fixed and random effects analysis. The anatomical labels and cluster size corresponding to the peak voxel Talairach coordinates (Talairach and Tournoux, 1988) are reported. In cases where an active cluster included significantly active voxels in more than one cortical region, these additional regions are also listed under that cluster. The order of listing represents the relative size of activity.

Table 3-3. *Anatomical localization of activity associated with left hand finger tapping in the group of PD patients*

Analysis	Area	Cluster Size	Talairach Coordinates		
			x	*y*	*z*
Fixed Effects	Right Postcentral/Precentral Gyrus	2763	39	-24	65
	Right Inferior Parietal Lobule				
	Right Superior Parietal Lobule				
	Right/Left SMA				
	Right Anterior Cingulate Gyrus				
	Right Superior Temporal Gyrus				
	Right Supramarginal Gyrus				
	Right Middle Frontal Gyrus				
	Right Thalamus	707	21	-19	5
	Right Lentiform Nucleus				
	Right Insula				
	Left Lentiform Nucleus	175	-23	-13	5
	Left Thalamus				
	Left Superior Temporal Gyrus	140	-56	-39	20
	Left Insula				
	Left Inferior Parietal Lobule				
	Left Precentral Gyrus	63	-28	-21	70
	Left Middle/Superior Frontal Gyrus				
	Right Angular Gyrus	54	39	-77	30
	Right Middle Temporal Gyrus				
	Right Superior Occipital Gyrus				
	Left Superior Frontal Gyrus	41	-13	-13	75
	Left Thalamus	41	-6	-28	-10
	Right Superior/Middle Frontal Gyrus	36	32	49	35
	Right Precentral Gyrus	29	56	4	35
	Right Inferior/Middle Frontal Gyrus				
	Left Postcentral Gyrus	29	-60	-24	25
	Left Inferior Parietal Lobule				
Random Effects	Right Insula	41	34	11	0
	Right Inferior Frontal Gyrus				

Table 3-3. Cortical regions showing significant ($p<0.05$) activity associated with left hand finger tapping in the group of PD patients assessed using fixed and random effects analysis. The anatomical labels and cluster size corresponding to the peak voxel Talairach coordinates (Talairach and Tournoux, 1988) are reported. In cases where an active cluster included significantly active voxels in more than one cortical region, these additional regions are also listed under that cluster. The order of listing represents the relative size of activity. Abbreviations: SMA, supplementary motor area.

Table 3-4. *Anatomical localization of activity associated with right and left hand finger tapping in the group of control subjects*

Analysis	Area	Cluster Size	Talairach Coordinates *x*	*y*	*z*
Right Hand Tapping					
Fixed Effects	Left Precentral/Postcentral Gyrus	729	-30	-24	70
	Left Middle Frontal Gyrus				
	Left Inferior Parietal Lobule				
	Left Precentral Gyrus	37	-53	4	20
	Left Inferior Frontal Gyrus				
Random Effects	Left Precentral/Postcentral Gyrus	79	-28	-26	65
Left Hand Tapping					
Fixed Effects	Right Precentral/Postcentral Gyrus	937	51	-38	45
	Right Inferior Parietal Lobule				
	Right Supramarginal Gyrus				
	Right Superior Temporal Gyrus				
	Right SMA	151	17	-15	50
	Right Anterior Cingulate Gyrus				
	Left Precentral Gyrus	61	-47	2	15
	Left Insula				
	Left Inferior Frontal Gyrus				
	Left Inferior Parietal Lobule	52	-53	-32	30
	Right Thalamus	44	21	-28	0
	Right Parahippocampal Gyrus				
	Left Inferior/Superior Parietal Lobule	43	-30	-49	60
	Left Postcentral Gyrus				
	Left Precentral Gyrus	33	-56	-2	25
	Left Inferior Frontal Gyrus				
	Right Superior Temporal Gyrus	23	56	0	0
Random Effects	No Suprathreshold Voxels				

Table 3-4. Cortical regions showing significant ($p<0.05$) activity associated with right and left hand finger tapping in the group of control subjects assessed using fixed and random effects analysis. The anatomical labels and cluster size corresponding to the peak voxel Talairach coordinates (Talairach and Tournoux, 1988) are reported. In cases where an active cluster included significantly active voxels in more than one cortical region, these additional regions are also listed under that cluster. The order of listing represents the relative size of activity. Abbreviations: SMA, supplementary motor area.

Figure 3-5. *Fixed and random effects analysis of activity associated with right and left hand finger tapping across sessions in the group of PD patients*

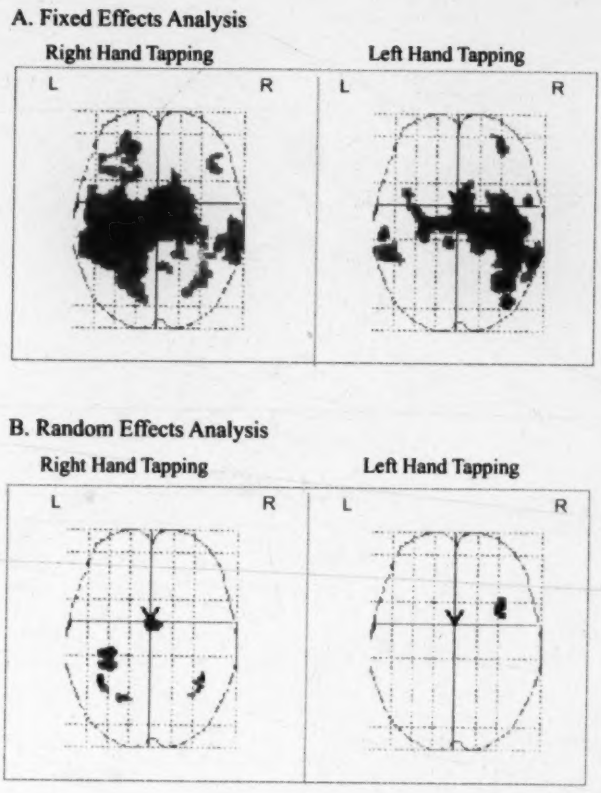

Figure 3-5. Maximum intensity projection (MIP) images showing the difference in activation associated with right and left hand tapping following a within group analysis of the data from the six PD patients using fixed effects analysis (A) and random effects analysis (B). Active voxels were significant at $p<0.05$.

Figure 3-6. *Fixed and random effects analysis of activity associated with right and left hand finger tapping across sessions in the group of healthy control subjects*

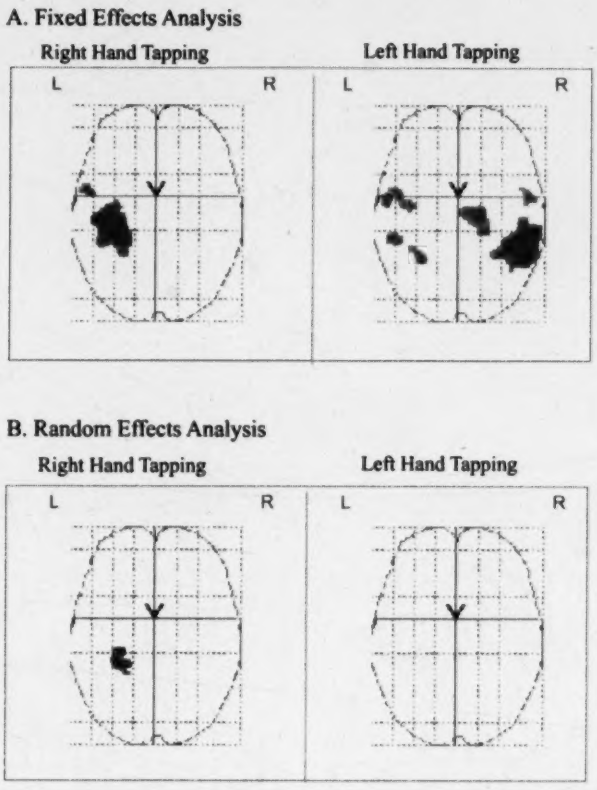

Figure 3-6. Maximum intensity projection (MIP) images showing the difference in activation associated with right and left hand finger tapping following a within group analysis of the data from the six control subjects using fixed effects analysis (A) and random effects analysis (B). Active voxels were significant at $p<0.05$.

Figure 3-7. *Fixed and random effects analysis of activity associated with right hand finger tapping in the group of PD patients and the group of control subjects*

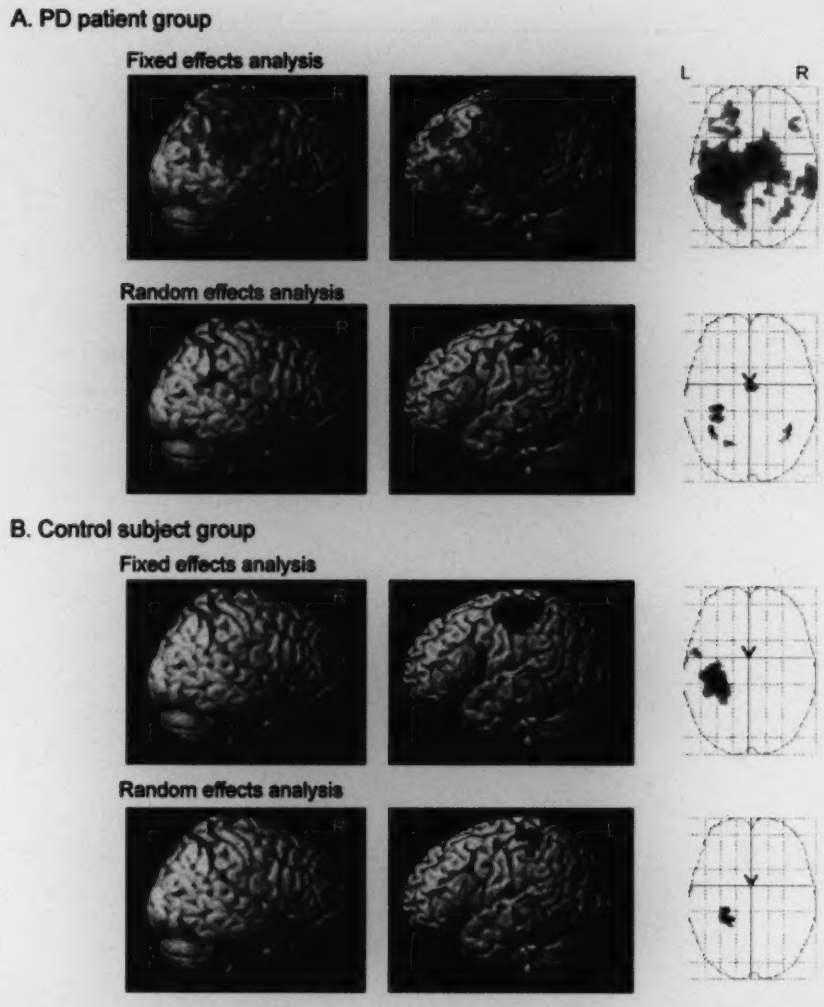

Figure 3-7. Activation associated with right hand finger tapping in the group of PD patients (A) and the group of control subjects (B). Active voxels in each group assessed using fixed and random effects analysis are shown superimposed onto surface renderings of the right and left hemispheres of a standardized brain with the corresponding MIP images. Surface rendering colour intensity was derived from the statistical value multiplied by an exponential decay function based on the distance of the active voxel from the surface of the brain.

Figure 3-8. *Fixed and random effects analysis of activity associated with left hand finger tapping in the group of PD patients and the group of control subjects*

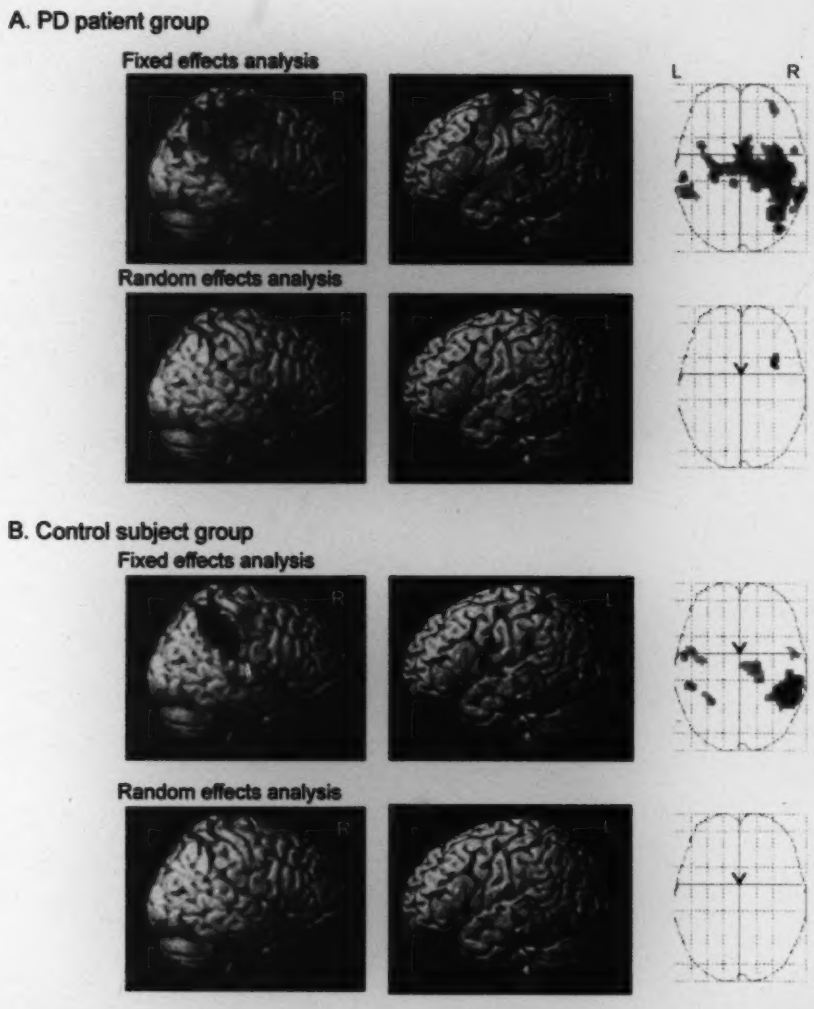

Figure 3-8. Activation associated with left hand finger tapping in the group of PD patients (A) and the group of control subjects (B). Active voxels in each group assessed using fixed and random effects analysis are shown superimposed onto surface renderings of the right and left hemispheres of a standardized brain with the corresponding MIP image. Surface rendering colour intensity was derived from the statistical value multiplied by an exponential decay function based on the distance of the active voxel from the surface of the brain.

3.3.4.1. Fixed effects analyses

A fixed effects analysis of a multisubject data set is implemented in a similar manner as the single subject analysis. However, the data from every subject in the group is included in the estimation of the model. As such, the results from a fixed effects analysis is indicative of the average activity of the data set (Friston et al., 1995). As shown in Figure 3-7, the results of the fixed effects analysis of activity associated with right and left hand finger tapping showed a substantial difference between the group of PD patients and control subjects. Perhaps the most remarkable observation is the large extent of activity associated with finger tapping in the group of PD patients. A total of 8536 and 4078 voxels were classified as active in PD patients during right and left hand tapping, respectively. As shown in Figure 3-5a, while the most robust activity detected within the group of PD patients was localized to the contralateral sensorimotor cortex, large clusters of active voxels were also found extensively throughout the ipsilateral cortex and in the medial frontal regions.

Within the group of control subjects (Figure 3-6a), the results of the fixed effects analysis more closely resemble the responses of individual analyses of motor activity in these subjects. As expected however, since a fixed effects model of group activity simply combines the data from multiple subjects into a single analysis (Friston et al., 1995), the extent of activity associated with finger tapping was more spatially extended. For example, while the mean number of active voxels associated with right hand tapping in the six single subject analyses was only 188.33 (± 55.43), 766 voxels were classified as active following the fixed effects analysis of the average group response. The 1344 voxels classified as active from the fixed effects analysis of activity associated with left

hand tapping in the group of control subjects included several smaller clusters of active voxels in the ipsilateral and medial regions of the cortex. Overall however, there is a clear distinction evident between the within group analysis of the average activity of PD patients and control subjects when assessed using a fixed effects model for statistical inference.

3.3.4.2. Random effects analyses

The results of the group analyses using a random effects model are more difficult to interpret. For example, while a random effects analysis of activity in the group of control subjects showed a cluster of active voxels restricted to the precentral and postcentral gyri, there were no significantly active voxels associated with left hand finger tapping (Figure 3-5b). Unlike fixed effects analysis, since a random effects analysis is sensitive to between subject variability, the power of the analysis is dependent on the number of subjects in the group (Holmes et al., 1998). Given that when analyzed independently clusters of significantly active voxels associated with left hand tapping were detected in every control subject, it is likely that the random effect analysis was inconclusive due to the low number of subjects in the group.

The analysis of the activity in the group of PD patients using a random effects model was also inconclusive. While right hand finger tapping was associated with small clusters of active voxels in the contralateral precentral gyrus, postcentral gyrus, inferior and superior parietal lobes, anterior cingulate gyrus, and ipsilateral inferior parietal lobe and supramarginal gyrus, the only active region associated with left hand finger tapping was the right insula. As the results of the independent analysis of each of the PD patients showed robust and reproducible activation during both right and left hand

tapping, it is again evident that more subjects are needed to increase the sensitivity of the random effects analysis of group activity.

3.3.5. Between group analysis

Since the between group comparison is based on a random effect analysis with a two sample t-test (Holmes et al., 1998), it is not surprising that there were also no significant differences between PD patients and controls in this analysis. There is nevertheless strong evidence from the independent analyses of the PD patients and controls that there are significant and meaningful differences between the two groups. Further investigation of these obvious trends with larger subject groups is clearly warranted.

3.4. Discussion

One of the main objectives of this study was to determine if there were any significant differences in the cortical activity in patients with early PD and healthy aged matched controls during a repetitive motor task. In both groups, robust activation was detected in the contralateral sensorimotor cortex. While there was no evidence of impaired cortical activity in PD patients, compared to age-matched controls every PD patient showed additional clusters of activity during both right and left hand tapping. However, although the mean spatial extent of activation across the whole brain and within the sensorimotor cortex was significantly higher in PD patients compared to controls, there were no differences in the mean amplitude of the BOLD response. In addition, fixed and random effects analyses of the activity within each group demonstrated that while a fixed effects analyses provided an inaccurate representation of

the typical responses within each group, the random effects analyses were inconclusive due to the low number of subjects in each group.

3.4.1. Repetitive finger tapping

Since PD patients generally experience difficulty with sequential, self-initiated movement, it is not surprising that functional imaging studies of PD are dominated by investigations of sequential motor tasks (Playford et al., 1992; Rascol et al., 1992, 1994, 1997; Jahanashahi et al., 1995; Samuel et al., 1997a; Sabatini et al., 2000; Haslinger at al., 2001). In addition, one of the earliest PET studies comparing PD patients to healthy control subjects, reported that a sequential task was more sensitive to impaired activity in PD patients than a repetitive task (Playford et al., 1992). Furthermore, functional imaging studies involving sequences of finger tapping (Rascol et al., 1992, 1994, 1997; Jahanashahi et al., 1995; Samuel et al., 1997a) or joystick movement (Playford et al., 1992) in PD patients consistently reported relatively impaired activity in the SMA, a region preferentially active during self-initiated sequential movement (Deiber et al., 1991, 1999; Rao et al., 1993; Van Oostende et al., 1997). Several more recent fMRI studies, including an event related fMRI study, localized this impairment in PD patients to the rostral, or more anterior subdivision of the SMA (Sabatini et al., 2000; Haslinger at al., 2001).

While only sequential motor tasks have been studied thus far, with the increased sensitivity of fMRI, it is possible that differences between PD patients and controls could also be detected during the performance of repetitive movement. Unlike sequential movement which is known to be difficult for PD patients, repetitive movement is relatively easy for both PD patients and healthy controls (Benecke et al., 1986; Georgiou

et al., 1994). Compared to sequential motor tasks, a repetitive motor task should therefore also minimize any undetectable variability in task performance and demands among subjects, improving the accuracy of observed data.

3.4.2. Single subject versus group analyses

While group analyses are important for generalizing the results of an activation study to a larger population, this may also conceal important details about the data (Holmes et al., 1998; McGonigle et al., 2000). In this study, activity associated with right and left hand finger tapping was detected in the contralateral sensorimotor cortex in every PD patient and control subject when analyzed individually. This suggests that the data is both valid and consistent.

While there was no obvious evidence of impaired cortical activity in any of the PD patients during repetitive finger tapping, compared to age-matched controls PD patients exhibited more widespread cortical activity. This included clusters of active voxels in the caudal SMA and anterior cingulate gyrus detected during both right and left hand tapping in every PD patient. Two PD patients also showed additional ipsilateral activity during left hand tapping. Although the clinical characteristics of the six PD patients in this study varied to some degree, there was no association between the duration of disease or history with dopaminergic medication and observed motor activation.

Previous functional imaging studies have reported relatively increased cortical activity in PD patients during sequential motor tasks (Rascol et al., 1997; Samuel et al., 1997a; Sabatini et al., 2000; Haslinger et al., 2001). In addition to impaired SMA activity, relatively increased activity in the lateral premotor cortex and inferior parietal

region were first reported in a PET study of PD patients during performance of a pre-learned finger tapping sequence (Samuel et al., 1997a). In the first published fMRI study with PD patients, Sabatini et al., (2000) reported increased activity in PD patients during performance of a pre-learned finger tapping sequence in "most of the other known cortical motor areas" (p.401). This included the caudal SMA, anterior cingulate, lateral premotor, primary sensorimotor and parietal cortices. An event related fMRI study also found increased activity in the bilateral motor cortex, caudal SMA, lateral premotor cortex and superior parietal cortex in PD patients during performance of freely selected joystick movements (Haslinger et al., 2001). In addition, in the first fMRI study of the effect of levodopa, Haslinger et al., (2001) showed that both impaired SMA activity and hyperactivity in PD patients partially recovered to the level of control subjects following the administration of levodopa (Haslinger et al., 2001).

While all three previous fMRI studies of PD patients have shown relatively increased activity associated with performance of self initiated sequences of movement, the results from this preliminary study demonstrate that relatively increased cortical activity in PD patients is also associated with repetitive movement with both hands, regardless of the lateralization of akinetic symptoms. Although the results from the random effects analyses were inconclusive, it is important to note that aside from the event related fMRI study by Haslinger et al., (2001), the only other fMRI study of PD reported only the average activity within the group of six PD patients and six age-matched control subjects (Sabatini et al., 2000). This may explain why the results were in agreement with the data from the present study that was either analyzed individually or using a fixed effects analysis.

3.4.3. Functional compensation

It has been suggested that increased activity observed in PD patients during movement is associated with functional compensation for disrupted SMA activity through the recruitment of cortical regions unaffected by striatal impairment (Rascol et al., 1997; Samuel et al., 1997a; Sabatini et al., 2000; Haslinger et al., 2001). This idea is supported by PET studies of recovered stroke patients who were shown to recruit the ipsilateral motor cortex when performing a movement with the affected hand (Chollet et al., 1991; Weiller et al., 1993; Cramer et al., 1997; Cao et al., 1998; Pineiro et al., 2001). However, in the present study there was no evidence of impaired cortical activation in any of the PD patients. Furthermore, increased activity in PD patients was associated with both right and left hand tapping, regardless of the lateralization of motor impairment. An alternative explanation is that heightened cortical activity in PD is associated with increased effort required to complete the task consistently and accurately. In order to consider this possibility, the functional significance of the regions associated with increased activity in PD will be briefly discussed.

3.4.3.1. Lateral premotor and parietal cortex

The lateral premotor cortex is involved in movements triggered by external sensory cues, and is therefore generally associated with sensory guided movement (Godschalk et al., 1981; Petrides, 1982; Passingham, 1985, 1988; Deiber et al., 1991; Mushiake et al., 1991; Halsband et al., 1994). The parietal cortex has also been shown to be important for the production of coordinated motor output by mediating the attentional control required to produce movements at the appropriate time and in an appropriate response to stimuli (Deiber et al., 1991; Jenkins et al., 1994).

There is evidence that activity in the lateral premotor and parietal cortices increases with task demands. For example, Winstein et al., (1997) demonstrated that lateral premotor and parietal activation increased linearly with task difficulty during visuomotor reaching movements in healthy subjects. In a related PET study, in both PD patients and healthy controls activation of parietal and lateral premotor regions increased during performance of sequential movements as the number of items in the sequence increased (Catalan et al., 1999). However, for sequences of all lengths, the foci of activation in lateral premotor and parietal regions were larger in PD patients relative to controls (Catalan et al., 1999). This suggests that although there were no differences in task performance, the task was generally more demanding for PD patients. While increased sensory or proprioceptive feedback may be a contributing factor, it is evident that heightened activity in these regions would be associated with increased task demands.

3.4.3.2. Caudal SMA

Unlike the rostral SMA, which has been shown to be relatively impaired during sequential movement in PD patients, the caudal SMA was reported to be more active in PD patients relative to healthy controls (Sabatini et al., 2000; Haslinger et al., 2001). While the rostral SMA is highly interconnected with striatal motor pathways, the caudal SMA receives input from the parietal lobe and has reciprocal connections with the primary sensorimotor cortex (Luppino et al., 1993). Therefore, while the rostral SMA is primarily associated with movement preparation, the caudal SMA is active more during movement execution (Samuel et al., 1998; Lee et al., 1999). Increased activity in the caudal SMA would therefore be expected during the performance of motor tasks that

required greater effort. Indeed, increased force or frequency of movement were shown to be associated with increased activity in the primary motor cortex and caudal SMA, but not in the rostral SMA (Dettmers et al., 1995; Blinkenberg et al., 1996; Sadato et al., 1996; Jenkins et al., 1997).

3.4.3.3. Anterior Cingulate

The anterior cingulate cortex, located below the rostral SMA, was shown to be more active during novel motor tasks, and thus decreased with task habituation (Colebatch et al., 1991; Deiber et al., 1991; Tyszka et al., 1994; Van Oostende et al., 1997). The anterior cingulate was also found to be correlated with the relative degree of emotional, attentional, or motivational involvement of the subject during the task (Devinsky et al., 1995). Although the role of the anterior cingulate is not as well understood as other regions, it is reasonable to expect that activity in this region would increase during tasks that required more effort and attention.

3.4.4. Conclusions

Since the present study is the first fMRI investigation of repetitive tapping with both the right and left hands in PD patients, the results provide additional insight into previous fMRI studies of functional compensation in PD during sequential movements (Sabatini et al., 2000; Haslinger et al., 2001). Although the group analyses were limited due to the low number of subjects in each group, the independent analysis of each subject and the fixed effects group analysis showed evidence of abnormal activity in PD patients during performance of repetitive finger tapping with the right and left hands.

While there was no evidence of impaired task performance or cortical activity in PD patients, relatively increased activity was detected in several regions during both

right and left hand tapping, regardless of the patients medication history or lateralization of motor symptoms. Surprisingly, all patients with PD showed large clusters of active voxels in the anterior cingulate and SMA, regions that have previously been shown to be relatively impaired in PD patients compared to age-matched control subjects (Playford et al., 1992; Jahanashahi et al., 1995; Samuel et al., 1997a). However, two more recent fMRI studies have localized this impairment in PD patients to the rostral region of the SMA (Sabatini et al., 2000; Haslinger et al., 2001), while activity in the caudal SMA was actually heightened (Sabatini et al., 2000; Haslinger et al., 2001). Therefore, increased activity in this study was likely also associated with the caudal SMA. Along with additional activation in a number of other regions, including the primary motor cortex, these results suggest that performing the repetitive motor task accurately and consistently was more demanding, and thus induced greater activation in regions associated with movement execution in PD patients compared to healthy age-matched controls.

In addition the sensorimotor cortex and caudal SMA, which are associated with movement execution, PD patients also showed additional activity in the parietal cortex and anterior cingulate cortex. These regions were previously shown to be more active during tasks that require greater attention (Colebatch et al., 1991; Deiber et al., 1991; Tyszka et al., 1994; Devinsky et al., 1995; Van Oostende et al., 1997). Even though there was no evidence of impaired movement or cortical activity, a repetitive motor task may be more difficult for PD patients to perform automatically. This may have been influenced both by mildly impaired motor processes and/or the patients cognitive state. For example, it is possible that patients with movement disorders are more aware of their

movement especially within the context of clinical evaluation. As such, even a simple motor task could be associated with increased attention and effort in PD patients. Unfortunately it is difficult to control the cognitive mind set and relative automaticity associated with a task. It may be interesting to look for a correlation between increased activity and individual experience with the task. Another option may be to try to reduce the automaticity of the task or increase the attention to task in healthy controls by introducing an unrelated task to be performed simultaneously.

Overall, it is evident that differences in cortical activation in PD patients and age-matched control subjects can be consistently detected in the individually analyzed data using a repetitive motor task. However, since the data from the random effects analyses were inconclusive due to the low number of subjects in each group, further investigation of the observed trends in a larger data set would be useful. In addition, more subtle experimental designs may provide more information about the functional significance of increased cortical activity in PD patients during motor tasks.

3.5. References

Benecke R, Rothwell JC, Dick JPR, Day BL, Marsden CD. Disturbance of sequential movements in patients with Parkinson's disease. Brain 1987; 110: 361-79.

Blinkenberg M, Bonde C, Holm S, Svarer C, Andersen J, Paulson OB. Rate dependence of regional cerebral activation during performance of a repetitive motor task: a PET study. J Cereb Blood Flow Metab 1996; 16: 794-803.

Bluml S, Kopyov O, Jacques S, Ross BD. Activation of neurotransplants in humans. Exp Neurol 1999; 158: 121-5.

Cao Y, D'Olhaberriage L, Vikingstad EM, Levine SR, Welch KMA. Pilot study of functional MRI to assess cerebral activation of motor function after poststroke hemiparesis. Stroke 1998; 29: 112-22.

Catalan MJ, Ishii K, Honda M, Samii A, Hallett M. A PET study of sequential finger movements of varying length in patients with Parkinson's disease. Brain 1999; 122: 483-95.

Ceballos-Baumann AO, Obeso JA, Vitek JL, DeLong MR, Bakay R, Linazasoro G, Brooks DJ. Restoration of thalamocortical activity after posteroventral pallidotomy in Parkinson's disease. Lancet 1994; 344: 814.

Ceballos-Baumann AO, Boecker H, Bartenstein P, VonFalkenhayn I, Riescher H, Conrad B, Moringlane JR, Alesch F. A positron emission tomographic study of subthalamic nucleus stimulation in Parkinson's disease. Arch Neurol 1999; 56: 997-1003.

Chollet F, Di Piero V, Wise RJ, Brooks DJ, Dolan RJ, Frackowiak RS. The functional anatomy of motor recovery after stroke in humans; A study with positron emission tomography. Ann Neurol 1991; 29: 63-71.

Colebatch JG, Deiber MP, Passingham RE, Friston KJ, Frackowiak RS. Regional cerebral blood flow during voluntary arm and hand movements in human subjects. J Neurophysiol 1991; 65; 1392-401.

Cramer SC, Nelles G, Bensom R, Kaplan J, Parker R, Kwong K, Kennedy D, Finklestein SP, Rosen BR. A functional MRI study of subjects recovered from hemiparetic stroke. Stroke 1997; 28: 2518-27.

Davis KD, Taub E, Houle S, Lang AE, Dostrovsky JO, Tasker RR, Lozano AM. Globus pallidus stimulation activated the cortical motor system during alleviation of parkinsonian symptoms. Nat Med 1997; 3: 671-74.

Deiber MP, Passingham RE, Colebatch JG, Friston KJ, Nixon PD, Frackowiak RS. Cortical areas and the selection of movement; a study with positron emission tomography. Exp Brain Res 1991; 84: 393-402.

Deiber MP, Honda M, Ibanez V, Sadato N, Hallet M. Mesial motor areas in self-initiated versus externally triggered movements examined with fMRI: Effect of movement type and rate. J Neurophysiol 1999; 81: 3065-77.

Dettmers C, Fink GR, Lemon RN, Stephan KM, Passingham RE, Silbersweig D, Holmes A, Ridding MC, Brooks DJ, Frackowiak RS. Relation between cerebral activity and force in the motor areas of the human brain. J Neurophysiol 1995; 74: 802-15.

Devinsky O,Morrell MJ, Vogt BA. Contributions of anterior cingulate cortex to behaviour. Brain 1995; 18: 279-306.

Friston KJ, Holmes AP, Worsley KJ, Poline JB, Frith CD, Frackowiak RSJ. Statistical parametric maps in functional imaging: a general linear approach. Hum Brain Mapp 1995; 2: 189-210.

Friston KJ, Williams S, Howard R, Frackowiak RSJ, Turner R. Movement related effects in fMRI time series. Mag Res Med 1996; 35: 346-55.

Georgiou N, Bradshaw JL, Iansek R, Phillips JG, Mattingley JB, Bradshaw JA. Reduction in external cues and movement sequencing in Parkinson's disease. J Neurol Neurosurg Psychiatry 1994; 57: 368-70.

Godschalk M, Lemon RN, Nijs HG, Kuypers HGJM. Behaviour of neurons in monkeys per-arcuate and precentral cortex before and during visually guided arm and hand movements. Exp Brain Res 1981; 44: 113-16.

Grafton ST, Waters C, Sutton J, Lew MF, Couldwell W. Pallidotomy increases activity of motor association cortex in Parkinson's disease: a positron emission topographic study. Ann Neurol 1995; 37: 776-83.

Halsband U, Matsuzaka Y, Tanji J. Neuronal activity in the primate supplementary, pre-supplementary and premotor cortex during externally and internally instructed sequential movements. Neurosci Res 1994; 20: 149-55.

Haslinger B, Erhard P, Kampfe N, Boecker H, Rummeny E, Schwaiger M, Conrad B, Ceballos-Baumann AO. Event-related functional magnetic resonance imaging in Parkinson's disease before and after levodopa. Brain 2001; 124: 558-70.

Holmes AP, Friston KJ. Generalisability, random effects and population inference. Neuroimage 1998; 7: 124.

Jahanshahi M, Jenkins IH, Brown RG, Marsden CD, Passingham RE. Brooks DJ. Self-initiated versus externally triggered movements. I. An investigation using measurement of regional cerebral blood flow with PET and movement-related potentials in normal and Parkinson's disease subjects. Brain 1995; 118: 913-33.

Jenkins IH, Fernandez W, Playford ED, Lees AJ, Frackowiak RSJ, Passingham RE, Brooks DJ. Impaired activation of the supplementary motor area in Parkinson's disease is reversed when akinesia is treated with apomorphine. Ann Neurol 1992; 32: 749-57.

Jenkins IH, Brooks DJ, Nixon PD, Frackowiak RSJ, Passingham RE. Motor sequence learning: a study with positron emission tomography. J Neurosci 1994; 14: 3775-90.

Jenkins IH, Passingham RE, Brooks DJ. The effect of movement frequency on cerebral activation: a positron emission tomography study. J Neurol Sci 1997; 151: 195-205.

Lee KM, Chang KG, Roh JK. Subregions within the supplementary motor area activated at different stages of movement preparation and execution. Neuroimage 1999; 9: 117-23.

Luppino G, Matelli M, Camarda R, Rizzolatti G. Corticocortical connections of area F3 (SMA-proper) and area F6 (pre-SMA) in the macaque monkey. J Comp Neuol 1993; 338: 114-40.

McGonigle DJ, Howseman AM, Athwal BS, Friston KJ, Frackowiak RSJ, Holmes AP. Variability in fMRI: an examination of intersession differences. Neuroimage 2000; 11: 708-34.

Mushiake H, Inase M, Tanji J. Neuronal activity in the primate premotor, supplementary, and precentral motor cortex during visually guided and internally determined sequential movements. J Neurophysiol 1991; 66: 705-18.

Passingham RE. Premotor cortex: sensory cues and movement. Behav Brain Res 1985; 18: 175-85.

Passingham RE. Premotor cortex and preparation for movement. Exp Brain Res 1988; 70: 590-96.

Petrides M. Motor conditional associative-learning after selective prefrontal lesions in the monkey. Behav Brain Res 1982; 5: 407-13.

Piccini P, Lindvall O, Bjorklund A, Brundin P, Hagell P, Ceravolo R, Oertel W, Quinn N, Samuel M, Rehncrona S, Widner H, Brooks DJ. Delayed recovery of movement-related cortical function in Parkinson's disease after striatal dopaminergic grafts. Ann Neurol 2000; 48: 689-95.

Pineiro R, Pendlebury S, Johansen-Berg H, Matthews PM. Functional MRI detects posterior shifts in primary sensorimotor cortex activation after a stroke: evidence of local adaptive reorganization? Stroke 2001; 32: 1134-39.

Playford ED, Jenkins IH, Passingham RE, Nutt J, Frackowiak RSJ, Brooks DJ. Impaired mesial frontal and putamen activation in Parkinson's disease: a positron emission tomography study. Ann Neurol 1992; 32: 151-61.

Rao SM, Binder JR, Bandettini PA, Hammeke TA, Yatkin FZ, Jesmanowicz A, Lisk LM, Morris GL, Mueller WM, Estkowski et al. Functional magnetic resonance imaging of complex human movements. Neurology 1993; 43: 2311-18.

Rascol O, Sabatini U, Chollet F, Celsis P, Monstastruc JL, Marc-Vernes JP, Rascol A. Supplementary and primary sensory motor area activity in Parkinson's disease. Regional cerebral blood flow changes during finger movements and effects of apomorphine. Arch Neurol 1992; 49: 144-48.

Rascol O, Sabatini U, Chollet F, Fabre N, Senard JM, Montastruc JL, Celsis P, Marc-Vergnes JP, Rascol A. Normal activation of the supplementary motor area in patients with Parkinson's disease undergoing long-term treatment with levodopa. J Neurol Neurosurg Psychiatry 1994; 57: 567-71.

Rascol O, Sabatini U, Fabre N, Brefel C, Loubinoux I, Celsis P, Senard JM, Montastruc JL, Chollet F. The ipsilateral cerebellar hemisphere is overactive during hand movements in akinetic parkinsonian patients. Brain 1997; 120: 103-10.

Sabatini U, Boulanouar K, Fabre N, Martin F, Carel C, Colonnese C, Bozzao L, Berry I, Montastruc JL, Chollet F, Rascol O. Cortical motor reorganization in akinetic patients with Parkinson's disease. A functional MRI study. Brain 2000; 123: 394-403.

Sadato N, Ibanez V, Deiber MP, Campbell G, Leonardo M, Hallett M. Frequency-dependent changes of regional cerebral blood flow during finger movements. J Cereb Blood Flow Metab 1996; 16: 23-33.

Samuel M, Ceballos-Baumann AO, Blin J, Uema T, Boecker H, Brooks DJ. Evidence for lateral premotor and parietal overactivity in Parkinson's disease during sequential and bimanual movements: A PET study. Brain 1997a; 120: 963-76.

Samuel M, Ceballos-Baumann AO, Turjanski N, Boecker H, Gorospe A, Linazasoro G, et al. Pallidotomy in Parkinson's disease increases SMA and prefrontal activation during performance of volitional movements: An $H_2{}^{15}O$ PET study. Brain 1997b; 120: 1301-13.

Samuel M, Williams SCR, Leigh PN, Simmons A, Chakraborti S, Andrew CM, Friston KJ, Goldstein LH, Brooks DJ. Exploring the temporal nature of hemodynamic responses of cortical motor areas using functional MRI. Neurology 1998; 51: 1567-75.

Talairach P, Tournoux J. A Stereotactic Coplanar Atlas of the Human Brain. 1988; Thieme, Stuttgart.

Tyszka JM, Grafton ST, Chew W, Woods RP, Colletti PM. Parceling of mesial frontal motor areas during ideation and movement using functional magnetic resonance imaging at 1.5 tesla. Ann Neurol 1994; 35: 746-49.

Weiller C, Chollet F, Friston KJ, Wise RJ, Frackowiak RSJ. Functional reorganization of the brain in recovery from striatocapsular infaction in man. Ann Neurol 1992; 31: 463-72.

Winstein CJ, Grafton ST, Pohl PS. Motor task difficulty and brain activity: investigation of goal-directed reciprocal aiming using positron emission tomography. J Neurophysiol 1997; 77: 1581-94.

Van Oostende S, Van Hecke P, Sunaert S, Nuttin B, Marchal G. FMRI studies of the supplementary motor area and the premotor cortex. Neuroimage 1997; 6: 181-90.

4. GENERAL DISCUSSION

4.1. Technical issues and limitations

There are technical issues associated with fMRI that are important to consider when interpreting fMRI results. These include image artifacts and spatial distortions associated with echo planar imaging, as well as the influence of inflow effects, draining veins, and physiological noise on the MR signal. Although each of these issues will be only briefly summarized here, they are described in more detail in several reviews (Edelman et al., 1994; Jezzard and Song, 1996; Turner et al., 1998; Jezzard and Clare, 1999).

4.1.1. Image artifacts and distortion

Echo planar imaging (EPI) is a method of rapid MR imaging that was originally developed by Mansfield (1977). In standard MR imaging, a single line of phase encoded data is acquired following each separate RF pulse. The imaging time therefore depends on the resolution of the image, which is in turn determined by the total number of phase encoding steps, and the time between RF excitations (repetition time, TR). In contrast, during EPI imaging the initial RF pulse is followed by a continuously oscillating readout gradient (see Edelman et al., 1994). The entire spatially encoded data set can therefore be sampled following a single RF pulse. Since each line of phase encoded data is acquired consecutively, the total imaging time is significantly reduced.

EPI is a popular imaging sequence for fMRI because of its speed, for example in the present study 20 image slices were acquired in 2 seconds. However, EPI images are particularly vulnerable to image artifacts. Since EPI is highly sensitive to the T_2^* dephasing that is the basis for BOLD contrast, it is also sensitive to magnetic field

inhomeogeneities associated with susceptibility differences between air, bone and tissue. Significant signal loss is therefore often seen in regions around the skull base and in the frontal area near the paranasal sinuses.

Inhomogeneity within the imaging plane also causes geometrical distortions of the image. More specifically, changes in the resonant frequency associated with magnetic field inhomogeneities within the frequency or phase encoding directions can cause the location of the signal to be misassigned, often appearing as a stretched image. EPI images are particularly vulnerable to geometric distortions due to the low receiver bandwidth (frequency per point in phase encoding direction). While these spatial distortions are typically worse at higher field strengths, they can be minimized prior to data acquisition by global shimming, which involves optimizing the external magnetic field to correct for field inhomogeneities. In addition, most post-processing software packages include warping schemes to correct for major spatial distortions.

In this study, spatial distortions were commonly observed in brain regions known to be particularly vulnerable to image artifacts. This included both the anterior region of the frontal cortex, and the region near the base of the skull that typically affected image slices within the occipital and cerebellar regions. While spatial normalization helped minimize image distortions by co-registering the images to a standard image template, this technique did not completely correct for spatial distortions (see Figure 2-2). Moreover, it is unclear if and how this post-processing technique affects the MR signal and observed cortical activation. Overall however, although spatial distortions were often observed in certain brain regions as described above, the cortical motor regions appeared to be relatively unaffected by spatial distortions and artifacts. Additional

activation in subcortical regions such as the basal ganglia would also have been of interest, especially when studying PD patients. However, imaging the basal ganglia using EPI is complicated both by relatively small changes in signal intensity compared to cortical areas, and the high concentration of iron, and artifactual noise resulting from the close proximity of this region to the ventricles (reviewed by Mattay and Weinberger, 1999).

The other common image artifacts are low intensity duplicate images called Nyquist ghosts that appear out of phase with the real image. Ghosting is caused by gradient eddy currents or field inhomogeneities which can result in slight differences in the timing of odd and even echoes acquired under the rapidly alternating positive and negative readout gradient. When the images are reconstructed, slight mismatches in the timing of odd and even echoes may result in a phase shift which causes part of the signal to appear 90° out of phase, or one half image away from the real image. Although correcting the phase mismatch during image reconstruction is an effective way to suppress ghosting artifacts, effective shimming and optimal gradient stability can also significantly minimize problems with ghosting. This is important since data analysis can be compromised if the intensities of the ghosts are correlated with the experimental task.

4.1.2. Inflow effects, draining veins, and physiological noise

Acquisition parameters are important when imaging with EPI. In an EPI experiment with a short repetition time, the spins of stationary protons may become saturated, which means that they have insufficient time to fully recover longitudinal magnetization before the next excitation. During the next excitation, fresh unsaturated (fully recovered) spins of blood flowing into the region will contribute more to the signal

than partially saturated protons already present in the region, thereby possibly interfering with the localization of neuronal activation. The effect of blood flow can be minimized using sequences with a longer repetition time. These sequences allow all the proton spins time to fully recover before the next excitation. Inflow effects are therefore generally assumed to be particularly problematic with repetition times that are less than one second (as reviewed by Jezzard and Song 1996; Jezzard and Clare 1999). The repetition time of 2 seconds that was implemented in this study should have helped minimized inflow effects.

Another concern with fMRI is that observed brain activity may actually be mislocated in large draining veins which have little or no close relationship with the truly active neurons. Indeed, fMRI studies have shown that the BOLD signal changes in macrovessels are larger than microvessels. In addition to minimizing the inflow effects, localization may be improved by including a minor diffusion weighting to remove the signal from draining veins while preserving the signals from capillaries and parenchyma (Boxerman et al., 1995; Song et al., 1996).

Physiological changes associated with cardiac and respiratory cycles can also influence the signal. Cardiac pulsations are directly associated with periodic blood flow and a pulsatile motion within vessels. Respiration is also associated with generalized changes in blood oxygenation as well as movement effects related to the physical act of breathing. These effects are especially disruptive in experiments with repetition times that are short relative to the cardiac and respiratory cycles (i.e., TR<1 second), where changes in signal associated with these effects will appear as peaks in images. While these effects cannot be avoided, retrospectively filtering these frequencies can minimize

signal associated with physiological noise (Le and Hu, 1995; Biswal et al., 1996).

While it is likely that corrections for physiological noise, inflow, and draining vein effects would influence observed motor activation, no such measures were implemented in this study. It is therefore possible that some of the reported variability in the size or extent of the observed BOLD contrast signal in this study could be due to variable influence of physiological noise both within and between subjects and imaging sessions.

4.2. Limitations of standard block-design fMRI experiments

In addition to the technical limitations associated with fMRI, there are also limitations related to experimental design. Standard block-design studies are effective for localizing cortical activity associated with a task, however the results provide no information pertaining to individual responses. Event related fMRI, in which a functional image is acquired following each single stimulus presentation or task execution rather than a block of continual activation, provides an alternative approach for activation studies.

In contrast to the rather limited options of a block design experiment, such as that implemented in this study, event related fMRI is capable of providing more information about the activation associated with various components of movement selection, preparation, and execution during motor tasks with varying degrees of physiological and cognitive demands. For example, event related experimental paradigms can be used to track the time course of changes in different regions of the brain (reviewed by Buckner, 1998). This could facilitate the evaluation of the processes or mechanisms contributing to widespread cortical overactivity in PD patients as reported both in this study, and in

previous functional imaging studies (Samuel et al., 1997; Sabatini et al., 2000; Haslinger et al., 2001).

4.3. General conclusions

4.3.1. Feasibility of investigating motor activity using fMRI at 3T

The experiments described in this thesis were designed to provide a comprehensive assessment of the technical feasibility and reproducibility of fMRI of motor activity at 3T. Assessing both single subject and group effects in each project provided an opportunity to fully characterize the consistency of the data and to identify potential limitations of the experimental design and analysis.

In both studies, cortical activity associated with repetitive finger tapping with the right and left hands was consistently detected in the contralateral sensorimotor cortex. This is consistent with the well established findings from previous fMRI studies (reviewed by Mattay and Weinberger, 1999). In addition, the results clearly demonstrated that there was no difference in the reproducibility of data acquired from multiple subjects versus data acquired from a single subject tested in several sessions. Thus, BOLD contrast fMRI at 3T is a valid and sensitive tool for localizing cortical motor activity.

4.3.2. Changes in cortical activation in PD

Results of this fMRI investigation of motor activation in patients with early Parkinson's disease demonstrated for the first time that differences between PD patients and healthy aged matched controls can be detected using a simple repetitive motor task. While there was no detectable impaired activity in this study, the individually analyzed images showed more widespread cortical activation in PD patients compared to controls.

Consistent with previous reports (Samuel et al., 1997; Sabatini et al., 2000; Haslinger et al., 2001), increased activity was detected in the parietal cortex, lateral premotor and primary motor cortex, caudal SMA, and anterior cingulate cortex. Previous reports attributed increased activity to compensatory recruitment of non-striatal motor pathways in PD (Samuel et al., 1997; Sabatini et al., 2000; Haslinger et al., 2001). It is important to note however, that increased activity was detected in PD patients during both right and left hand tapping, regardless of the lateralization of motor symptoms, and the duration or severity of disease. While there were no obvious changes in cortical activation associated with the patients' medication history, the number of medicated versus non-medicated subjects was essentially too small to determine this unequivocally.

Heightened activity in PD patients was primarily localized to regions associated with movement execution (i.e., caudal SMA, sensorimotor cortex), and task related attention or motivation (i.e., anterior cingulate, parietal regions). It is therefore possible that although the task was relatively simple, performing the task accurately and consistently was more challenging for PD patients. While previous functional imaging studies have restricted their experiments to sequential tasks which are effective for detecting impaired (rostral) SMA activity in PD (Jenkins et al., 1992; Playford et al., 1992; Rascol et al., 1992, 1994, 1997; Jahanashahi et al., 1995; Samuel et al., 1997; Sabatini et al., 2000; Haslinger et al., 2001), we have demonstrated that repetitive motor tasks are also useful for investigating more diverse changes in cortical activation. However, since the data from the random effects analyses were inconclusive due to the low number of subjects in each group, these preliminary results clearly warrant further investigation, both with larger group sizes, and more specific experimental paradigms.

Our data suggests that there may be a reduction in BOLD signal change with increasing age in healthy subjects. The mean BOLD signal changes associated with right and left hand movement in the group of younger healthy subjects (mean age 25.6 years) described in Chapter 2 were 2.2% and 2.5% compared to 1.5% and 1.3% in the older healthy control subjects (mean age 55.6 years) described in Chapter 3. Although presently little is known about age-related changes in the size or amplitude of BOLD signal changes associated with movement, it would be interesting to determine what these changes were, and how they differ in PD patients and healthy controls. In addition, it is obvious that more detailed information is needed regarding the influence of task demands on cortical motor activation in PD. Our understanding of the physiological and/or cognitive processes associated with the changes in activation in PD will therefore undoubtedly benefit from the development of more elegant experimental paradigms with larger groups of subjects.

In sum, we have demonstrated that BOLD fMRI at 3T is a feasible, reliable and consistent strategy to evaluate changes in cortical activity in both healthy volunteers and individuals with PD. Our results are compatible with what has been previously described in the literature and may provide new insight into the pathological changes underlying PD.

4.4. References

Biswal V, DeYoe AE, Hyde JS. Reduction of physiological fluctuations in fMRI using digital filters. Magn Reson Med 1996; 35: 107-13.

BoxermanJL, Bandettini PA, Kwong KK, Baker JR, Davis TL, Rosen BR, Weisskoff RM. The intravascular contribution to fMRI signal change: Monte Carlo modeling and diffusion weighted studies in vivo. Magn Reson Med 1995; 34: 4-10.

Buckner R. Event-related fMRI and the hemodynamic response. Hum Brain Mapp 1998; 6: 373-77.

Edelman RR, Wielopolski P, Schmitt F. Echo-planar MR imaging. Radiology 1994; 192: 600-12.

Haslinger B, Erhard P, Kampfe N, Boecker H, Rummeny E, Schwaiger M, Conrad B, Ceballos-Baumann AO. Event-related functional magnetic resonance imaging in Parkinson's disease before and after levodopa. Brain 2001; 124: 558-70.

Jahanshahi M, Jenkins IH, Brown RG, Marsden CD, Passingham RE. Brooks DJ. Self-initiated versus externally triggered movements. I. An investigation using measurement of regional cerebral blood flow with PET and movement-related potentials in normal and Parkinson's disease subjects. Brain 1995; 118: 913-33.

Jenkins IH, Fernandez W, Playford ED, Lees AJ, Frackowiak RSJ, Passingham RE, Brooks DJ. Impaired activation of the supplementary motor area in Parkinson's disease is reversed when akinesia is treated with apomorphine. Ann Neurol 1992; 32: 749-57.

Jezzard P, Song AW. Technical foundations and pitfalls of clinical fMRI. Neuroimage 1996; 4: S63-S75.

Jezzard P, Clare S. Sources of distortion in functional MRI data. Hum Brain Mapp 1999; 8: 80-85.

Le TH, Hu X. Restrospective estimation and correction of physiological artifacts by direct extraction of physiological activity from MR data. Magn Reson Med 1996; 35: 290-98.

Mansfield P. Multi-planar image formation using NMR spin echoes. J Phys 1977; 10: 349-52.

Mattay VS, Weinberger DR. Organization of the human motor system as studied by functional magnetic resonance imaging. Eur J Radiol 1999; 30: 105-14.

Playford ED, Jenkins IH, Passingham RE, Nutt J, Frackowiak RSJ, Brooks DJ. Impaired mesial frontal and putamen activation in Parkinson's disease: a positron emission tomography study. Ann Neurol 1992; 32: 151-61.

Rascol O, Sabatini U, Chollet F, Celsis P, Monstastruc JL, Marc-Vernes JP, Rascol A. Supplementary and primary sensory motor area activity in Parkinson's disease. Regional cerebral blood flow changes during finger movements and effects of apomorphine. Arch Neurol 1992; 49: 144-48.

Rascol O, Sabatini U, Chollet F, Fabre N, Senard JM, Montastruc JL, Celsis P, Marc-Vergnes JP, Rascol A. Normal activation of the supplementary motor area in patients with Parkinson's disease undergoing long-term treatment with levodopa. J Neurol Neurosurg Psychiatry 1994; 57: 567-71.

Rascol O, Sabatini U, Fabre N, Brefel C, Loubinoux I, Celsis P, Senard JM, Montastruc JL, Chollet F. The ipsilateral cerebellar hemisphere is overactive during hand movements in akinetic parkinsonian patients. Brain 1997; 120: 103-10.

Sabatini U, Boulanouar K, Fabre N, Martin F, Carel C, Colonnese C, Bozzao L, Berry I, Montastruc JL, Chollet F, Rascol O. Cortical motor reorganization in akinetic patients with Parkinson's disease. A functional MRI study. Brain 2000; 123: 394-403.

Samuel M, Ceballos-Baumann AO, Blin J, Uema T, Boecker H, Brooks DJ. Evidence for lateral premotor and parietal overactivity in Parkinson's disease during sequential and bimanual movements: A PET study. Brain 1997; 120: 963-76.

Song AW, Wong EC, Tan SG, Hyde JS. Diffusion weighted fMRI at 1.5T. Magn Reson Med 1996; 35: 155-58.

Turner R, Howseman A, Rees GE, Josephs O, Friston K. Functional magnetic resonance imaging of the human brain: data acquisition and analysis. Exp Brain Res 1998; 123: 5-12.